The Interplay of Physical and Biogeochemical Processes in Determining Water Cap Oxygen Concentrations within Base Mine Lake, the First Oil Sands Pit Lake

The Interplay of Physical and Biogeochemical Processes in Determining Water Cap Oxygen Concentrations within Base Mine Lake, the First Oil Sands Pit Lake

By

Daniel Arriaga B.Sc., M.Sc.

A Thesis Submitted to the School of Graduate Studies

In Partial Fulfilment of the Requirements of

the Degree of Doctor of Philosophy

McMaster University

McMaster University DOCTOR OF PHYLOSOPHY (2018) Hamilton, Ontario

TITTLE: The Interplay of Physical and Biogeochemical Processes in Determining Water Cap Oxygen Concentrations within Base Mine Lake, the First Oil Sands Pit Lake

AUTHOR: Daniel Arriaga B.Sc., M.Sc. (The University of Texas at El Paso)

SUPERVISOR: Dr. Lesley A. Warren

Pages: x, 189

ABSTRACT

Syncrude Canada's Base Mine Lake (BML), is the first oil sands pit lake and is being used to evaluate water-capped tailings technology for fluid fine tailings (FFT) management. To be successful, pit lakes must achieve the ecological role of a natural lake, requiring the development of oxygenated water cap capable of supporting macrofauna. Due to the reductive nature of the FFT stored at the bottom, oxygen-consuming constituents (OCC) such as methane, sulfide and ammonium can be mobilized into the water cap of oil sands pit lakes, posing a threat to the success of the reclamation. Results from BML are vital to inform successful pit lake design with a further 10+ pit lakes projected for collective waste reclamation required in the region, currently awaiting permitting. This field study established BML water cap depth dependent oxygen consumption rates (OCR), identified the key OCC driving those rates and modeled the roles of biogeochemical oxygen consumption and physical mixing in establishing water cap oxygen profiles during early stage development (< 5 years post commissioning). The balance between these two discrete processes underpins the likely viability of this management strategy for oil sands FFT. Results identify high OCR, in the range of highly productive eutrophic to hyper eutrophic lakes, in the vicinity of the FFT water interface, i.e. where concentrations of OCC are highest. Observed OCR rates decreased away from the FFT water interface, as concentrations of OCC decreased. The important OCC associated with high OCR were methane and ammonium. While the OCR values in the hypolimnion were extremely high, a minimally oxic FFT water interface persisted (<10 μM O_2) contrasting the anoxic hypolimnetic waters typically observed in highly productive systems. Water cap oxygen mass balance modeling revealed physical mixing of oxygen into the hypolimnion from the metalimnetic region of the BML water cap currently slightly exceeds the oxygen being consumed through biogeochemical redox cycling, explaining the persistence of low levels of oxygen to the FFT water interface in the BML water cap (~ 10 m in depth). However, higher mobilization of OCC from the FFT as FFT consolidates, and/or higher rates of microbial biogeochemical cycling as microbial communities continue to establish and grow within BML, and/or decreased physical vertical transport of O_2 into the hypolimnion, would all shift the oxygen balance towards greater consumption and thus would result in the migration of the oxic-anoxic boundary and OCC higher up into the water cap where they would directly impact the surface zone oxygen concentrations. Modeling results here identify that without the physical injection of oxygen into the hypolimnion, currently observed, OCR rates

would generate anoxic conditions that would reach the middle of the metalimnion within this system within 24 hours. The development of an anoxic zone would facilitate greater generation of OCC directly within the water cap through anaerobic microbial biogeochemical cycling, the high levels of sulfate (~ 2 mM) observed within the BML water cap, which exceeds water cap oxygen concentrations by 3 orders of magnitude, indicate that generation of ΣH_2S within this pit lake water cap would be a substantive risk to the development of a stable surface oxic zone that can support macro fauna. In addition, the emergence of nitrification, as one of the main oxygen-consuming reactions, was assessed experimentally to determine the potential effects on the oxygen depletion in BML water. Experimental results identified active nitrification with rates in the comparative range of marine to eutrophic estuary environments, with BML water collected from the metalimnion-hypolimnion interface, i.e. where the highest conversion of ammonia to nitrate was observed in field results. However, a comparison of oxygen consumption due to nitrification based on experimental, nitrification only results versus results from the field where nitrification as well as methanotrophy and other oxygen consuming processes are possible indicate oxygen consumption due to nitrification alone in the field is six times lower than the experimental oxygen consumption observed. These results highlight the competition for oxygen by multiple processes within BML, which suppress nitrification below levels observed under ideal experimental conditions. Characterization and modelling results of BML water cap oxygen concentrations carried out in this doctoral research reveal a new understanding of the important processes driving observed oxygen concentrations. These new insights delineate the potential effects of mobilized reduced constituents in the water cap from FFT and processes that may mitigate or exacerbate these impacts. Thus these results are of significant relevance to both the oil sands industry as well as other natural or anthropogenically impacted environments with high oxygen demand.

ACKNOWLEDGEMENTS

Over the course of my research, I have been supported (financially, academically and emotionally) from a variety of sources. I would like to express my sincerest gratitude to my supervisor, Lesley Warren, for her guidance, and support. Thank you for your patience, insight, and for being a strong advocate for my success. I would also like to thank the members of my supervisory committee, Drs. Luc Bernier, Ian Droppo, Greg Slater, who consistently made time to attend meetings and offer up helpful and challenging comments.

A special thanks to the closure and reclamation group at Syncrude. Their charismatic and cheerful assistance facilitated field work and enabled the collection of samples and data required for this research. Thanks to Janna Lutz, Wendy Kline, Jessica Piercey, Mohamed Salem, Dallas Heisler, Tara Penner, Carla Wytrykush, Geoff Halferdahl, Lori Cyprien; field leads Mike Arsenault, John Arnold; and boat operators Chris Beierling, and Richard Kao.

Over my years in this department, I have shared ideas, equipment, and incredible experiences with a number of colleagues. I would like to thank all the members of the microbial geochemistry research group for advising, teaching, and supporting me over the past four years. Tara Colenbrander, Katie Kendra, Stephanie Marshall, Michelle Reid, Maya Winland-Gaetz, Darla Bennett, Carlo Cilio, Kelly Martin, Patrick Morris, and Florent Risacher. Enjoying being around the people you work with definitely makes for a superior grad school experience. My deepest gratitude to David Camacho for several days of fruitful talks and liming. Thanks for your help in checking my work and your great suggestions over the years.

I would also like to acknowledge the generous financial support of the School of Geography and Earth Science, which set aside funds during the Fort McMurray fire, where some of us lost our belongings. To all the staff and administrative personnel, I appreciate all your help during these years.

I want to thank all my family who has never stopped believing in me. They are the pillar that has sustained my academic and professional career. To my siblings, I have always felt your love and affection regardless of where I live. Also, to my partner in crime, Mai Yamamoto. Thanks for these amazing years together. To my father Antonio, you introduced me to my two favourite hobbies: Science and Futbol. I have worked hard to deserve every penny you have invested in my academic career. Gracias por todo Papa.

If I were to dedicate this thesis to someone it would be my mother, who has been the source of my strength during my life. Thanks for every smile, message, meal, laugh and your wise guidance. There are no words to describe my infinity appreciation for being my mother. Te Amo abue

This work was funded by grants from Canada's Oil Sands Innovation Alliance (COSIA), Syncrude Canada and, the National Science and Engineering Research Council (NSERC).

TABLE OF CONTENTS

LIST OF FIGURES

LIST OF TABLES

LIST OF ABBREVIATIONS

AOSR ..... Alberta Oil Sands Area

BML ..... Base Mine Lake

DO ..... Dissolved Oxygen

DOC ..... Dissolved Organic Carbon

FFT ..... Fluid Fine Tailings

FWI ..... FFT water interface

IRB ..... Iron-Reducing Bacteria

MLSB ..... Mildred Lake settling basin

PL ..... Pit Lake

OCC ..... Oxygen consuming constituent

OCR ..... Oxygen consumption rate

ORP ..... Oxidation-Reduction potential

OSPW ..... Oil Sand Processed Water

WCTT ..... Water Capped Tailings Technology

PREFACE

This thesis includes two original papers that will be submitted for publication in peer-reviewed journals, as follows:

Thesis Chapter	Publication title/full citation	Publication status
Chapter 3	Arriaga D., Colenbrander T., Morris P. K., Risacher F., Goad C., Slater G.F., Warren L. A., The precarious balance between physical transport and biogeochemical consumption in determining water cap oxygen concentrations in the first oil sands pit lake, Base Mine Lake	To be submitted to the journal, Chemosphere January 2019
Chapter 4	Arriaga D., Warren A. L. Nitrification in BML, the first oil sands pit lake: Investigating the effects of NH_4^+ on the oxygen consumption	In preparation

DECLARATION OF ACADEMIC ACHIEVEMENT

I am the primary contributor to this thesis in terms of analyses, experimental work, data collection, analysis and writing. Dr. Lesley Warren supervised the work reported in Chapters 2-4, providing intellectual and technical guidance, assistance in the interpretation of findings and written and editorial work on the written thesis. Chapters 3 and 4 incorporate results not collected by myself: methane concentrations for 2015 and 2016 analyzed by Corey Goad, areal-volume data from BML provided by Geoff Halferdahl (Syncrude Canada), and August 2017 physicochemical and geochemical data collected by Dr. Jiro Mori and Dr. Gerhard Jessen.

CHAPTER 1: Base Mine Lake: the first Oil Sand Pit Lake in the Alberta oil sands area

1.1 The Athabasca oil sand region

Alberta is one of the world's main producers of oil. The Athabasca Oil Sands Region (AOSR), in northern Alberta (Figure 1.1), has one of the largest oil reservoirs in the world (GOA, 2012). The oil deposits are estimated to hold 165 billion barrels of bitumen (Allen, 2008; Frank et al., 2014; Holden et al., 2011; Teare et al., 2012a). These oil sands deposits in northern Alberta are the third in size after Saudi Arabia and Venezuela (Giesy et al., 2010; Honarvar et al., 2011). Oil sand is composed of bitumen (12 wt %), an assortment of sand, silts, and clays (85 wt %); and water (3–5 wt %). Bitumen contains saturated hydrocarbons, high aromatic compounds, resins, and asphaltenes.

Figure 1.1 The Athabasca Oil Sands Region in northern Alberta, Canada. Created by Alberta Environment and Sustainable Resource Development, (2014)

1.1.1 Extraction

Bitumen is recovered from oil sands using surface mining or in situ methods depending on where the deposit is located. Near-surface oil sands deposits are extracted by open-pit mining. Deep oil sands reserves are recovered using in situ methods (Bergerson and Keith, 2006). In the AOSR, only 20% is excavated through surface mining, the rest is extracted using in situ techniques (CAPP, 2018; Carrera-Hernandez et al., 2012; GOA, 2012; Peacock, 2010). Each oil sands collector varies in the technology used for

extraction and upgrading. Overall, the oil sands material collected is crushed and broken into smaller pieces. This mixture is hydro-transported in a pipeline to stirred tanks. During this process, oil sands are separated from oil and bitumen is liberated from sand grains. In traditional processing, caustic hot water is added to the oil sands to cause the asphaltic acids in bitumen to become water soluble and act as surfactants. This permits the bitumen to be removed from the sand and clays (Chalaturnyk et al., 2002; Giesy et al., 2010; Kavanagh et al., 2009; Li et al., 2011; OSDG, 2009). After this, there is residual tailings slurry, which is made up of solids and dissolved salts mixed with oil sands process water (OSPW). Tailing ponds are engineered to allow the settlement of the sand and fines within this tailing slurry. These tailing ponds allow dewatering of entrapped water in the slurry, which can then be recycled. Bitumen, in this slurry, is extracted by flotation (Masliyah et al., 2004). Typical bitumen recovery ranges from 88% to 95% (Beier et al., 2013; Beier and Sego, 2008).

The bitumen extraction process is a complex and expensive process that consumes large amounts of water. Water is initially withdrawn from freshwater sources (i.e., the Athabasca River) to use during the extraction process (Allen, 2008). During the in situ extraction process, 12 barrels of water are used to produce one barrel of bitumen. From this water, approximately 85% is reused from settling (tailing) basins, decreasing the use to four barrels of water (Giesy et al., 2010; Holowenko et al., 2000; Mikula et al., 2008). Management of the large quantities of tailings water is one of the major challenges of the oil sands industry. Tailings are comprised of process-affected water, coarse and fine particles, inorganic and organic by-products and residual bitumen left behind after

extraction. OSPW contains dissolved metals, ions, and organic compounds (Allen, 2008). After several rounds of tailing water recycling, the concentrations of dissolved ions and toxic compounds gradually increase. Elevated concentrations of these dissolved ions and compounds lead to detrimental water that can be used for extraction recovery of bitumen (Allen, 2008). In addition, the tailings water becomes highly saline and acutely toxic. These make it inappropriate for release or use outside the oil sand site (Drzewicz et al., 2010; Kotylar et al., 1996). Nonetheless, the oil sands manufacturers, following the Alberta Environmental Protection and Enhancement Act, have successfully (i.e., Gateway Hill) returned the used land to a productive capability equivalent to that of the pre-disturbance landscape.

1.1.2 Tailings Management

Current estimations predict that oil sands crude oil production will grow from 2.5 million barrels per day (bbl/d) in 2016 to approximately 3.5 million barrels per day between 2020 and 2025 (Kelly et al., 2010; Kurek et al., 2013; Teare et al., 2012b). This could generate almost 20,000 cubic meters of tailing material daily (GOA, 2012, 2009). It is estimated these tailing ponds cover an area of more than 240 km^2 (GOA, 2009; Sobkowicz, 2013). The total tailing volume reported by the mine operators for 2015 included approximately 1 billion cubic meters of processed water, which is expected to grow to more than 1.1 billion cubic meters by 2020 (Parajulee and Wania, 2014; Schindler, 2014).

Tailings, with time, separate into four segments or layers within the ponds: 1) a rapidly settling silt (>44 μm) fraction settles out upon discharge into the ponds; 2) after 2–3 years, the remaining suspended fines content achieves 30 to 40 wt %, referred to as mature fine tailings (MFT) (Farkish and Fall, 2013); 3) this fines content continues to increase its proportional content of the suspended aqueous fine particles (20 to 80 wt % clays and silts) referred to as fluid fine tailings (FFT); and lastly, 4) there is the processed-water layer (Allen, 2008; GOA, 2009; Powter et al., 2011). FFT behaves as a viscous fluid, made up of clay particles, sand, and residual bitumen mixed with water (Headley et al., 2010; Powter et al., 2011). FFT remains in suspension because it does not efficiently self-consolidating into a solid layer, thus presenting a great concern for the oil sands industry. Therefore, FFT must be stored in tailing ponds to allow for dewatering, settlement, and recycling of water (Eckert et al., 1996). Dewatering and settling rates for tailings are normally greatest during the first year after deposition but the consolidation rate is slow and tailings can remain in suspension for decades (Eckert et al., 1996; Kasperski, 1992; Kasperski and Mikula, 2011; MacKinnon, 1989).

1.1.3 Tailings Reclamation Strategies for FFT

The Government of Alberta introduced, in 2015, the tailings management framework (TMF) to delineate regulations for managing FFT in the AOSR (GOA, 2015). The TMF establishes site-specific thresholds for FFT volumes over the life of an oil sands mine. These thresholds mandate the total FFT to reach suitable conditions after 10 years of the end of bitumen extraction. Currently, two methods of reclamation are under development for oil sands tailing ponds: dry reclamation and wet reclamation. The latter,

wet landscape approach, consists of large FFT deposits capped with OSPW within decommissioned open pits. A self-sustaining freshwater ecosystem is projected to develop eventually (List and Lord, 1997). Oil sands pit lakes are characterized in the TMF as a prospective approach to manage the reducing constituents released from the FFT, and for simplifying FFT assimilation into reclamation landscapes (GOA, 2015).

Some of the main water quality parameters of concern (see more details in the next section) for the oil sands pit lake are: elevated dissolved solids, elevated ammonia concentrations, elevated acute and chronic toxicants and low dissolved oxygen concentrations (Westcott and Watson, 2005). FFT will consolidate over time and express pore water that can affect the water quality of the cap water. The dissolved oxygen concentration within a pit lake is a key water quality issue that will be influenced by the chemical composition of the OSPW and subsequently by the pore-water release. At first, the chemical composition of the water cover will be governed by the legacy of OSPW constituents. However, freshwater inputs (i.e., water pump in, water runoff and precipitation) and in situ (bio) geochemical processes are projected to improve the quality of the water over time. A complete understanding of FFT pore-water and water-cap geochemistry, as well as the relationships between geochemical processes and FFT settlement, are critical for anticipating the long-term oxygen evolution as a key water quality parameter.

Syncrude Canada has built the first oil sands pit lakes, Base Mine Lake (BML; Figure 1.2) and is currently assessing its viability as a tailings management strategy. BML consists of a mixed freshwater and oil sands process water (OSPW) cover of about

10 meters overlying a suspended layer of FFT (Figure 1.3) deposited over the years using Syncrude's tailings ponds. It should be mentioned that while BML is an excellent approach to study oil sands pit lake, it is not a true pit lake given Syncrude is still using the water for production and/or supply of OSPW to BML. A critical regulatory requirement for these pit lakes will be the demonstration that they can support a viable ecosystem; i.e., turbidity, oxygen, and salinity levels within the water cap will reach levels that enable a self-sustaining higher aquatic life to develop. BML, commissioned at the end of 2012, is the first commercial-scale demonstration of the WTCC in the AOSR and thus the evolution of water quality within such a pit lake is currently unknown given the current short existence of BML.

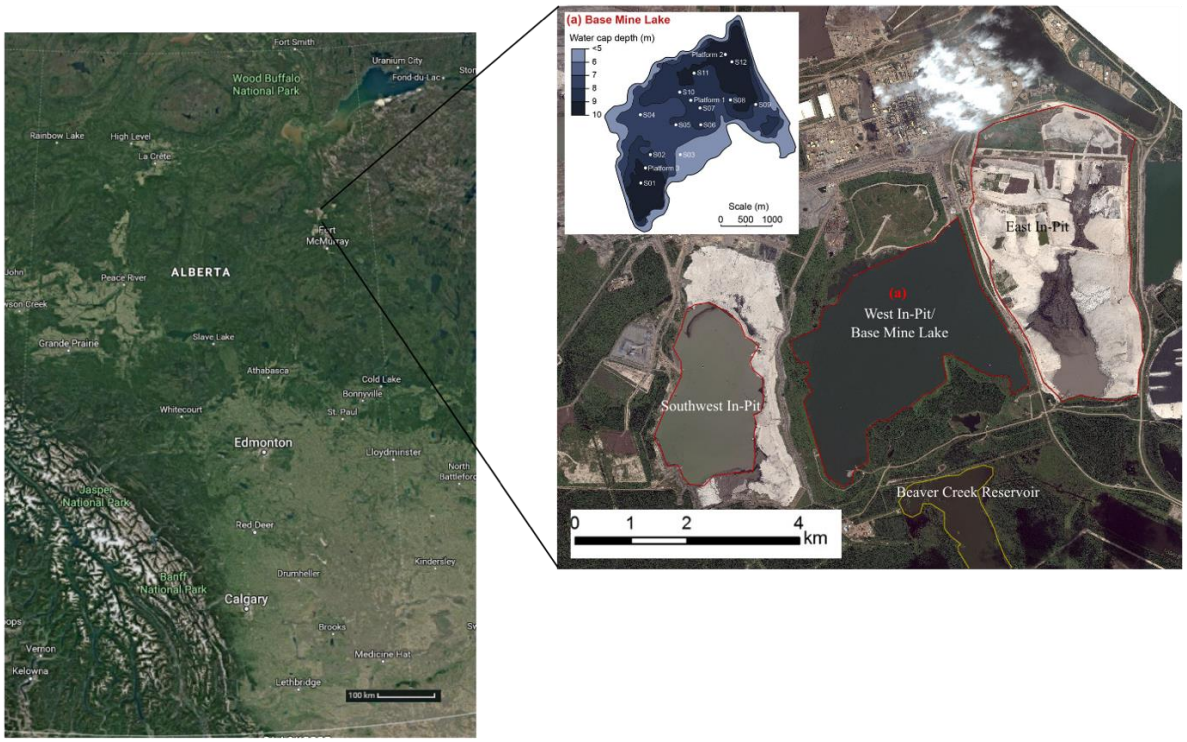

Figure 1.2 Fort McMurray in northern Alberta and satellite image of Base Mine Lake at Syncrude Ltd. with the tailings impoundments outlined in red and Beaver Creek Reservoir outlined in yellow; inset (a) shows a detailed image of the Base Mine Lake monitoring stations and water cap depth (Dompierre and Barbour, 2016)

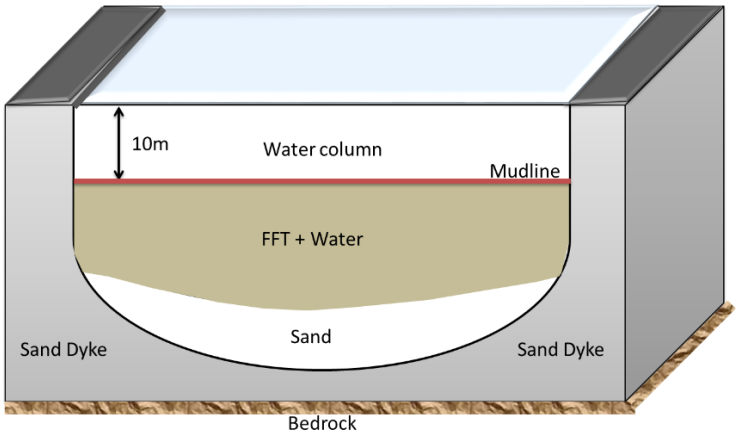

Figure 1.3 Schematic of BML; ~ 10 m of a mixture of freshwater/OSPW overlies FFT. Mudline is the interface between solids and overlying expressed pore water

1.2 Pit Lake water cap oxygen controls

1.2.1 Mine Pit Lakes

Water capped tailings technology (WCTT) has been widely used in the metal mining industries for almost a century (Castro and Moore, 2000). Similar to WCTT in the oil sands, abandoned mine pits are filled with overburden rocks and tailings from the mining operations and are then capped with fresh water to act as a natural lake (Castro and Moore, 2000). Despite the similarities in the practices, the distinct nature of the tailings in metal mining create problems that are specific to the industry. For example, metal release and metal contamination has been associated with coal and metal mining pit lakes (Miguel-Chinchilla et al., 2014; Levy et al., 1997). The success of pit lakes and WCTT has driven the oil sands industries to investigate this solution for the application to reclamation of oil sands tailings.

BML is the first oil sands pit lake with no analogous system however, pit lakes in the coal and metal base mining could provide some insights into the projected water quality progress based on the cumulative impact of biological, chemical and physical aspects. The literature is vast for pit lakes in the mining sector with many studies focusing on using predictive geochemical models to predict the fate of various constituents (Table 1.2) (see Castendyk et al. 2015 for a full list of studies). A few studies (Stevens and Lawrence, 1997; von Rohden et al., 2009, 2007; von Rohden and Ilmberger, 2001) have demonstrated that physical mixing is important to assess the vertical exchange processes into the water cap of coal/metal tailings pit lakes. A limited number

of studies have demonstrated the importance of how these two processes could influence O_2 distribution and concentrations in natural lakes, where turbulent mixing will transfer oxygen across thermally stratified regions, resulting in locally enhanced *in situ* oxygen consumption at deeper depths (Crowe et al., 2008; Katsev et al., 2010; Kreling et al., 2017; Stauffer, 1987). It is therefore of significant relevance to include both the biogeochemical and physical mixing processes to explain observed oxygen concentrations within the water cap of pit lakes.

Table 1.1 Comparison of number studies assessing physical mixing or geochemistry processes in pit lakes and natural systems. Sources: INAP Pit lakes database http://pitlakesdatabase.org; Castendyk and Eary, 2009; Gammons et al. 2009.

Environment	Category	Reference
Mining Pit Lakes	Combined physical limnology & geochemistry	Saskatchewan, Canada Tones (1982)
		Nevada, USA Atkins et al. (1997)
		Saskatchewan, Canada Doyle and Runnells (1997)
		British Columbia, Canada Stevens and Lawrence (1998)
		British Columbia, Canada Hamblin et al. (1999)
		Nevada, USA Atkin and Schrand (2000)
		British Columbia, Canada Fisher and Lawrence (2000)
		Montana, USA Jonas (2000)
		NW Territory, Australia Boland and Padovan (2002)
		Nevada, USA Jewell and Castendyk (2002)
		Central Germany Boehrer et al. (2003)
		Lusatian, Germany Karakas et al. (2003)
		Nevada, USA Parshley and Bowell (2003)
		Quebec, Canada Tassé (2003)
		British Columbia, Canada Stevens and Fisher (2005)

	Montana, USA Davis and Ashenberg (1989)
	Nevada, USA Price et al. (1995)
	USA Miller et al. (1996)
	USA Davis and Eary (1997)
	Germany Klapper and Schultze (1997)
	Montana, USA Robins et al. (1997)
	Nevada, USA Shevenell et al. (1999)
	California, USA Savage et al. (2000, 2009)
	Nevada, USA Shevenell (2000)
	Nevada, USA Shevenell and Connors (2000)
	Global Bowell (2002)
	Montana, USA Madison et al. (2003)
	Nevada, USA Bowell and Parshley (2005)
	Montana, USA Pellicori et al. (2005)
	Germany Schultze et al. (2010)
	California, USA Levy et al. (1997)
	Utah, USA Castendyk and Jewell (2002)
	Northern Sweden Ramstedt et al. (2003)
	Vermont, USA Seal et al. (2006)
	Montana, USA Gammons and Duaime (2006)
	Spain Sánchez España et al. (2008
Predictive geochemistry modelling	Nevada, USA Connors et al. (2000)
	Morin and Hutt (2006)
	New Zealand Castendyk et al. (2005)
	Eary (1998)
	Flite and Eidson (2003)
	Havis and Worthington (1997)
	Marinelli and Niccoli (2000)
	Nevada, USA Shevenell and Pasternak (2000)
	Germany Werner et al. (2001)

		Kuma et al. (2002)
		Nevada, USA Lyons et al. (1994)
		Central Germany Böhrer et al. (1998)
		Stevens et al. (2002)
		Nevada, USA Balistrieri et al. (2006)
		New Zealand Castendyk and Webster-Brown (2007a)
		Bird et al. (1994)
		Pillard et al. (1996)
		Nevada, USA Kempton et al. (1997)
		Davis and Fennemore (1998)
		Lewis (1999)
		Nevada, USA Tempel et al. (2000)
		New Zealand Castendyk and Webster-Brown (2007b)
		WA Australia Oldham et al. (2009)
		California Savage et al. (2009)
		Germany Werner (2009)
	Physical mixing	Stevens and Lawrence, 1997
		von Rohden et al., 2009, 2007
		von Rohden and Ilmberger, 2001
Natural Lakes	Combined physical mixing and geochemistry for O_2 transport	Crowe et al., 2008
		Katsev et al., 2010
		Kreling et al., 2017
		Stauffer, 1987

1.2.2 Oil Sands Tailings Pond and Pit Lake Water Quality

The oil sands industry has identified several factors that must be considered in the design of a viable and biologically productive pit lake ecosystem (Golder, 2001; Nix, 1988). These factors include the optimum depth for cap water, lake shape, littoral zone extent, and shoreline construction. Possible nutrient limitations, biological characteristics of the tailings and the influences of groundwater have also been investigated (CEMA, 2012; Golder, 1995). Habitat availability, oxygen concentrations, nutrient concentrations, salinity, mixing profiles and temperatures in pit lakes will limit the plant and animal species that can live in them. The design and construction of a pit lake will have to include different types of habitat features, such as deep water and shallow water environments. Most pit lakes are expected to have relatively low nutrient concentrations, which will limit biological productivity (EMA, 1993). Other concerns include physical (e.g., morphometry, volume, residence time, shoreline erosion, pore water release from tailings), chemical (e.g., water and tailing toxicity, bioremediation), and biological (e.g., extent and stability of littoral zone, biodiversity, productivity) issues that have to be considered when planning and designing a pit lake. For a more comprehensive breakdown of all these aspects and pit lake design, the reader is directed to previous technical reports (CEMA, 2012; Westcott and Watson, 2005).

Research on test environments in the oil sands region indicates that careful design is needed for aquatic life to become established and self-sustainable in pit lakes (CEMA, 2012). Natural lakes in the Athabasca oil sands region are often high in nutrients, which can support large plankton and algal populations (Golder, 1995). Ideally, the pit lake

would meet both sediment quality guidelines and water quality guidelines established by Alberta (AENV, 1999) and the Canadian Council of Ministers of the Environment (CCME, 2018). Any acute and/or chronic toxicity within the pit lake environment would prevent or slow the establishment of both plant and animal life. Therefore, the oil sands industry will attempt to minimize the toxicity of the tailings and process-affected waters within the pit lakes.

1.2.3 Oxygen Importance

Oxygen is often considered one of the most fundamental water-quality parameters of lakes because dissolved oxygen is essential to the metabolism of all aquatic organisms that have aerobic respiratory biochemistry (Wetzel, 2001).. The Canadian guideline for the minimum oxygen concentration required to protect aquatic life is between 5.5 and 6 mg/L (CCME, 1999). Low or insufficient oxygen levels in any lake would hamper the ability of aquatic organisms to develop sustainable communities. Depending on the depth and turbidity of the pit lake, the surface layer will likely have insufficient light for photosynthetic organisms to grow and increase the dissolved oxygen throughout the water cap.

Oxygen concentrations also depend on whether the lake is thermally/chemically stratified. In highly productive lakes, the decomposition of large amounts of organic material can consume oxygen and may result in a decline in oxygen concentrations during the summer and fall. Without mixing with the metalimnion, the hypolimnion can eventually become anoxic. Oil Sands tailing ponds have been shown to have high levels

of oxygen consumption (Westcott and Watson, 2005). Recent microcosm experiments using FFT showed that both microbially and chemically mediated processes play a key role in the oxygen equilibrium at the FFT–water interface (Chen et al., 2013). It is expected that legacy constituents from the extraction processes as well as pore water released chemicals will have an important impact on the BML water cap, especially the dissolved oxygen concentration (Westcott and Watson, 2005). FFT contains a number of particulate (e.g. sulfur pools, acid volatile sulfide, and acid extractable sulfate; iron oxide minerals, particulate organic nitrogen; and particulate organic carbon), gaseous (e.g. volatile organic compounds, hydrogen sulfide H_2S, methane CH_4,) and dissolved reduced compounds such as aqueous ammonia (NH_4^+), HS^-, Fe^{2+}, NO_2-, CH_4 (Allen, 2008; Quagraine et al., 2005; Siddique et al., 2014a; Small et al., 2015; Westcott and Watson, 2005). These reduced species can migrate into the oxygenated layer where their oxidation can deplete oxygen from the deep waters and potentially throughout the water column. These constituents can be mobilized into the overlying water by a variety of physical processes, such as FFT densification, ebullition, mixing, and diffusion.

1.2.4 The Role of Mixing Processes

Oxygen exchange with the atmosphere is a critical physical process in aquatic systems that allow aquatic organisms to form a livable ecosystem. With the exception of molecular diffusion, mixing and transport mechanisms are controlled by external forces such as the wind, surface heat flux, and turbidity currents (Lerman et al., 1995). Some of the principal water mixing mechanisms occurring in lakes are shown in Figure 1.4.

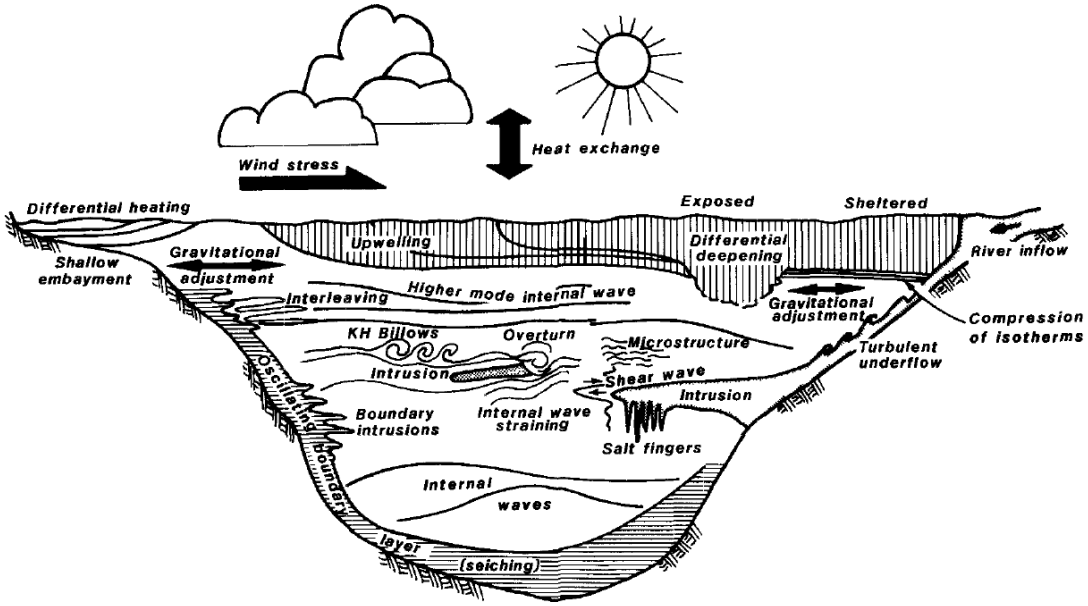

Figure 1.4. A schematic of the major water transport and mixing mechanisms that can occur in lakes (from Lerman et al., 1995)

As an open system, the surface water of aquatic environments is often saturated with respect to oxygen, which can be transferred downwards throughout the water column into the sediments by turbulent motions. Diffusion of atmospheric oxygen is a slow process, therefore, away from boundaries, turbulent mixing becomes the dominant transport mechanism in the lake and marine settings (Chapra, 2008; Lerman et al., 1995). Nevertheless, some physical factors can restrict this mixing process. For instance, stratification can limit turbulence and consequently limit mixing above the thermocline or chemocline; this prevents vertical oxygen flux, minimizing oxygen supply to deeper water layers (Wetzel, 2001). Furthermore, mixing is important in the resuspension of sediment, or FFT in the case of BML, which can mobilize reduced compounds into the water column where they may negatively impact oxygen concentrations.

In regard to tailing ponds, there are estimations that ponds with a water depth of 10 m would reduce the probability of tailings resuspension with a fetch-limited wind velocity of 17 m/s (Lawrence et al., 1991). Therefore, oil sands pit lake morphometry should be designed to reduce water column mixing (Westcott, 2007a). Recently, Lawrence and coworkers (Lawrence et al., 2015) proposed several mixing processes that can potentially occur in BML. For instance, wind waves can cause mixing throughout the water column extending to the FFT surface. Ward and colleagues (Ward et al., 1994) noted that winds strong enough to erode the FFT in the Mildred Lake Settling Basing (MLSB), one of the earliest tailing ponds, were infrequent, and for the most part, changes in turbidity were caused by the vertical movement of particles already in the water cap. During calm periods, particles settled to form an intermediate, turbid layer at the base of the water cap analogous to the fluid mud often found in estuaries (McAnally et al., 2007) which is far less dense and far more mobile than the gel-like FFT. This naturally formed material was subsequently resuspended during storms that were not strong enough to erode the underlying FFT.

BML is approximately 10 m depth (as of 2017) and increasing because of the FFT dewatering every year. Given that the oscillating currents beneath surface wind waves decrease exponentially with depth, these currents are far less likely to disturb the FFT in BML than in MLSB. Other potential mixing mechanisms include convection due to salt-water exclusion during ice formation, penetrative convection due to surface cooling, gas emission from the FFT, and internal wave activity. Advection was considered to be the governing mass transport process during the initial periods of the oil sands pit lake

(Westcott, 2007b). Consequently, the release of dissolved constituents, caused by advective transport, across the FFT–water interface could delay expected water quality improvements. Advective processes will decline over time as FFT settlement and dewatering rates decrease (Jeeravipoolvarn et al., 2009). Nevertheless, there is the potential for mixing of the BML water cover to occur such that surface inputs of atmospheric oxygen may be mixed into the underlying water column to some depth, while reduced constituents and FFT particles may be mixed in the overlying water column (Figure 1.4). The redox biogeochemistry of the water cover is thus likely to be highly dynamic and if periodic mixing events occur, such that FFT and aqueous and gaseous reduced constituents are mobilized into the oxic portion of the water column, the potential of episodic, substantive oxygen consumption events exists.

1.2.5 Redox Biogeochemistry

Geochemical gradients can change significantly during the consolidation process and are affected by the constituents brought up from the FFT in addition to the complex microbial consortia found in each tailing pond (Fedorak et al., 2002; Fru et al., 2013; Penner and Foght, 2010). Further, biogeochemical activity, by producing dissolved and gaseous constituents, within the FFT will have a direct impact on the quality of the cap water. Furthermore, exhaustion of dissolved oxygen, associated with major biogeochemical cycles can directly or indirectly regulate the progress of a self-sustaining ecosystem through impacts on oxygen concentrations (Figure 1.5).

Aerobic

- Respiration: $CH_2O + O_2 \rightarrow CO_2 + H_2O$
- Nitrification: $NH_4^+ + 2O_2 \rightarrow NO_3^- + 2H^+ + H_2O$
- Iron oxidation: $Fe^{2+} + 0.5O_2 + H^+ \rightarrow Fe^{3+} + 3H_2O$
- Sulfide oxidation: $HS^- + 2O_2 \rightarrow SO_4^{2-} + H^+$
- Methane oxidation: $CH_4 + 2O_2 \rightarrow CO_2 + 2H_2O$

Anaerobic

- Denitrification: $2CH_2O + NO_3^- + 2H^+ \rightarrow 2CO_2 + NH_4^+ + H_2O$
- Fe Reduction: $CH_2O + 4FeOOH + 8H^+ \rightarrow CO_2 + 4Fe^{2+} + 7H_2O$
- Sulfate reduction: $2CH_2O + SO_4^{2-} + 2H^+ \rightarrow 2CO_2 + H_2S + 2H_2O$
- Methanogenesis: $CO_2 + 4H_2 \rightarrow CH_4 + 2H_2O$

Figure 1.5. Potential aerobic and anaerobic processes that can affect oxygen concentrations within a PL either directly or indirectly through the production of reductants (i.e. anaerobic reactions).

Methane

Methanogenesis plays a major role as a hydrocarbon degradation mechanism within FFT deposits (Fedorak et al., 2003; Siddique et al., 2011, 2007, 2006; Stasik et al., 2014; Stasik and Wendt-Potthoff, 2014). Anaerobic degradation of hydrocarbons in tailing ponds, comprising n-alkanes and BTEX (benzene, toluene, ethylbenzene, xylenes), under methanogenic conditions produces CH_4 and CO_2 (Siddique et al., 2011, 2007, 2006) Methane has been produced during the tailing containment, which remains in gaseous form. Confined and dissolved gases estimations; predominantly methane, comprised between 2% to and 5% (v/v) of MLSB (Holowenko et al., 2000). Thus, it is expected that this legacy methane present in the FFT will diffuse throughout the water column, where it will get oxidized in the presence of aerobic heterotrophs (i.e.,

methanotrophs). BML will likely have a substantial concentration of methane within the FFT layer that will dominate oxygen consumption at least in the early evolution of BML, if not over longer timescales. However, methanogenesis was not observed, or minimal, to be occurring in the water cap during initial stages of tailing pond construction on both MSLSB and BML (Foght et al., 1985; Stasik et al., 2014). For example, methane emissions in old tailing ponds (e.g., MLSB) were reported almost eight times higher (3278 Kg CH_4 m^{-2} y^{-1}) in comparison with a young tailing pond, West In-Pit (later known as BML) (301 Kg CH_4 m^{-2} y^{-1}) (Small et al., 2015). It was suggested that these processes were likely suppressed by the activity of sulfate-reducing bacteria (SRB), which outcompete methanogenesis until sulfate is depleted (Fedorak et al., 2002). However, the coexistence of SRB and methanogens populations was found in microcosm using FFT, where high sulfate ion concentration were present, suggesting that either there is an abundance of acetate ion and H_2 present to support both populations or that the two populations are consuming different substrates and are not in direct competition (Holowenko et al., 2000). Moreover, some of the highest rates of both sulfate ion reduction and methanogenesis were reported at the same depth in the FFT of BML, indicating that there may not be inhibition of methanogenesis in situ by competition with SRB (Stasik et al., 2014). Tailings ponds can release approximately 40 million litres of methane gas per day (Holowenko et al., 2000; Penner and Foght, 2010). Tailings started to produce methane gas after nearly 15 years of storage in the ponds when it became anaerobic in nature (Penner and Foght, 2010; Yeh et al., 2010).

Recent studies found that microbial methane production processes in the tailing ponds increased the densification rate of FFT particles (Bordenave et al., 2010; Holowenko et al., 2000; Siddique et al., 2014b). Biogenic end products (CH_4, CO_2, and organic acids) changed the chemistry of both pore water and solid phases in several interrelated ways. Consequently, an improvement in the consolidation of fine tailings was observed as long there is methanogenic activity present. Methanogenic conditions increased dissolved CO_2 to promotes carbonate-mineral dissolution and releases divalent cations (i.e., Ca^{2+}, Mg^{2+}) to FFT pore water, enhancing FFT dewatering and settlement by reducing the electrical double layer thickness and facilitate facilitating closer packing of FFT solids (Siddique et al., 2014b). It is unknown which are the mechanisms responsible for the consolidation of tailings (Bordenave et al., 2010; Fedorak et al., 2003; Ramos-Padron et al., 2011). Biodensification and FFT dewatering has been observed in BML at a rate of 0.85 m per year (Lawrence et al., 2015).

Sulfate

Early attempts to consolidate fine tailings caused an increase in sulfate ion and a substrate for sulfidic bacteria to thrive. During the mid-1990s, oil companies decided to address the slow settling of fine particles through the use of gypsum in their tailings ponds (List and Lord, 1997). The addition of gypsum produces a fast release of water from the FFT, thus accelerating their densification and reducing their volumes. This, in turn, increases the concentration of sulfate ion in the water column from the FFT. Sulfate ion concentrations, in tailing ponds, can range from 4.7 mM at the surface to less than 0.5 mM below the mudline (the hypothetical interface separating the water from the FFT at

5% FFT) reflecting sulfate ion reduction by indigenous sulfate-reducing bacteria (SRB) and conversion to hydrogen sulfide (Holowenko et al., 2000; Stasik et al., 2014). However, hydrogen sulfide ion concentration was detected low or below detection limits in the water column for all tailing ponds (Small et al., 2015). The lack of hydrogen sulfide ion emissions was attributed to sulfur cycling and specifically sulfide oxidation which decreased oxygen concentrations within the tailings ponds (Ramos-Padron et al., 2011).

Sulfate ion reduction rates were also observed to range from 0 to 10 nmol mL^{-1} d^{-1} in the water cap and less than 10 mmol mL^{-1} d^{-1} below the FFT–water interface in oil sands tailing ponds (Chen et al., 2013; Stasik et al., 2014). Furthermore, Salloum and colleagues (2002) found that nitrate was rapidly depleted, 88% of sulfate ion was reduced and no methane was produced in experimental FFT amended microcosms indicating SRB activity will likely be important at some point in the pit lake evolution for generating hydrogen sulfide ion, which can be both abiotically and biotically oxidized. The importance of sulfide ion (or any other sulfur-oxidative intermediate) as the main oxygen-consumer will depend on the sulfate ion reduction rates, the presence of more energetically favoured electron acceptors and the potential to form metal sulfides.

Iron

Iron (Fe) redox reactions may also be important to consider in the oil sands pit lake, as the generation of ferrous ion by microbial iron reduction will impact oxygen concentrations, however the generation of ferrous iron may provide a mechanism to strip ΣH_2S from the water column through iron sulfide formation. Although low levels of

dissolved iron have been detected in tailing ponds, it is argued that ferric ion occurs as particulate crystalline iron oxides and (oxy) hydroxide coatings associated with clay minerals (Kaminsky et al., 2008). Mineralogy analysis in microcosms with FFT (Chen et al., 2013) identified quartz, accessory Fe (II) sulfides, and amorphous Fe (III) oxides.

Depletion of sulfate via sulfate reduction and subsequent formation of iron sulfides was observed in tailing ponds (Stasik et al., 2014) and laboratory studies (Boudens et al., 2016; Chen et al., 2013; Fru et al., 2013; Siddique et al., 2014b) suggesting that sulfide-mineral precipitation may serve as an additional control on Fe concentrations in the FFT pore water. A black sulfidic zone below the mudline was reported by several studies at all the tailing ponds, suggesting the presence of precipitated metal sulfides (Fru et al., 2013; Holowenko et al., 2000; MacKinnon, 1989; Penner and Foght, 2010). The rate of iron reduction increased below the mudline in tailing ponds, with a significant number of iron-reducing bacteria (IRB), suggesting that IRB is accessing ferric ion from the FFT. In addition, acid-volatile sulfide was found to be the dominant hydrogen sulfide fraction in the FFT, indicating that Fe^{2+} was present to remove the H_2S from solution (Salloum et al., 2002; Stasik et al., 2014). Thus, the concentration of available ferrous ion to react with hydrogen sulfide will be an important factor in determining the concentration of ΣH_2S that ultimately mobilize into the water cap, where it can undergo chemical and/or microbial oxidation.

Nitrogen

Nitrification is the microbially mediated oxidation of ammonium to nitrite and the further oxidation of nitrite to nitrate; and, a major pathway in the overall nitrogen cycle of

freshwater systems (Curtis et al., 1975; Harris, 2012; Sprent, 1987; Wetzel, 1983). Overall, the nitrification process has been reported to be influenced by a number of several physical and ambient conditions, including: temperature, pH, salinity, dissolved oxygen, NH_4^+/NH_3 concentration, light, and the presence of synthetic organic chemicals and heavy metals (Berounsky and Nixon, 1990; Grady Jr et al., 2011; Sharma and Ahlert, 1977). Ammonia exists in aqueous solution in two forms: NH_3 (unionized ammonia) and NH_4^+ (ionized ammonia or ammonium). Both forms of aqueous ammonia can be toxic to fish, but NH_3 is the more toxic form at low concentrations (Meade, 1985).

In a pit lake, nitrification could play an important role in the observed oxygen-consumption rate (OCR), perhaps not in early-stage evolution, when hypothesized methane oxidation will dominate, but over time it could become an important process if ideal conditions for nitrification are established within the pit lake water cap. For instance, in hypoxic waters of the Black Sea, nitrification significantly consumed oxygen associated with bacterial ammonia oxidation to nitrite and ultimately to nitrate (Yakushev and Newton, 2012). Studies on oil sands tailing ponds have reported ammonia concentrations ranging from 220 to 775 μM in the water column (Penner and Foght, 2010; Stasik et al., 2014). Likewise, observed concentrations of nitrate and nitrite in MLSB were low or below the detection limit. Interestingly, studies have shown a significant amount of denitrifying bacteria ranging from 10^4 to 10^9 most probable number (MPN/g) in the FFT layer of MLSB (Fedorak et al., 2002), identifying that the FFT within tailing ponds is likely to produce ammonia. Studies have shown that competition between NH_4^+ and CH_4-oxidizing bacteria for oxygen can inhibit methane oxidation by

nitrification (Bedard and Knowles, 1989; Roy and Knowles, 1994). However, when there is a high level of CH_4 and low oxygen concentration, methane-oxidizing bacteria outcompete NH_4^+-oxidizing bacteria because of their higher affinity for oxygen (Roy and Knowles, 1994; Van Luijn et al., 1999), suggesting that nitrifying microorganisms are not likely to be an important oxygen-consuming metabolism until methane levels decrease.

1.2.6 Microbial Activity Occurring in Tailing Ponds

Microbial activity is key to redox biogeochemical cycling. The microbial type, abundances, and occurrences of microorganisms in addition to available redox reactive substrates within aquatic systems are key aspects that will shape *in situ* biogeochemical processes. Microorganisms are naturally found throughout the entire process of oil production, starting from the formation of oil sands deposits to the tailing ponds and FFT. Bacterial and archaeal population studies have shown distinct communities between the tailing ponds and the Athabasca River (Yergeau et al., 2012). These results suggest microbial communities have developed unique and specialized characteristics that may originate from the river, oil sands bitumen or the extraction process itself. Once the tailing pond is established, microorganisms adapt to their environment (gene expression) by creating syntrophic relationships between each other (for instance, gene transfer). These microbial consortia will dominate the pond, generating a microbial community exclusively adapted to this environment.

The earliest microbial study (Foght et al., 1985) surveyed the microbial community in the FFT of MLSB. Both aerobic and anaerobic microorganisms were

identified, including SRB and methanogens. Methane production was measured in the FFT but in a concentration below detection limits. Tailing ponds create a highly anaerobic environment preventing light and oxygen from entering the ponds. The accumulation of large quantities of hydrocarbons, in tailing ponds, and reduced chemicals such as hydrogen sulfide, can create reducing conditions favourable for methanogenesis (Quagraine et al., 2005; Saidi-Mehrabad et al., 2013). By the early 1990s, methane production increased in MLSB and consequently, methanogens were detected in larger numbers. SRB can inhibit methanogens unless low sulfate concentrations allow methanogenesis. During the mid-1990s, oil companies added gypsum to FFT, which in turn could inhibit methanogenesis in tailing ponds (Holowenko et al., 2000).

The oil sands pit lake is expected to shift, from OSPW at some point, toward becoming a freshwater system. During a long-term study of an active tailing pond, the same microbial species were observed at every sampling time, although their relative abundance changed with time, depending on the availability of electron acceptors and fresh tailings input (Ramos Padron, 2013). The microbial activity in an active tailing pond decreased with the reduction of fresh tailings input. An active tailing pond converted to an inactive state after it stopped receiving fresh tailings input. A shift in the major microbial community structure and functions were observed when an active tailing pond became inactive. Methanogens no longer dominated the inactive pond and a few hydrocarbon degraders became prevalent. *Pseudomonas* and *Acidovorax* species were mainly identified in the inactive tailings pond. Unlike an active storage pond, microbial activity was concentrated only near the surface water of the inactive pond (Ramos-Padron

et al., 2011; Ramos Padron, 2013). The success of pit lakes in the AOSR will rely on the water quality improvement which will be directly influenced by the microbial activity and oxygen-consuming constituents (OCC) mobilized from the FFT.

1.3 Base Mine Lake

BML is the pilot model pit lake created in the AOSR that is under inspection to assess the reliability of this reclamation method for oil sands FFT. BML contains FFT, which has high organic and inorganic content, and high microbial activity. The main concern is the development of an oxygenated layer capable of sustaining higher life forms. To date, BML has shown stratification during the summer and a progressive evolution in five years toward mimicking a freshwater system (Risacher et al., 2018).

Deposition of FFT began in 1994 when BML, then referred to as West In-Pit, was used as a tailings storage facility. This deposition ceased in 2012 prior to the establishment of BML as an oil sands pit lake. FFT deposited in the BML was approximately 186 million m^3, over a series of discharges between 1994 and 2012. By late 2012, BML was comprised of 48m FFT deposit layer, which was capped under a 52 million m^3 water cover. BML has a surface area of 6.5 km^2 and an initial average water cap depth of 6.5m. BML was established on December 31, 2012 (Dompierre et al., 2016).

Freshwater has been pumped in from the adjacent Beaver Creek Reservoir (Figure 1.3) to maintain a water surface level. Estimation of freshwater addition ranges from 5 to 10 million m^3 to BML yearly (Dompierre et al., 2016). Water discharge from BML is presently prohibited. It is expected the freshwater input from Beaver Creek Reservoir, to

maintain the water level, to decline over the following years as additional landforms provide alternative natural water input. Water gain caused by annual precipitation, water runoff, and snowfall comparable to evaporation (≈3 Mm^3).

The initial physicochemical analysis was performed in 2013 (Dompierre et al., 2016). The water cap showed the highest temperature (19 ± 1.0°C) and the temperature decreased near the FFT layer (13 ± 1.2°C) during the summer. Nevertheless, the FFT has shown the potential for heat transfer into the water cap (Lawrence et al., 2015). In addition, during this season a variation throughout the FFT–water interface (FWI) ranging from 3 to 8 °C was observed, which suggests the presence of vertical thermal mixing in this zone. BML presented an oligotrophic thermal profile during the summer season (i.e., July through September 2013). The water column was alkaline in nature with a mean water surface pH value of 8.26. Moreover, BML is expected to exhibit winter stratification (December through March) when average open-air temperatures in Fort McMurray are −13 ± 4.5°C (Canada, 2015).

A recent study of BML water geochemical parameters analyzed trends observed during the summer seasons in 2015 and 2016 (Risacher et al., 2018). In BML, mobilization of important OCC's was observed, in both years, with intense redox cycling and oxidation occurring right at the FWI, where oxygen concentrations were the lowest. Redox potentials generally described anoxic conditions at this interface, with average values ranging from –250 to –100 mV in BML. This indicates an active biogeochemical redox zone where the oxic–anoxic interface occurred. In comparison with active tailing ponds, ΣH_2S concentrations in BML were lower (≈80 μM vs ≈1 μM, respectively) (Chen

et al., 2013; Salloum et al., 2002; Stasik et al., 2014), because most oil sands tailing ponds water caps are characterized by an anoxic water column. This has allowed ΣH_2S to persist until it reached the oxic–anoxic boundary near the surface where it rapidly interacts with oxygen. In contrast, the BML water cap showed oxic to suboxic (5–15 μM) conditions in both years, resulting in near depletion of ΣH_2S in the proximity of the FWI. Sulfate concentration in the water column was high in comparison with other aquatic systems and decreases as it reaches the FWI. Sulfate concentration ranges between 1600 and 2300 μM throughout the water cap. Previous studies, using FFT microcosms, predicted concentrations 10 to 100 times higher than those observed in BML (Chen et al., 2013; Fru et al., 2013). Depletion of sulfate via sulfate reduction and formation of iron sulfides was observed in tailing ponds (Stasik et al., 2014) and laboratory studies (Boudens et al., 2016; Chen et al., 2013; Fru et al., 2013; Siddique et al., 2014b) suggesting that sulfide-mineral precipitation may serve as an additional control of Fe concentrations in FFT pore water. A narrow zone immediately below the FWI was identified, which was characterized by a sharp decrease in pore-water sulfate concentrations and a small increase in dissolved Fe (Dompierre et al., 2016). This was argued to be caused by microbial Fe and sulfate reduction, mechanisms observed in tailing ponds (Chen et al., 2013; Ramos-Padron et al., 2011; Siddique et al., 2012; Stasik et al., 2014; Stasik and Wendt-Potthoff, 2014).

1.3.1 2015-2016 Physicochemical and Geochemical Trends

Physicochemical and geochemical analysis indicated that the FFT layer in the overlying water cap has a great influence on its development toward a freshwater system

(Risacher et al., 2018). FFT is an important source of OCC mobilizing up into the water cap where they affect extant oxygen concentrations. Moreover, the cessation of FFT inputs and the development of a thick water cap, by dewatering and settling of the FFT, allowed summer thermal stratification and oxygen zonation, with epilimnetic oxygen saturations reaching 70% (2015) and 85% (2016), while hypolimnetic oxygen saturation decreased to < 5% in 2015 and 2016. These consistent epilimnetic increases in dissolved oxygen concentration can support several warm water fish species and macrofauna. In addition, an increase in photosynthetic activity was observed in 2016 (Risacher et al., 2018) which would also increase oxygen levels in the water cap.

Furthermore, CH_4 and NH_4^+ concentrations were measured throughout the water column where there was observed rapid loss of CH_4 in the metalimnion–hypolimnion interface (≈15μM O_2) while NH_4^+ accumulated in the water cap over the summer of 2015. During this period, CH_4 concentrations alone best explain the consumption of oxygen within the BML water cap, however, both NH_4^+ and CH_4 were important in explaining water cap decreases in oxygen concentration in 2016. Methane oxidation played a more dominant role in oxygen consumption than nitrification, as the decrease in the mean 2015 CH_4 concentration from the hypolimnetic maxima to epilimnetic minima were greater than those observed for NH_4^+ concentrations. In addition, isotopic trends in hypolimnion samples indicate dissolved CH_4 origins from microbial methanogenic activity occurring in the FFT layer below the water cap (Goad et al., 2016). In addition, a slight enrichment trend was observed with decreasing dissolved CH_4 concentration in the hypolimnion, suggesting methanotrophy has a consistent role in the oxygen consumption

of oxygen in the deep waters of BML. However, the on going development of BML is unclear, as to whether nitrification will persist and whether the water cap will remain oxic to the FFT water interface (Figure 1.6).

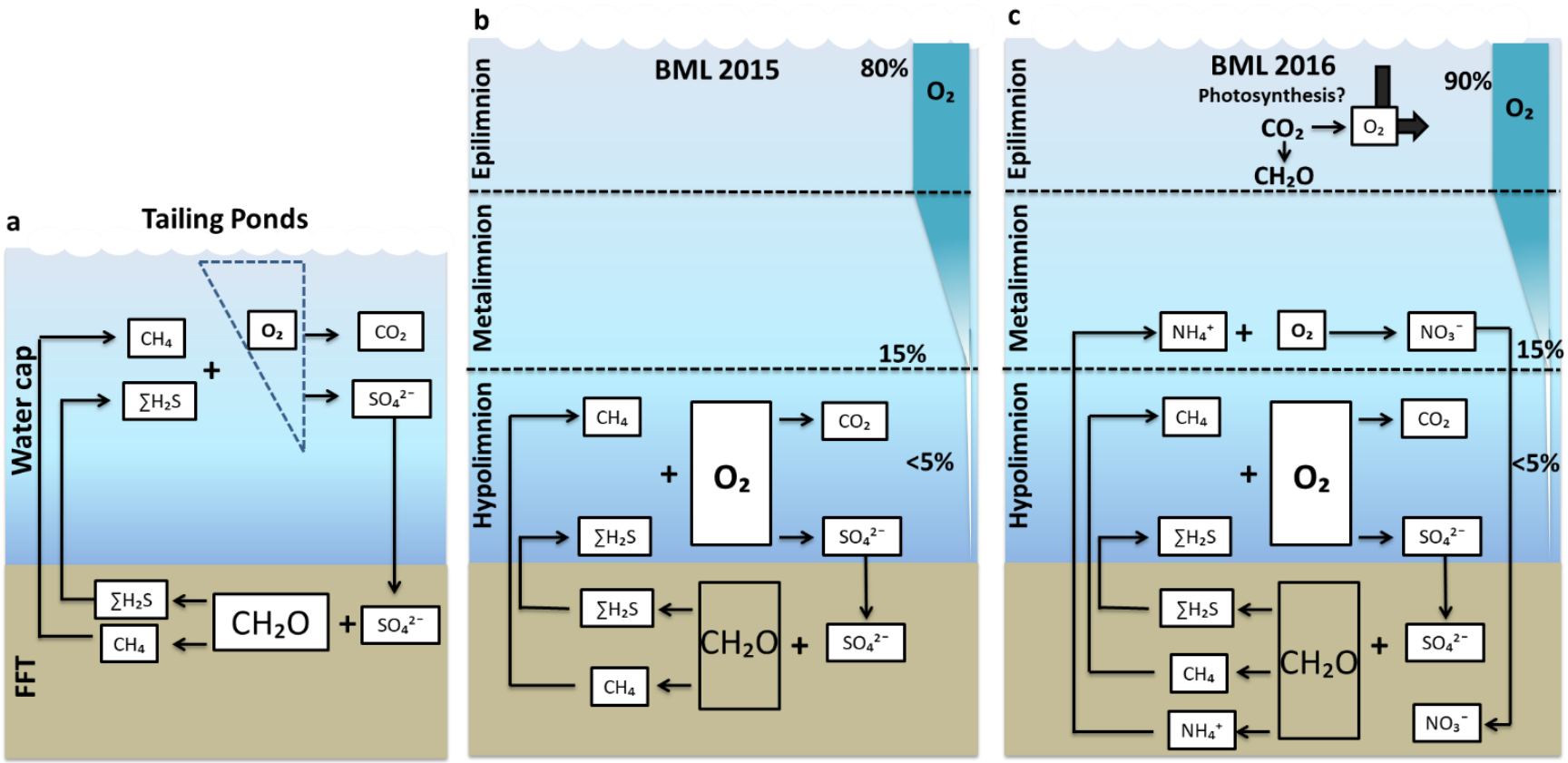

Figure 1.6 Comparison of the physicochemistry and oxygen–consumption dynamics between tailing ponds (a) and BML for the summers of 2015 (b) and 2016 (c). Modified after Risacher et al., 2018

The late occurrence of nitrification, three years after BML was decommissioned, has been attributed to a delay in the establishment of nitrifying archaeal and/or bacterial microorganisms in BML (Risacher et al., 2018). Previously, microbial nitrification was argued to be delayed because of the inhibition caused by naphthenic acids, which was suggested to explain why this metabolism has not been observed to play a significant role in oil sands tailing pond biogeochemical cycling (Misiti et al., 2013). In early oil sands PL development, nitrifying microorganisms could take some time to establish and/or heterotrophic microorganisms (e.g., methanotrophs) may outcompete nitrifying microorganisms for highly limited oxygen in the vicinity of the FWI, where heterotrophs may tolerate lower oxygen concentrations better. CH_4 and ΣH_2S constituents have been recognized as the key OCC impacting oxygen concentrations within tailing ponds (Chen et al., 2013; Reid et al., 2016; Saidi-Mehrabad et al., 2013). Nonetheless, results from the water–cap geochemistry and correlation to oxygen decrease indicate that after interruption of FFT deposition and a development of a deeper water cap, which allowed stratification, nitrifying microorganisms were able to establish within the water cap and thus NH_4^+ release from the FFT may be an important OCC that needs to be considered in addition to CH_4 and ΣH_2S in future PL. The emergence of microbial nitrification processes as important to oxygen consumption within the BML water cap in 2016 indicates that this process will be an important player in determining PL water column oxygen concentrations over the longer development trajectory.

1.4 Research Objectives and Hypotheses

This research combines a field and experimental approach to characterizing the water cap biogeochemistry of the Oil Sands Base Mine Lake. Thus, the focus of the proposed research is the determination of OCR and the mechanisms involved in oxygen development in BML. The findings of this thesis are expected to highlight the oxygen consumption throughout the water column of BML with important implications for understanding the behaviour of *in situ* (bio) geochemical processes and physical oxygen transport.

Water Cap O_2 controls (addressed in Chapter 3):

Determine depth–dependent OCR using specialized oxygen consumption chambers targeting zones of significant biogeochemical impact, such as the FWI, and identify which OCC are influencing those OCR within the BML water cap.

Specifically, this field-based study aimed to:

1) Establish depth-dependent OCR values for stratified BML water column;
2) Determine the role (if any) of physical processes in the overall net O_2 concentration profile of the water cap of BML; and
3) Determine the key redox biogeochemical processes linked to the oxygen consumption in the water cap.

To address the field research objectives, the following hypotheses were tested:

1) BML water cap will show depth-dependent oxygen consumption rates (OCR)
2) The FWI will have the highest OCR values associated with the proximity of the FFT as the principal source of OCC
3) CH_4 concentrations will be the primary OCC driving observed oxygen consumption in BML water cap
4) The overall net oxygen concentration in the water cap of BML will reflect the interaction of both oxygen mass physical transport and in situ biogeochemical processes consuming oxygen.

Nitrification contribution to O_2 consumption (addressed in Chapter 4):

Examine experimentally the importance of nitrification on the oxygen consumption using hypolimnetic BML water and identify the impact of nitrification on oxygen depletion in BML.

More precisely, this laboratory-based study aimed to:

(1) Determine the potential for nitrification in BML methane-free water and its contribution to OCR,

(2) Assess if nitrification rates are ammonia concentration-dependent, and

(3) Establish the O_2 consumption contributions of laboratory-determined nitrification to field based BML water ammonium oxidation.

To address the experimental objectives, the following hypotheses were tested:

1) BML water amended with ammonia will show nitrification activity associated with oxygen and ammonia consumption and nitrate and nitrite production
2) Nitrification and associated consumption of oxygen rates will be ammonia concentration dependent;
3) The experimentally determined nitrification O_2 consumption will correspond to the expected O_2 consumed by bulk water ammonia concentration of BML water.

1.5 References

(AESRD), A. environment and sustainable resource development, 2014. Reclamation Information System, 2013, Annual Conservation and Reclamation Report Submissions.

AENV, 1999. Regional sustainable development strategy for the Athabasca oil sands area : progress report. Alberta Environment, [Edmonton].

Alberta Government, 2017. Oil Sands Information Portal [WWW Document]. Oil sands Inf. portal. URL http://osip.alberta.ca/map/ (accessed 1.31.18).

Allen, E.W., 2008. Process water treatment in Canada's oil sands industry: I. Target pollutants and treatment objectives. J. Environ. Eng. Sci. 7, 123–138. https://doi.org/10.1139/s07-038

An, D., Brown, D., Chatterjee, I., Dong, X., Ramos-Padron, E., Wilson, S., Bordenave, S., Caffrey, S.M., Gieg, L.M., Sensen, C.W., Voordouw, G., 2013. Microbial community and potential functional gene diversity involved in anaerobic hydrocarbon degradation and methanogenesis in an oil sands tailings pond. Genome 56, 612–618. https://doi.org/10.1139/gen-2013-0083

An, D., Caffrey, S.M., Soh, J., Agrawal, A., Brown, D., Budwill, K., Dong, X., Dunfield,

P.F., Foght, J., Gieg, L.M., Hallam, S.J., Hanson, N.W., He, Z., Jack, T.R., Klassen, J., Konwar, K.M., Kuatsjah, E., Li, C., Larter, S., Leopatra, V., Nesbø, C.L., Oldenburg, T., Pagé, A.P., Ramos-Padron, E., Rochman, F.F., Saidi-Mehrabad, A., Sensen, C.W., Sipahimalani, P., Song, Y.C., Wilson, S., Wolbring, G., Wong, M.L., Voordouw, G., 2013. Metagenomics of hydrocarbon resource environments indicates aerobic taxa and genes to be unexpectedly common. Environ. Sci. Technol. 47, 10708–10717. https://doi.org/10.1021/es4020184

ASTM, 2005. ASTM F838-05, Standard Test Method for Determining Bacterial Retention of Membrane Filters Utilized for Liquid Filtration.

Bedard, C., Knowles, R., 1989. Physiology, biochemistry, and specific inhibitors of CH4, NH4+, and CO oxidation by methanotrophs and nitrifiers. Microbiol Rev 53, 68–84.

Beier, N., Sego, D., 2008. The oil sands tailings research facility. Geotech. news 26, 72–77.

Beier, N., Wilson, W., Dunmola, A., Sego, D., 2013. Impact of flocculation-based dewatering on the shear strength of oil sands fine tailings. Can. Geotech. J. 50, 1001–1007.

Bergerson, J., Keith, D., 2006. Life cycle assessment of oil sands technologies.

Berounsky, V.M., Nixon, S.W., 1990. Temperature and annual cycle of nitrification in waters of Narragansett Bay. Limnol. Oceanogr. 35, 1610–1617.

Bordenave, S., Kostenko, V., Dutkoski, M., Grigoryan, A., Martinuzzi, R.J., Voordouw, G., 2010. Relation between the activity of anaerobic microbial populations in oil sands tailings ponds and the sedimentation of tailings. Chemosphere 81, 663–668.

Boudens, R., Reid, T., VanMensel, D., Prakasan, M.R.S., Ciborowski, J.J.H., Weisener, C.G., 2016. Bio-physicochemical effects of gamma irradiation treatment for naphthenic acids in oil sands fluid fine tailings. Sci Total Env. 539, 114–124. https://doi.org/10.1016/j.scitotenv.2015.08.125

Bowman, F.W., Calhoun, M.P., White, M., 1967. Microbiological methods for quality control of membrane filters. J. Pharm. Sci. 56, 222–225.

BRENNER, F.J., EDMUNDSON, J., WERNER, M., McGRATH, T., 1987. Plankton, chlorophyll characteristics and fishery potential of surface coal mine lakes in western Pennsylvania, in: Proceedings of the Pennsylvania Academy of Science. JSTOR, pp. 147–152.

Canada, E., 2015. Canadian Climate Data [WWW Document]. URL http://climate.weather.gc.ca

CAPP, 2018. Canada's oil sands. Canadian Association of Petroleum Producers (CAPP) [WWW Document]. URL http://www.capp.ca/

Carrera-Hernandez, J.J., Mendoza, C.A., Devito, K.J., Petrone, R.M., Smerdon, B.D., 2012. Reclamation for aspen revegetation in the Athabasca oil sands: Understanding soil water dynamics through unsaturated flow modelling. Can. J. Soil Sci. 92, 103–116.

Castendyk, D.N., Eary, L.E., Balistrieri, L.S., 2015. Modeling and management of pit lake water chemistry 1: Theory. Appl. Geochemistry 57, 267–288.

Castro, J.M., Moore, J.N., 2000. Pit lakes: their characteristics and the potential for their remediation. Environ. Geol. 39, 1254–1260.

CCME, 2018. Water Quality Guidelines for the Protection of Aquatic Life, Freshwater, Marine [WWW Document]. URL http://st-ts.ccme.ca/en/index.html?chems=all&chapters=1&pdf=1

CCME, 1999. Canadian water quality guidelines for the protection of aquatic life:Dissolved oxygen (freshwater).

CEMA, 2012. End pit lakes guidance document 2012. Cumul. Environ. Manag. Assoc. Fort McMurray, Alberta. CEMA Contract.

Chalaturnyk, R.J., Don Scott, J., Özüm, B., 2002. Management of oil sands tailings. Pet.

Sci. Technol. 20, 1025–1046.

Chapra, S.C., 2008. Surface water-quality modeling. Waveland press.

Chen, M., Walshe, G., Fru, E.C., Ciborowski, J.J.H., Weisener, C.G., 2013. Microcosm assessment of the biogeochemical development of sulfur and oxygen in oil sands fluid fine tailings. Appl. geochemistry 37, 1–11. https://doi.org/10.1016/j.apgeochem.2013.06.007

Cheryan, M., 1998. Ultrafiltration and microfiltration handbook. CRC press.

Crowe, S.A., O'Neill, A.H., Katsev, S., Hehanussa, P., Haffner, G.D., Sundby, B., Mucci, A., Fowle, D.A., 2008. The biogeochemistry of tropical lakes: A case study from Lake Matano, Indonesia. Limnol. Oceanogr. 53, 319–331.

Curtis, E.J.C., Durrant, K., Harman, M.M.I., 1975. Nitrification in rivers in the Trent Basin. Water Res. 9, 255–268.

Davis, A., Eary, L.E., 1997. Pit lake water quality in the western United States: An analysis of chemogenetic trends. Min. Eng. 49, 98–102.

Dompierre, K.A., Barbour, S.L., 2016. Thermal properties of oil sands fluid fine tailings: laboratory and in situ testing methods. Can. Geotech. J. 54, 428–440.

Dompierre, K.A., Lindsay, M.B., Cruz-Hernandez, P., Halferdahl, G.M., 2016. Initial geochemical characteristics of fluid fine tailings in an oil sands end pit lake. Sci Total Env. 556, 196–206. https://doi.org/10.1016/j.scitotenv.2016.03.002

Drzewicz, P., Afzal, A., El-Din, M.G., Martin, J.W., 2010. Degradation of a model naphthenic acid, cyclohexanoic acid, by vacuum UV (172 nm) and UV (254 nm)/H2O2. J. Phys. Chem. A 114, 12067–12074.

Eary, L.E., 1999. Geochemical and equilibrium trends in mine pit lakes. Appl. Geochemistry 14, 963–987.

Eckert, W.F., Masliyah, J.H., Gray, M.R., Fedorak, P.M., 1996. Prediction of

sedimentation and consolidation of fine tails. AIChE J. 42, 960–972.

EMA, 1993. Suncor/Syncrude Wet Landscape Simulation Model 1992/93. Prepared for Suncor Inc. Oil Sands Group and Syncrude Canada Ltd. Calgary, Alberta.

Espana, J.S., Pamo, E.L., Pastor, E.S., Ercilla, M.D., 2008. The acidic mine pit lakes of the Iberian Pyrite Belt: An approach to their physical limnology and hydrogeochemistry. Appl. Geochemistry 23, 1260–1287.

Farkish, A., Fall, M., 2013. Rapid dewatering of oil sand mature fine tailings using super absorbent polymer (SAP). Miner. Eng. 50, 38–47.

Fedorak, P.M., Coy, D.L., Dudas, M.J., Simpson, M.J., Renneberg, A.J., MacKinnon, M.D., 2003. Microbially-mediated fugitive gas production from oil sands tailings and increased tailings densification rates. J. Environ. Eng. Sci. 2, 199–211. https://doi.org/10.1139/s03-022

Fedorak, P.M., Coy, D.L., Salloum, M.J., Dudas, M.J., 2002. Methanogenic potential of tailings samples from oil sands extraction plants. Can J Microbiol 48, 21–33. https://doi.org/10.1139/w01-129

Foght, J.M., Fedorak, P.M., Westlake, D.W.S., Boerger, H.J., 1985. Microbial content and metabolic activities in the Syncrude tailings pond. AOSTRA J Res 1, 139–146.

Foght, J.M., Gieg, L.M., Siddique, T., 2017. The microbiology of oil sands tailings: past, present, future. FEMS Microbiol. Ecol. 93.

Frank, R.A., Roy, J.W., Bickerton, G., Rowland, S.J., Headley, J. V, Scarlett, A.G., West, C.E., Peru, K.M., Parrott, J.L., Conly, F.M., 2014. Profiling oil sands mixtures from industrial developments and natural groundwaters for source identification. Environ. Sci. Technol. 48, 2660–2670.

Friese, K., Wendt-Potthoff, K., Zachmann, D.W., Fauville, A., Mayer, B., Veizer, J., 1998. Biogeochemistry of iron and sulfur in sediments of an acidic mining lake in Lusatia, Germany. Water. Air. Soil Pollut. 108, 231–247.

Fru, E.C., Chen, M., Walshe, G., Penner, T., Weisener, C., 2013. Bioreactor studies predict whole microbial population dynamics in oil sands tailings ponds. Appl. Microbiol. Biotechnol. 97, 3215–3224.

Gammons, C.H., Harris, L.N., Castro, J.M., Cott, P.A., Hanna, B.W., 2009. Creating Lakes from Open Pit Mines: Processes and Considerations, Emphasis on Northern Environments.

Geller, W., Klapper, H., Schultze, M., 1998. Natural and anthropogenic sulfuric acidification of lakes, in: Acidic Mining Lakes. Springer, pp. 3–14.

Giesy, J.P., Anderson, J.C., Wiseman, S.B., 2010. Alberta oil sands development. Proc Natl Acad Sci U S A 107, 951–952. https://doi.org/10.1073/pnas.0912880107

GOA, 2015. Lower Athabasca Region – Tailings Management Framework for the Mineable Athabasca Oil Sands.

GOA, 2012. Oil sands information portal. Government of Alberta (GOA) [WWW Document]. URL http://environment.alberta.ca/apps/osip/

GOA, 2009. Environmental management of Alberta's oil sands.

Goad, C., Arriaga, D., Risacher, F., Morris, P., Slater, G., Warren, L.A., 2016. Methane Biogeochemical Cycling over Seasonal and Annual Scales in an Oil Sands Tailings End Pit Lake, in: AGU Fall Meeting Abstracts.

Golby, S., Ceri, H., Gieg, L.M., Chatterjee, I., Marques, L.L., Turner, R.J., 2012. Evaluation of microbial biofilm communities from an Alberta oil sands tailings pond. FEMS Microbiol Ecol 79, 240–250. https://doi.org/10.1111/j.1574-6941.2011.01212.x

Golder, 2001. End Pit Lake Background Information Summary.

Golder, 1995. Draft report on the effect of littoral zone area on lake productivity. Golder Associates Ltd.

Grady Jr, C.P.L., Daigger, G.T., Love, N.G., Filipe, C.D.M., 2011. Biological wastewater treatment. CRC press.

Gulley, J.R., MacKinnon, M., 1993. Fine tails reclamation utilization using a wet landscape approach, in: Energy, Mines & Resources Canada, Oil Sands: Our Petroleum Future Conference.

Harris, G., 2012. Phytoplankton ecology: structure, function and fluctuation. Springer Science & Business Media.

Headley, J. V, Armstrong, S.A., Peru, K.M., Mikula, R.J., Germida, J.J., Mapolelo, M.M., Rodgers, R.P., Marshall, A.G., 2010. Ultrahigh-resolution mass spectrometry of simulated runoff from treated oil sands mature fine tailings. Rapid Commun Mass Spectrom 24, 2400–2406. https://doi.org/10.1002/rcm.4658

Headley, J. V, Barrow, M.P., Peru, K.M., Fahlman, B., Frank, R.A., Bickerton, G., McMaster, M.E., Parrott, J., Hewitt, L.M., 2011. Preliminary fingerprinting of Athabasca oil sands polar organics in environmental samples using electrospray ionization Fourier transform ion cyclotron resonance mass spectrometry. Rapid Commun. Mass Spectrom. 25, 1899–1909.

Hernandez-Aviles, J.S., Bertoni, R., Macek, M., Callieri, C., 2012. Why bacteria are smaller in the epilimnion than in the hypolimnion? A hypothesis comparing temperate and tropical lakes. J. Limnol. 71, 10.

Holden, A.A., Donahue, R.B., Ulrich, A.C., 2011. Geochemical interactions between process-affected water from oil sands tailings ponds and North Alberta surficial sediments. J. Contam. Hydrol. 119, 55–68.

Holowenko, F.M., MacKinnon, M.D., Fedorak, P.M., 2000. Methanogens and sulfate-reducing bacteria in oil sands fine tailings waste. Can J Microbiol 46, 927–937.

Honarvar, A., Rozhon, J., Millington, D., Walden, T., Murillo, C.A., Walden, Z., 2011. Economic impacts of new oil sands projects in Alberta (2010-2035). Can. Energy

Res. Institute,. Study.

Jeeravipoolvarn, S., Scott, J.D., Chalaturnyk, R.J., 2009. 10 m standpipe tests on oil sands tailings: long-term experimental results and prediction. Can. Geotech. J. 46, 875–888.

Johnson, E., Castendyk, D.N., 2012. The INAP Pit Lakes Database: A novel tool for the evaluation of predicted pit lake water quality, in: Proceedings of the 9th International Conference on Acid Rock Drainage: Ottawa, Canada. pp. 1–12.

Jornitz, M.W., Agalloco, J.P., Akers, J.E., Madsen, R.E., Meltzer, T.H., 2001. Filter Integrity Testing in Liquid Applications, Revisited. Pharm. Technol.

Kaminsky, H.A.W., Etsell, T.H., Ivey, D.G., Omotoso, O., 2008. Characterization of heavy minerals in the Athabasca oil sands. Miner. Eng. 21, 264–271.

Karakas, G., Brookland, I., Boehrer, B., 2003. Physical characteristics of acidic mining lake 111. Aquat. Sci. 65, 297–307.

Kasperski, K.L., 1992. A review of properties and treatment of oil sands tailings. AOSTRA J. Res. 8, 11.

Kasperski, K.L., Mikula, R.J., 2011. Waste streams of mined oil sands: characteristics and remediation. Elements 7, 387–392.

Katsev, S., Crowe, S.A., Mucci, A., Sundby, B., Nomosatryo, S., Douglas Haffner, G., Fowle, D.A., 2010. Mixing and its effects on biogeochemistry in the persistently stratified, deep, tropical Lake Matano, Indonesia. Limnol. Oceanogr. 55, 763–776.

Kavanagh, R.J., Burnison, B.K., Frank, R.A., Solomon, K.R., Van Der Kraak, G., 2009. Detecting oil sands process-affected waters in the Alberta oil sands region using synchronous fluorescence spectroscopy. Chemosphere 76, 120–126.

Kelly, E.N., Schindler, D.W., Hodson, P. V, Short, J.W., Radmanovich, R., Nielsen, C.C., 2010. Oil sands development contributes elements toxic at low concentrations to the Athabasca River and its tributaries. Proc. Natl. Acad. Sci. 107, 16178–16183.

Kotylar, L.S., Sparks, B.D., Schutte, R., 1996. Effect of salt on the flocculation behavior of nano particles in oil sands fine tailings. Clays Clay Miner. 44, 121–131.

Kreling, J., Bravidor, J., Engelhardt, C., Hupfer, M., Koschorreck, M., Lorke, A., 2017. The importance of physical transport and oxygen consumption for the development of a metalimnetic oxygen minimum in a lake. Limnol. Oceanogr. 62, 348–363.

Kurek, J., Kirk, J.L., Muir, D.C., Wang, X., Evans, M.S., Smol, J.P., 2013. Legacy of a half century of Athabasca oil sands development recorded by lake ecosystems. Proc Natl Acad Sci U S A 110, 1761–1766. https://doi.org/10.1073/pnas.1217675110

Lawrence, G.A., Tedford, E.W., Pieters, R., 2015. Suspended solids in an end pit lake: potential mixing mechanisms. Can. J. Civ. Eng. 43, 211–217.

Lawrence, G.A., Ward, P.R.B., MacKinnon, M.D., 1991. Wind-wave-induced suspension of mine tailings in disposal ponds–a case study. Can. J. Civ. Eng. 18, 1047–1053.

Lerman, A., Imboden, D., Gat, J., 1995. Physics and chemistry of lakes. New York.

Levy, D. B., Custis, K. H., Casey, W. H., & Rock, P. A. (1997). A comparison of metal attenuation in mine residue and overburden material from an abandoned copper mine. Applied Geochemistry, 12(2), 203-211.

Li, C., 2010. Methanogenesis in oil sands tailings: An analysis of the microbial community involved and its effects on tailings densification.

Li, X., Sun, W., Wu, G., He, L., Li, H., Sui, H., 2011. Ionic liquid enhanced solvent extraction for bitumen recovery from oil sands. Energy & Fuels 25, 5224–5231.

List, B.R., Lord, E.R.F., 1997. Syncrude's tailings management practices from research to implementation. CIM Bull. 90, 39–44.

MacKinnon, M., Sethi, A., 1993. A comparison of the physical and chemical properties of the tailings ponds at the Syncrude and Suncor oil sands plants, in: Proceedings of Our Petroleum Future Conference, Alberta Oil Sands Technology and Research Authority (AOSTRA), Edmonton, Alta.

MacKinnon, M.D., 1989. Development of the tailings pond at Syncrude's oil sands plant: 1978–1987. AOSTRA J. Res 5, 109–133.

MacKinnon, M.D., Retallack, J.T., 1981. Preliminary characterization and detoxification of tailings pond water at the Syncrude Canada Ltd. Oil Sands Plant. L. Water Issues Relat. to Energy Dev. Ann Arbor Sci. Denver, Colo 185–210.

Madigan, M.T., Martinko, J.M., Dunlap, P. V, Clark, D.P., 2008. Brock Biology of microorganisms 12th edn. Int. Microbiol 11, 65–73.

Masliyah, J., Zhou, Z.J., Xu, Z., Czarnecki, J., Hamza, H., 2004. Understanding water-based bitumen extraction from Athabasca oil sands. Can. J. Chem. Eng. 82, 628–654.

McAnally, W.H., Friedrichs, C., Hamilton, D., Hayter, E., Shrestha, P., Rodriguez, H., Sheremet, A., Teeter, A., 2007. Management of fluid mud in estuaries, bays, and lakes. I: Present state of understanding on character and behavior. J. Hydraul. Eng. 133, 9–22.

McCullough, C.D., van Etten, E.J.B., 2011. Ecological restoration of novel lake districts: new approaches for new landscapes. Mine Water Environ. 30, 312–319.

Meade, J.W., 1985. Allowable ammonia for fish culture. Progress. Fish-Culturist 47, 135–145.

Miguel-Chinchilla, L., González, E., & Comín, F. A. (2014). Assessing metal pollution in ponds constructed for controlling runoff from reclaimed coal mines. *Environmental monitoring and assessment*, *186*(8), 5247-5259.

Mikula, R., Munoz, V., Bjornson, B., Cox, D., Marks, A., 2008. Processing of oil sand ore which contains degraded bitumen.

Misiti, T., Tandukar, M., Tezel, U., Pavlostathis, S.G., 2013. Inhibition and biotransformation potential of naphthenic acids under different electron accepting conditions. Water Res. 47, 406–418. https://doi.org/10.1016/j.watres.2012.10.019

Morris, P., 2018. Depth Dependent Roles of Methane, Ammonia and Hydrogen Sulfide in the Oxygen Consumption of Base Mine Lake, the pilot Athabasca Oil Sands Pit Lake.

Nix E. Power., P., 1988. An Evaluation of Sludge Capping for the Disposal of Oil Sand Sludge.

OSDG, 2009. Responsible oil sands development: the process. Oil Sands Developers Group.

Parajulee, A., Wania, F., 2014. Evaluating officially reported polycyclic aromatic hydrocarbon emissions in the Athabasca oil sands region with a multimedia fate model. Proc Natl Acad Sci U S A 111, 3344–3349. https://doi.org/10.1073/pnas.1319780111

Peacock, M.J., 2010. Athabasca oil sands: reservoir characterization and its impact on thermal and mining opportunities, in: Geological Society, London, Petroleum Geology Conference Series. Geological Society of London, pp. 1141–1150.

Penner, T.J., Foght, J.M., 2010. Mature fine tailings from oil sands processing harbour diverse methanogenic communities. Can J Microbiol 56, 459–470. https://doi.org/10.1139/w10-029

Powter, C.B., Biggar, K.W., Silva, M.J., McKenna, G.T., Scordo, E.B., 2011. Review of oil sands tailings technology options, in: Tailings and Mine Waste.

Quagraine, E.K., Peterson, H.G., Headley, J. V, 2005. In situ bioremediation of naphthenic acids contaminated tailing pond waters in the Athabasca oil sands region—demonstrated field studies and plausible options: a review. J. Environ. Sci. Heal. 40, 685–722.

Ramos-Padron, E., Bordenave, S., Lin, S., Bhaskar, I.M., Dong, X., Sensen, C.W., Fournier, J., Voordouw, G., Gieg, L.M., 2011. Carbon and sulfur cycling by microbial communities in a gypsum-treated oil sands tailings pond. Env. Sci

Technol 45, 439–446. https://doi.org/10.1021/es1028487

Ramos Padron, E., 2013. Physiology and Molecular Characterization of Microbial Communities in Oil Sands Tailings Ponds. University of Calgary.

Reid, M.L., Warren, L.A., 2016. S reactivity of an oil sands composite tailings deposit undergoing reclamation wetland construction. J. Environ. Manage. 166, 321–329.

Reid, T., Boudens, R., Ciborowski, J.J.H., Weisener, C.G., 2016. Physicochemical gradients, diffusive flux, and sediment oxygen demand within oil sands tailings materials from Alberta, Canada. Appl. geochemistry 75, 90–99.

Risacher, F.F., Morris, P.K., Arriaga, D., Goad, C., Nelson, T.C., Slater, G.F., Warren, L.A., 2018. The interplay of methane and ammonia as key oxygen consuming constituents in early stage development of Base Mine Lake, the first demonstration oil sands pit lake. Appl. Geochemistry 93, 49–59. https://doi.org/10.1016/j.apgeochem.2018.03.013

Rogers, V. V, Liber, K., MacKinnon, M.D., 2002. Isolation and characterization of naphthenic acids from Athabasca oil sands tailings pond water. Chemosphere 48, 519–527.

Roy, R., Knowles, R., 1994. Effects of methane metabolism on nitrification and nitrous oxide production in polluted freshwater sediment. Appl Env. Microbiol 60, 3307–3314.

Saidi-Mehrabad, A., He, Z., Tamas, I., Sharp, C.E., Brady, A.L., Rochman, F.F., Bodrossy, L., Abell, G.C., Penner, T., Dong, X., Sensen, C.W., Dunfield, P.F., 2013. Methanotrophic bacteria in oilsands tailings ponds of northern Alberta. ISME J 7, 908–921. https://doi.org/10.1038/ismej.2012.163

Salloum, M.J., Dudas, M.J., Fedorak, P.M., 2002. Microbial reduction of amended sulfate in anaerobic mature fine tailings from oil sand. Waste Manag. Res. 20, 162–171.

Schindler, D.W., 2014. Unravelling the complexity of pollution by the oil sands industry.

Proc Natl Acad Sci U S A 111, 3209–3210. https://doi.org/10.1073/pnas.1400511111

Segers, P., Vancanneyt, M., Pot, B., Torck, U., Hoste, B., Dewettinck, D., Falsen, E., Kersters, K., De Vos, P., 1994. Classification of Pseudomonas diminuta Leifson and Hugh 1954 and Pseudomonas vesicularis Büsing, Döll, and Freytag 1953 in Brevundimonas gen. nov. as Brevundimonas diminuta comb. nov. and Brevundimonas vesicularis comb. nov., respectively. Int. J. Syst. Evol. Microbiol. 44, 499–510.

Sharma, B., Ahlert, R.C., 1977. Nitrification and nitrogen removal. Water Res. 11, 897–925.

Shevenell, L., Connors, K.A., Henry, C.D., 1999. Controls on pit lake water quality at sixteen open-pit mines in Nevada. Appl. Geochemistry 14, 669–687.

Siddique, T., Fedorak, P.M., Foght, J.M., 2006. Biodegradation of short-chain n-alkanes in oil sands tailings under methanogenic conditions. Env. Sci Technol 40, 5459–5464.

Siddique, T., Fedorak, P.M., MacKinnon, M.D., Foght, J.M., 2007. Metabolism of BTEX and naphtha compounds to methane in oil sands tailings. Env. Sci Technol 41, 2350–2356.

Siddique, T., Foght, J., 2013. Biogeochemical pathways that influence de-watering and consolidation of fluid fine tailings, in: AGU Fall Meeting Abstracts.

Siddique, T., Kuznetsov, P., Kuznetsova, A., Arkell, N., Young, R., Li, C., Guigard, S., Underwood, E., Foght, J.M., 2014a. Microbially-accelerated consolidation of oil sands tailings. Pathway I: changes in porewater chemistry. Front Microbiol 5, 106. https://doi.org/10.3389/fmicb.2014.00106

Siddique, T., Kuznetsov, P., Kuznetsova, A., Li, C., Young, R., Arocena, J.M., Foght, J.M., 2014b. Microbially-accelerated consolidation of oil sands tailings. Pathway II:

solid phase biogeochemistry. Front Microbiol 5, 107. https://doi.org/10.3389/fmicb.2014.00107

Siddique, T., Penner, T., Klassen, J., Nesbo, C., Foght, J.M., 2012. Microbial communities involved in methane production from hydrocarbons in oil sands tailings. Env. Sci Technol 46, 9802–9810. https://doi.org/10.1021/es302202c

Siddique, T., Penner, T., Semple, K., Foght, J.M., 2011. Anaerobic biodegradation of longer-chain n-alkanes coupled to methane production in oil sands tailings. Env. Sci Technol 45, 5892–5899. https://doi.org/10.1021/es200649t

Slater, G.F., Cowie, B.R., Harper, N., Droppo, I.G., 2008. Variation in PAH inputs and microbial community in surface sediments of Hamilton Harbour: implications to remediation and monitoring. Env. Pollut 153, 60–70. https://doi.org/10.1016/j.envpol.2007.08.009

Small, C.C., Cho, S., Hashisho, Z., Ulrich, A.C., 2015. Emissions from oil sands tailings ponds: Review of tailings pond parameters and emission estimates. J. Pet. Sci. Eng. 127, 490–501.

Small, C.C., Ulrich, A.C., Hashisho, Z., 2012. Adsorption of acid extractable oil sands tailings organics onto raw and activated oil sands coke. J. Environ. Eng. 138, 833–840.

Sobkowicz, J.C., 2013. Developments in treating and dewatering oil sand tailings, in: Proceedings 16th International Seminar on Paste and Thickened Tailings, Belo Horizonte, Brazil. pp. 17–20.

Sprent, J.I., 1987. The ecology of the nitrogen cycle. Cambridge University Press.

Stasik, S., Loick, N., Knöller, K., Weisener, C., Wendt-Potthoff, K., 2014. Understanding biogeochemical gradients of sulfur, iron and carbon in an oil sands tailings pond. Chem. Geol. 382, 44–53.

Stasik, S., Wendt-Potthoff, K., 2014. Interaction of microbial sulphate reduction and

methanogenesis in oil sands tailings ponds. Chemosphere 103, 59–66. https://doi.org/10.1016/j.chemosphere.2013.11.025

Stauffer, R.E., 1987. Effects of oxygen transport on the areal hypolimnetic oxygen deficit. Water Resour. Res. 23, 1887–1892.

Stevens, C.L., Lawrence, G.A., 1997. The effect of sub-aqueous disposal of mine tailings in standing waters. J. Hydraul. Res. 35, 147–159.

Teare, M., Burrowes, A., Baturin-Pollock, C., Rokosh, D., Evans, C., Gigantelli, P., Marsh, R., Banafsheh, A., Tamblyn, C., Ito, S., 2012a. Energy Resources Conservation Board ST98-2012: Alberta's energy reserves 2011 and supply/demand outlook 2012–2021. Calgary, AB.

Teare, M., Burrowes, A., Baturin-Pollock, R.D., Evans, C., Gigantelli, D., Marsh, R., Ashrafi, B., Tamblyn, C., Ito, S., Willwerth, A., 2012b. Alberta's Energy Reserves 2011 and Supply/Demand. Outlook 2021.

Van Luijn, F., Boers, P.C.M., Lijklema, L., Sweerts, J.-P., 1999. Nitrogen fluxes and processes in sandy and muddy sediments from a shallow eutrophic lake. Water Res. 33, 33–42.

Viollier, E., Inglett, P.W., Hunter, K., Roychoudhury, A.N., Van Cappellen, P., 2000. The ferrozine method revisited: Fe (II)/Fe (III) determination in natural waters. Appl. geochemistry 15, 785–790.

von Rohden, C., Ilmberger, J., 2001. Tracer experiment with sulfur hexafluoride to quantify the vertical transport in a meromictic pit lake. Aquat. Sci. 63, 417–431.

von Rohden, C., Ilmberger, J., Boehrer, B., 2009. Assessing groundwater coupling and vertical exchange in a meromictic mining lake with an SF6-tracer experiment. J. Hydrol. 372, 102–108.

von Rohden, C., Wunderle, K., Ilmberger, J., 2007. Parameterisation of the vertical transport in a small thermally stratified lake. Aquat. Sci. 69, 129–137.

Ward, P.R.B., Lawrence, G.A., MacKinnon, M.D., 1994. Wind driven re-suspension of sediment in a large tailings pond, in: Proceedings, International Symposium on Ecology and Engineering. pp. 37–57.

Warren, L.A., Kendra, K.E., Brady, A.L., Slater, G.F., 2015. Sulfur biogeochemistry of an oil sands composite tailings deposit. Front. Microbiol. 6.

Westcott, F., 2007a. Oil sands end pit lakes: a review to 2007. Prep. by Clear. Environ. Consult. Inc. Cumul. Environ. Manag. Assoc. Pit Lakes Subgr.

Westcott, F., 2007b. End Pit Lakes technical guidance document. Cumul. Environ. Manag. Assoc. End Pit Lakes Subgr. 61.

Westcott, F., Watson, L., 2005. End Pit Lakes technical guidance document. Clear. Environ. Consult. CEMA end Pit Lakes subgroup, Proj. 61.

Wetzel, R.G., 2001. Limnology: lake and river ecosystems. Gulf Professional Publishing.

Wetzel, R.G., 1983. Limnology (2nd edn). Saunders Coll. Publ. Philadelphia 767, R81pp.

Winkler, M.K.H., Yang, J., Kleerebezem, R., Plaza, E., Trela, J., Hultman, B., van Loosdrecht, M.C.M., 2012. Nitrate reduction by organotrophic Anammox bacteria in a nitritation/anammox granular sludge and a moving bed biofilm reactor. Bioresour. Technol. 114, 217–223.

Yakushev, E. V, Newton, A., 2012. Introduction: redox interfaces in marine waters, in: Chemical Structure of Pelagic Redox Interfaces. Springer, pp. 1–12.

Yeates, P.S., Imberger, J., 2003. Pseudo two-dimensional simulations of internal and boundary fluxes in stratified lakes and reservoirs. Int. J. River Basin Manag. 1, 297–319.

Yeh, S., Jordaan, S.M., Brandt, A.R., Turetsky, M.R., Spatari, S., Keith, D.W., 2010. Land use greenhouse gas emissions from conventional oil production and oil sands. Environ. Sci. Technol. 44, 8766–8772.

Yergeau, E., Lawrence, J.R., Sanschagrin, S., Waiser, M.J., Korber, D.R., Greer, C.W., 2012. Next-generation sequencing of microbial communities in the Athabasca River and its tributaries in relation to oil sands mining activities. Appl Env. Microbiol 78, 7626–7637. https://doi.org/10.1128/AEM.02036-12

Yokom, S., Axler, R., McDonald, M., Wilcox, D., 1997. Recovery of a mine pit lake from aquacultural phosphorus enrichment: model predictions and mechanisms. Ecol. Eng. 8, 195–218.

Yokom, S., Axler, R., McDonald, M., Wilcox, D., 1997. Recovery of a mine pit lake from aquacultural phosphorus enrichment: model predictions and mechanisms. Ecol. Eng. 8, 195–218.

Chapter 2: Field Site, water sampling and analysis, and laboratory experiments

2.1 Introduction

For this thesis, field- and laboratory-based methods were used to investigate the oxygen dynamics in the water cap of base mine lake (BML) and the relationships linked to the constituents coming out of the fluid fine tailing (FFT) layer. This chapter is intended to provide (1) greater detail concerning the field site that was stated in the two results chapters (Chapter 3-4), and (2) a synthetic overview and justification of the methods employed to collect and analyze water samples and characterize oxygen-consuming constituents (OCC). In both the field and experimental results a primary focus was on the determination of oxygen consumption rates (OCR) and identification of the key OCC involved and their relative impact. Specifically field-based ad laboratory based oxygen consumption experiments were performed to determine: (1) *in-situ* oxygen depletion associated with the release of OCC from the FFT layer (Chapter 3); and (2) the contribution of ammonium to oxygen consumption in experimental microcosms (Chapter 4; Figure 2.1).

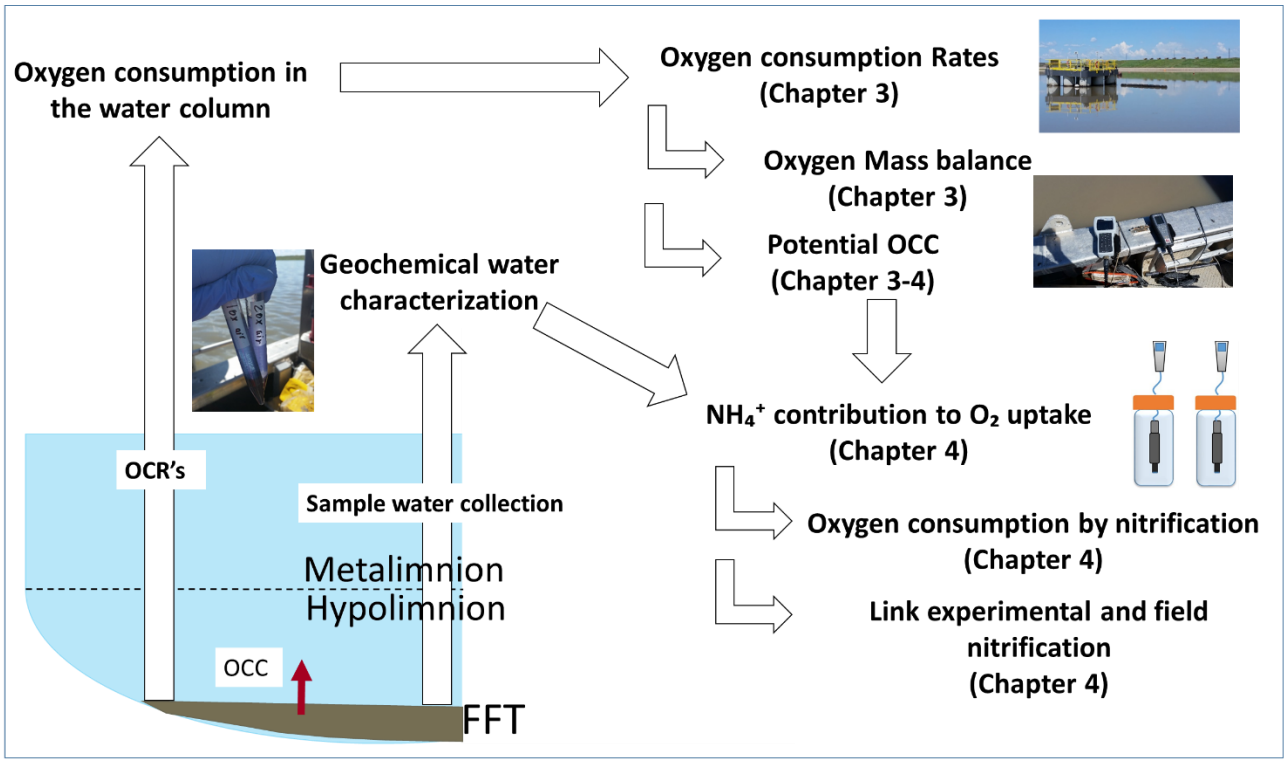

Figure 2.1 Schematic of the proposed field and laboratory study

2.2 Field Investigation of BML water cap oxygen concentrations, OCR and the role of mixing in oxygen distribution (Chapter 3)

2.2.1 Field Site

Field sampling campaigns were carried out at Base Mine Lake, Syncrude Canada, Fort McMurray AB, over diurnal timeframes during the summer of 2016. The lake is located in northern Alberta (coordinates: 57° 0' 38.88"N, 111° 37' 22.44"W; Figure 2.2). The lake is only accessible by Syncrude permission and is currently closed to the public.

Base Mine Lake, a shallow lake (mean depth ~ 10 m, maximum depth ~ 12 m) covering approximately 6.5 km^2, was commisioned in 2012 and is comprised of ~40 m of

FFT material overlying mixed freshwater/OSPW layer (Figures 2.2). Infrastructure has been installed to pump in and pump out water as an analogue for natural flows until a more substantial upstream surface watershed is reclaimed and connected to BML and outflow is permitted into the Athabasca River. Syncrude has added additional fresh water to bring the level to the final designed elevation. Commisioning is defined as no further tailings solids either added (transferred in from MLSB) or removed (pumped out to the composite tailings process); water flow in and out are part of the operation of the lake. Prior to commisioning, FFT was deposited at this site through a series of discharge pipes over the span of several years, such that the oldest FFT layers are found at the bottom of the deposit with the most recent FFT layers towards the surface. Water was opaque and murky with occasional bitumen mats (10 cm^2 to several square meters) covering the surface. There is regular ebullition, in the form of bubbles, coming out which are associated to bring up bitumen, as well as other compounds, to the surface from the FFT layer. The lake area is subjected to moderate wind action and thunderstorms during the summer. Three permanent sampling platforms have been installed along a southwestern-northeastern transect in BML.

BML monitoring program (Westcott and Watson, 2005) consists of two main objectives: Objective 1 (early, 5 to 10 years) demonstration of water capped FFT technology at BML and Objective 2 (later, 20 to 30+ years) development toward a self-sustaining aquatic system in the closure landscape. A crucial part of the first objective is the positive development of the water quality. The water quality within BML will determine the timing and ability for sustainable aquatic populations to become

established. One of the biggest water quality concerns is the dissolved oxygen concentration, to the extent that low or insufficient oxygen levels in BML would hamper the ability of aquatic organisms to develop sustainable communities. The sampling campaign was planned to assess different aspects of the oxygen dynamics across the water column: temporal and spatial water column oxygen consumption rates throughout the water column and potential OCC (Chapter 3) and, the importance of nitrification in the oxygen consumption of BML (Chapter 4).

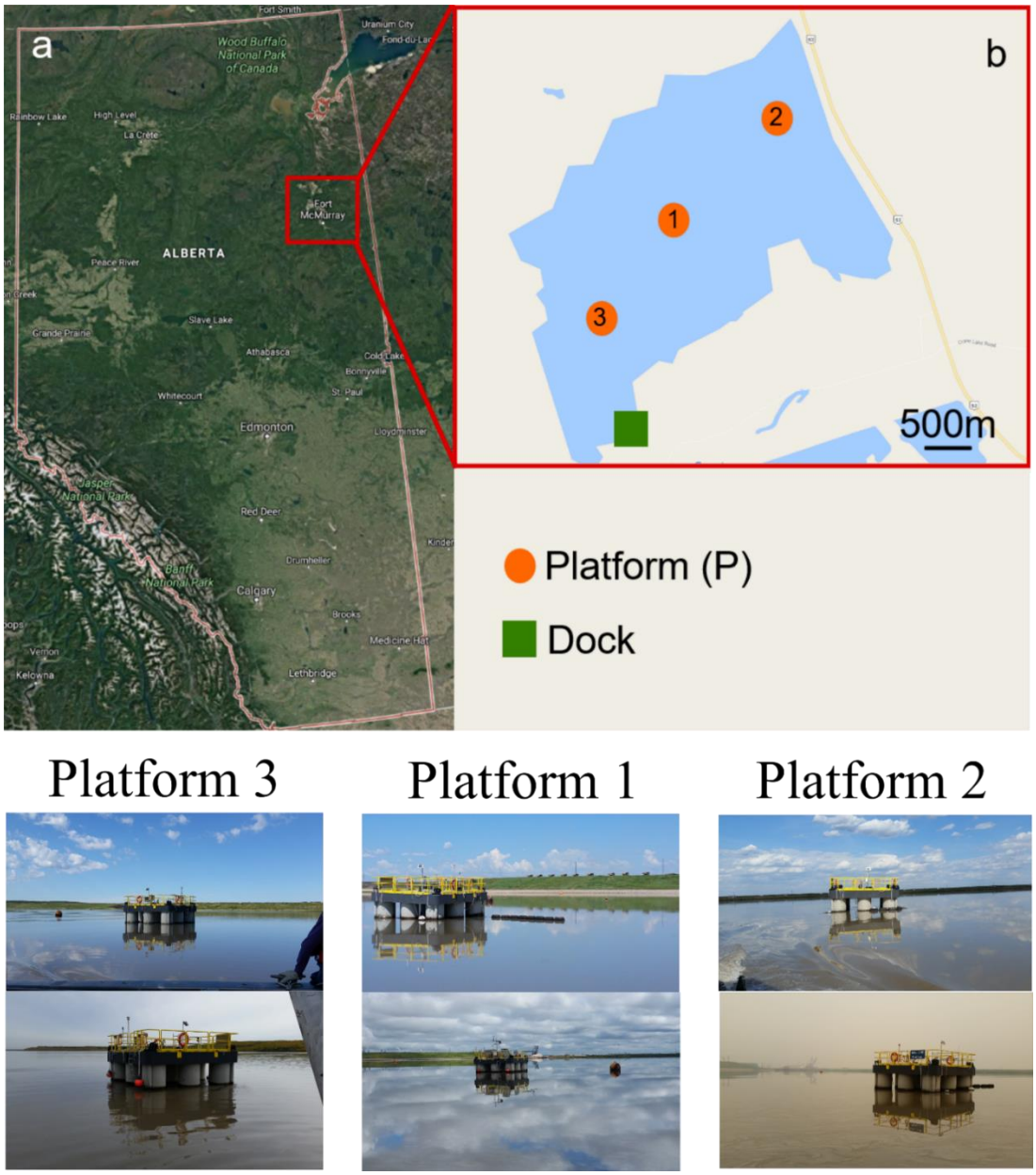

Figure 2.2 Base Mine Lake, Syncrude, in northern Alberta Canada. A) Satellite view of the province of Alberta, B) schematic diagram of BML in the AOSR and photographic pictures of each platform

2.2.2 Field Site Characterization and Water Sample Collection

Water sample collection and characterization occurred from July 04th to September 06th 2016 at a central platform in BML. BML has three permanent platforms, platform 1 (P1), platform 2 (P2) and platform 3 (P3) have been installed on the lake (Figure 2.1). These three platforms, serving as monitoring stations on BML, were the sites for all sampling completed in BML during the 2016 field season. The focus on this thesis was the oxygen dynamics at the water column from the water surface to the FFT-water interface (FWI). At BML, diurnal water column profiling was carried out daily. Physicochemical profiling of the BML water column (~9-10m of depth) was carried on for each sampling campaign, prior to water sampling. Profiles, at each platform, were conducted at ~ 50 cm intervals from the BML surface to the FFT-water interface (FWI) for pH, specific conductivity, temperature, dissolved oxygen, turbidity, oxidation-reduction potential (ORP), and salinity (YSI Professional Plus 6-Series Sonde, YSI Incorporated). Physicochemical zonation was identified and observed gradients served as a sampling point selection method. FWI and metalimnion-hypolimnion interface were prioritized as crucial zones where oxygen flux plays an important role in the water column geochemistry. The dissolved oxygen concentration was determined using an O_2 sensor (Yellow Spring Instruments) that was lowered through the water column. Once desired depth was selected, a van dorn bottle was deployed and stirred for a few seconds before close it, capturing the water from that depth. The van dorn is retrieved back to the surface where samples are collected as described below.

All sample collection, preservation and analyses followed well-established protocols developed in our research groups (Reid and Warren, 2016; Slater et al., 2008; Warren et al., 2015). Water samples were collected from three depths covering the epilimnion, metalimnion and hypolimnion as identified from the physicochemical profile for each sampling campaign using a 9.3 L sampling van dorn (WaterMark, Forestry supplies). Upon retrieval of the van dorn sampler to the boat, sample collection proceeded in the following order: CH_4, ΣH_2S, Fe^{2+}, Fe^{3+}, and a bulk water sample for NO_3^-, NO_2^-, NH_4^+ and SO_4^{2-}. Three to seven replicates were analyzed for all geochemical analytes. Field blanks (filtered and preserved ultrapure water on site) and process blanks (3) were collected and analyzed for each analyte.

To minimize organic, and trace metal contamination, all equipment (excluding syringes and needles, which were maintained under sterile conditions until use) and containers used for the collection and storage of water samples were cleaned via a three-step process before use: (1) washing with detergent and rinsing with ultrapure water (18.2 MΩ cm), (2) soaking in a 4% (v/v) HCl solution prepared using ultrapure water for >24 h (exception: 10% (v/v) HCl for bottles used for measuring organic carbon), and (3) rinsing eight times with ultrapure water. For larger equipment (i.e. YSI sonde and pelican case), only surfaces in direct contact with the collected water sample were thoroughly cleaned. In the field, all samples were stored in coolers with ice packs until such time that they could be placed in refrigerators or freezers for long-term storage. Samples for iron and total sulfur analyses were acidified prior to storage using optima HCl and trace metal grade HNO_3, respectively, to minimize any changes from the time of their collection (e.g.

microbial growth or oxidation). Concentrations of reduced species were analyzed to determine the impact on the oxygen consumption (Table 2.1).

Table 2.1 Summary of each analyte methodology, collection procedure and the storage details

Constituent	**Details**	**Storage**
ΣH_2S	Methylene Blue Colorimetric Test • Method 8131, Hach Company • 2 mL of Reagent 1 is added to a clean 15 mL polypropylene tube to stabilize any H_2S present • 10 mL of sample is directly extruded (in triplicates) into the tube under anaerobic conditions • Addition of 2 mL of Reagent 2 is added • tube contents are homogenized and reacted for 5 minutes • The sample analyzed using HACH spectrophotometer	Analyzed on site
Sulfate	• SulfaVer4 Method 8051 Hach Company • The prespiked SulfaVer4 reagent is added to clean 15 mL polypropylene tube to stabilize any sulfate present • 10 mL of sample is directly extruded (in triplicates) into the tube • tube contents are homogenized and reacted for 5 mins • The sample analyzed using HACH spectrophotometer	Analyzed on site
Ammonium	Salicylate Method • Method 8151, Hach Company • 1 mL of sample is collected (in triplicates) and mixed with reagent 1 (Ammonia Salicylate) in a test vial • Reagent dissolved and react with the sample for 3 minutes, after which reagent 2 (Ammonia Cyanurate) is mixed and shaken and wait for 15 minutes • The sample analyzed using HACH spectrophotometer	Analyzed on site
Nitrate	Cadmium Reduction Method • Method 8192, Hach Company • 15 mL of sample is collected (in triplicates) and mixed with reagents • After the 20-minute reaction, the sample is analyzed using HACH colorimetry	Analyzed on site
Nitrite	Diazotization Method • Method 8507, Hach Company • 10 mL of sample is collected (in	Analyzed on site

	triplicates) and mixed with the reagent • After the 20-minute reaction, the sample is analyzed using HACH colorimetry	
Fe^{2+}/Fe^{3+}	• Retrieve a pre-spiked HCl 15 mL/50 mL corning tube • pH on the sample is brought up to 7 and rapidly mixed with reagents, recording values for Fe^{2+}/Fe^{3+} • Fe^{2+}/Fe^{3+} values are normalized using standard curves	The sample is preserved with 2% (v/v) optima HCl Analyzed on-site following the Ferrozine method (see details on text)
Methane	• 30 mL of the sample is collected using a 60 mL syringe • Samples were fixed with a saturated solution of mercuric chloride • Methane is analyzed on an SRI GC (Gas chromatography) and an FID (flame ionization detector)	Sample vials were transported back to the lab at McMaster University for analysis by Slater lab group (Gas chromatography)
Organic-inorganic carbon: particle and dissolved	• 120 mL of samples (2) are collected in in carbon-clean amber glass • The unfiltered sample was analyzed using a Total Organic Carbon Analyzer • Sample filtered with a syringe-driven 0.7μm glass microfiber filter unit were analyzed using a Total Organic Carbon Analyzer • Dissolved inorganic carbon (DIC) and dissolved organic carbon (DOC) were analyzed on each sample	Preserved and stored at -20°C. Samples analyzed using a Total Organic Carbon Analyzer at McMaster University

For organic carbon, water samples were collected in carbon-clean amber glass 120mL bottles. Bottles were cleaned with detergent, rinsed with ethanol, and placed in a 10% HCl bath overnight. After 7 rinses with MilliQ water, bottles were muffled in a furnace at 450°C for 8h to remove any residual carbon. Lids were rinsed with a 1:1:1 mixture of dichloromethane, hexane, and methanol and allowed to evaporate dry. In the field, each bottle was rinsed twice with sample before filling and then frozen at -20°C until filtration for dissolved organic carbon (DOC) and dissolved inorganic carbon (DIC) characterization in the laboratory back at McMaster. Similarly, TOC sample bottles were rinsed twice with sample before filling, and then stored on ice until on water activities

have finished and then frozen at -20°C until filtration for organic and inorganic carbon characterization at McMaster University.

Samples for carbon analysis were thawed and immediately filtered with a syringe-driven 0.7µm GF/F glass microfiber filter unit (13mm, GE Life Sciences). The filtrate was analyzed for TOC/TIC on a Shimadzu TOC-L Total Organic Carbon Analyzer with an autosampler ASI-L using the 680°C combustion catalytic oxidation method as per manufacturer recommended protocols (Mandel Scientific). Particulate total carbon and inorganic carbon were measured on the 0.7µm filters by combustion in the solid sampler SSM-5000A attachment for the Shimadzu TOC-Analyzer (Mandel Scientific). Analyses were conducted using a Shimadzu TOCL Total Organic Carbon Analyzer with an autosampler ASI-L (Mandel Scientific, Guelph, Ontario, Canada) using the 680°C combustion catalytic oxidation method as per manufacturer recommended protocols. The autosampler runs sample replicates (minimum three) until obtaining a peak area below 1 standard deviation. All samples were compared against a corresponding standard curve for either total C or inorganic C with a correlation value (R^2) of 0.99 or higher. Total C standards were prepared from a 1000 mg/L stock solution of potassium hydrogen phthalate (Sigma Aldrich) and all inorganic C standards were prepared from a 1000 mg C/L stock solution of 3.5 g $NaHCO_3$ and 4.41 g Na_2CO_3 (Sigma Aldrich) prepared in 1 L volumetric flasks as per manufacturer recommended protocols. Standard curves were made fresh at the time of each analysis. Organic carbon values were obtained by subtracting the inorganic C values from the total C values. Dissolved inorganic carbon (DIC) and dissolved organic carbon (DOC) were analyzed on each sample.

Dissolved methane was analyzed by Corey Goad (see Goad, 2017 MSc thesis) in the Slater lab at McMaster University following the method described by Slater et al. (2008). Samples were collected in the field using wheaton serum vials (60mL) which were crimped sealed with a 20 mm chlorobutyl stopper (Bellco glass) and pre-spiked with ~3.7mg mercuric chloride to stop any biological activity. The vials were then plugged with 13mm blue butyl septum stoppers and sealed with an aluminum crimped ring prior to evacuation (Eby et al., 2015).

Samples for ferrous and ferric iron were preserved by the addition of 2% v/v Optima-Grade hydrochloric acid. Quantification of total aqueous Fe (dissolved, <0.45 μm) and particulate Fe (>0.45 μm) was accomplished by colorimetric analysis (Ultraspec 3000, UV/visible, spectrophotometer, Pharmacia Biotech, Cambridge, U.K) by following a modified ferrozine method (Viollier et al., 2000) at McMaster University, once on water activities were finished. Standard curves for determination of Fe (II)/Fe (III) concentrations were prepared by serial dilution of an acidified $FeCl_3$ solution (1.786×10^{-2} mol/L $FeCl_3$, in 2% v/v HCl). Fe (II) and Fe (III) were quantified on a single preserved water sample before and after a reduction step as described by Viollier et al. (2000).

For sulfide analysis, 60mL syringes were pre-spiked with 1.5mL of sulfide 1 reagent. The water sample was collected from the identified sampling depth by a clean van dorn bottle and 30mL of sample water was extracted into a pre-filled 50 mL syringe from the closed van dorn bottle with the fixative for the sulfide analyses by spectrophotometry (Risacher et al. 2018). The reagent fixed sulfide without exposing to the atmosphere. The fixed sample was then filtered directly through 0.45 μm sterile

syringe filters into three replicate 15mL falcon tubes, and analyzed using a HACH spectrophotometer (Hach DR/2800 spectrophotometer, HACH Company, Loveland, CO, USA) directly on the sampling boat using the methylene blue method (Method 8131). One litre of sample water was stored in coolers with ice packs for subsequent sulfate, nitrate, nitrite and ammonia analyses. Samples contain large particles and interference was observed during analysis. Because of this, aliquots of sample water were centrifuged and filtered (0.45 μm) before analysis. Sample water was analyzed following HACH methods for ammonia (Method 10031), nitrate (method 8192), nitrite (method 8507) and sulfate (SulfaVer4 Method 8051). These samples were stored refrigerated until analyses were performed either on site within the field laboratory or upon return to McMaster University.

2.2.3 Oxygen Consumption Chamber

In order to evaluate OCR in the field, a customized pelican case was used for OCR experiments (Figure 2.3). Pelican™ cases (case 1400) made of polypropylene plastic with interior dimensions 30 x 22.5 x 13.2 cm (LxWxD) with a volume of approximately 9.3 Liters were deployed. The interior of the pelican case uses an O-ring seal and it is watertight, crushproof, and dustproof (as per manufacturer). The case was drilled to make an inlet, outlet and probe ports. Both inlet and outlet fitted a half an inch threaded port (Figure 2.3). The inlet consists of a through-wall fitting holding a compact threaded plastic on/off valve attached to the barbed fitting which was attached to a plastic tube. The outlet comprises a through-wall fitting attached to a pipe fitting that has a closure screw on it. Another threaded hole was made to insert the probe (YSI

ProODO™) inside the case. A customized fitting was designed to seal the hole using a through-wall system with O-rings on each side. All the pieces were attached to the case and tested before each experiment. Inside and outside of the case was bleached and ethanol-cleaned every time a new experiment was set up. A total of 6 customized pelican cases were prepared.

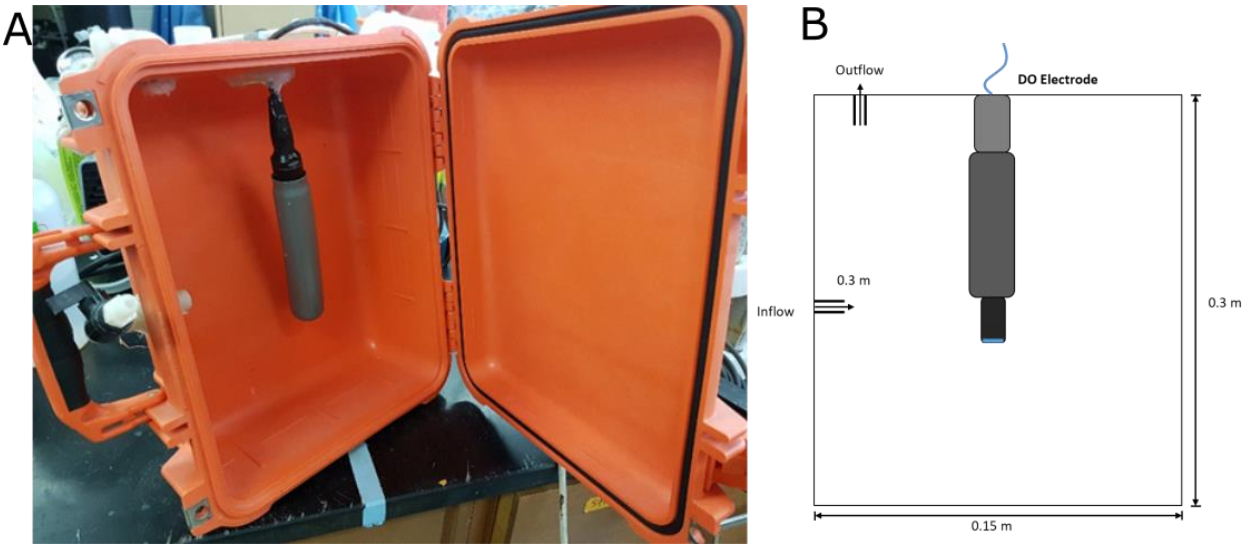

Figure 2.3 Specialized oxygen consumption chamber. A) Inside view of the oxygen chamber, B) Schematic view of the oxygen chamber with dimensions

2.2.4 Oxygen Probe

The YSI optical dissolved oxygen probes (6) were calibrated to check the instrument read zero in a dissolved oxygen free solution by using a solution of sodium sulfite according to the manufacturer's instructions. The oxygen probes were calibrated daily using the DO% in water saturated air method according to the manufacturer's instructions. The DO probe can measure barometer, temperature and dissolved oxygen (% saturation and concentration). The DO probe has an accuracy of 0 to 200% air

saturation ± 1% of the reading and 0 to 20 mg/L ± 0.1 mg/L. Temperature and barometer accuracy is ± 0.2°C and ± 1.5 mmHg from 0 to 50°C, respectively. The DO probe has a resolution of 0.1% air saturation, 0.01 or 0.1 mg/L (auto-scaling); temperature 0.1°C and barometer 0.1 mmHg. Also, the DO probe has a salinity manual calibration input range 0 to 70 ppt. DO readings compensate with temperature between -5 and 50°C.

2.2.5 Sample Collection for OCR Experiments

Sample water for the OCR experiments was collected using a van dorn bottle from the desired depth. Once retrieved the van dorn was attached to the case via a 1cm polyurethane tube, allowing the transfer of water into the case without opening either the van dorn bottle or the OCR chamber. Water was first allowed to run through the tube, before connecting to the case, to expel any oxygen from the tube prior to filling the case. The outlet port was opened to allow the air inside to escape and allow water to fill the case. Once the case was filled, water was left to runoff to get rid of any air/oxygen remaining. After this, the outlet port was closed and the case was deployed in the water column at the same depth of collection to mimic *in-situ* conditions. Oxygen concentrations were continuously measured at 60 seconds time series until depletion. OCR's were determined as the difference in concentration between time samples (uM/h).

2.2.6 Field OCR Experimental Design

A total of 31 OCR experiments were performed over spatial and temporal scale between July and August 2016 (Table 2.3). Sampling depths varied from the water surface to the FFT-water interface (FWI) in the water column. Rates closer to the source

(i.e. FFT) of OCC were hypothesized to be higher than those observed at the water surface. This zone was targeted during the OCR experiments. Zones of interested were replicated to corroborate if rates differ over time differences. Sample collection and physicochemical characterization were carried out according to established field protocols (Table 2.2). The experiments lasted from a few hours to a few days, depending on the starting oxygen concentration and oxygen demand. The OCR was determined by the least squares method of the change in oxygen concentration (e.g. HagMan and la Cour Jansen, 2007) after the oxygen concentration neared zero (~5 μM) inside the chamber.

Table 2.2 OCR experiments timeline

Year/Month/ Day	Experiments	Military start time	Zones assessed
14 July 2016	1	10:00	FWI
26 July 2016	6	12:30	Epilimnion, metalimnion, hypolimnion, FWI
27 July 2016	5	10:00	Epilimnion, metalimnion, hypolimnion, FWI
August 03 2016	5	11:00	Epilimnion, metalimnion, hypolimnion, FWI
August 10 2016	6	11:30	Hypolimnion, FWI
August 17 2016	5	10:20	Metalimnion, hypolimnion
August 17 2016	3	11:30	Epilimnion, metalimnion, FWI

Using the same sample water to fill the case, samples were collected for geochemical characterization including redox reactive oxygen constituents of concern (OCC): suspended particle matter concentration, CH_4, H_2S, bulk CH_2O (i.e. dissolved organic carbon, and dissolved inorganic carbon, DIC), Fe^{2+}/ Fe^{3+}, NH_4^+, NO_2^-, NO_3^-, SO_4^{2-} (see details in section 2.3; Table 2.4).

Table 2.3 Parameter analyzed and collected during the oxygen consumption experiments and methods of analysis

Parameter	Sample storage	Amount Required	Method of analysis
Total soluble nitrite (NO_2−-N) concentration	In the dark at 4C Analyzed on site	1/2 Dilution, 20 mL Triplicates + sample blank	Spectrophotometric nitrite method (Hach Company)
Total soluble nitrate (NO_3−N) concentration		1/2 Dilution, 20 mL Triplicates + sample blank	Spectrophotometric nitrate method (Hach Company)
Total soluble ammonia (NH_4^+−N) concentration		1/5 Dilution, 8 mL Triplicates + sample blank	Spectrophotometric ammonia method (Hach Company)
Total soluble sulfate (SO_4^{2-}) concentration		1/5 Dilution, 8 mL Triplicates + sample blank	Spectrophotometric sulfate method (Hach Company
Total suspended solids concentration		1/1 Dilution, 30 mL Triplicates	Spectrophotometric method based on the absorbance of a homogenized sample at 810 nm (Hach Company)
Total soluble reactive sulfide (H_2S) concentration	Analyzed immediately	1/1 Dilution, 30 mL Triplicates	Spectrophotometric blue methylene method (Hach Company)
Particulate and dissolved (<0.45 μm) organic carbon	In the dark at -20C	2xContainer 250 mL, Teflon	Total Organic Carbon Analyzer
Total Sulfur	In the dark at 4C	3x40mL Acidify with trace metal grade HNO_3 (2% (v/v)	Gas chromatography with sulfur chemiluminescence detection (SCD)
Methane	At room temperature	30mL Fixed with a saturated solution of mercuric chloride	Gas chromatography couple with a thermal conductivity detector
Fe^{2+}/Fe^{3+}	In the dark at 4C	2x14mL Filtered 2x14mL Unfiltered Acidify with trace metal grade HNO_3 (5% (v/v) final)	Ferrozine method

2.3 Experimental Laboratory Assessment of Ammonium Amendment (Chapter 4)

To assess the contribution of ammonium to the oxygen consumption in BML, an experimental assessment was performed using customized bottles containing ammonia amended BML water. 500-mL Pyrex lids were customized to attach oxygen probes within the experimental bottles to measure oxygen concentrations directly within the bottles. The lid was drilled to attach the O_2 probe (Figure 2.5) and sealed to avoid any gas escape. The experiments tested NH_4^+ as an emergent constituent to the oxygen consumption contribution in BML. The analyses will be the same as the field description as described in section 2.2.2.

2.3.1 Water Sample Collection and NH_4^+ Experimental Design

Prior to water collection for the experiments, physicochemical profiling (as described in section 2.2.1) of the BML water cap was conducted to identify the thermal zones. Sample water units (2) were collected at the interface between the metalimnion and hypolimnion (7.5 m; August 4th, 2017). Upon retrieval of the van dorn sampler to the boat, the water units were stored at room temperature in 20 litres buckets. The goal of sample collection was to provide a BML sample that contained viable endemic nitrifying bacteria, not to maintain the geochemical conditions at the time of collection. Thus the sample was subsequently stored at room temperature and shipped back to McMaster University for subsequent experimentation within 14 days of collection. The BML water was characterized immediately prior to initiation of the experiment, as discussed

subsequently to establish the geochemical conditions of the water and confirm the loss of any methane within the original water sample, which would remove confounding influences of methanotrophy on experimental OCR values.

The experiments were performed following three treatments: non-random, pre-test and post-test design (Table 2.4). Three treatment levels of NH_4^+ concentration were assessed: 50 μM, 200 μM and 500 μM. The sample water was amended with an ammonium sulfate stock solution (3.5 mM) to bring the NH_4^+ concentration up to the treatment level being examined in a 500 mL media bottle. These concentrations were selected based on bulk water NH_4^+ concentration observed in BML (50 μM), maximum NH_4^+ observed in the FFT (~200 μM) and concentration of NH_4^+ in tailing ponds (<500 μM). Two media bottles served as control group, one with unamended water and the other, as abiotic control, which received the NH_4^+ treatment. All bottles had an oxygen sensor measuring oxygen continuously inside the bottle. Constituents directly related to the nitrification process (i.e. NH_4^+, O_2, NO_3^-, NO_2^-) had a pre-test (initial) and post-test (final) analysis. In addition, a full water geochemistry characterization of other constituents of interest such as DOC, DIC, Fe^{2+}/ Fe^{3+}, ΣH_2S, and SO_4^{2-} (See section 2.2, Table 2.1), identified the contribution of other oxygen-consuming processes. For each experimental group (amended and control groups), an initial (pre-test) water sample was characterized for all the nitrogen species (i.e. NH_4^+, NO_3^-, NO_2^-). Similarly, a final analysis (post-test) was determined after oxygen concentration reaches near zero (~5 μM O_2).

Table 2.4 Experimental design: three groups, non-random selection, pre-test, post-test

Group	Pre-test	Treatment	Post-test
Experimental group = Amended	O	X	O
Control Group = Abiotic	O		O
Control Group = Unamended	*O*		*O*

2.3.2 Experimental Oxygen Chamber Incubations

From each water unit (20L), sample water was separated in 2.5 bottles. Each 2.5L bottle, previously homogenized from the selected sample water unit, was divided into five 500mL bottles. These bottles represented three amended bottles, one unamended water sample and one pre-test bottle. For each treatment experiment three amended replicates, one abiotic control and one unamended water control ran in parallel (Figure 2.4).

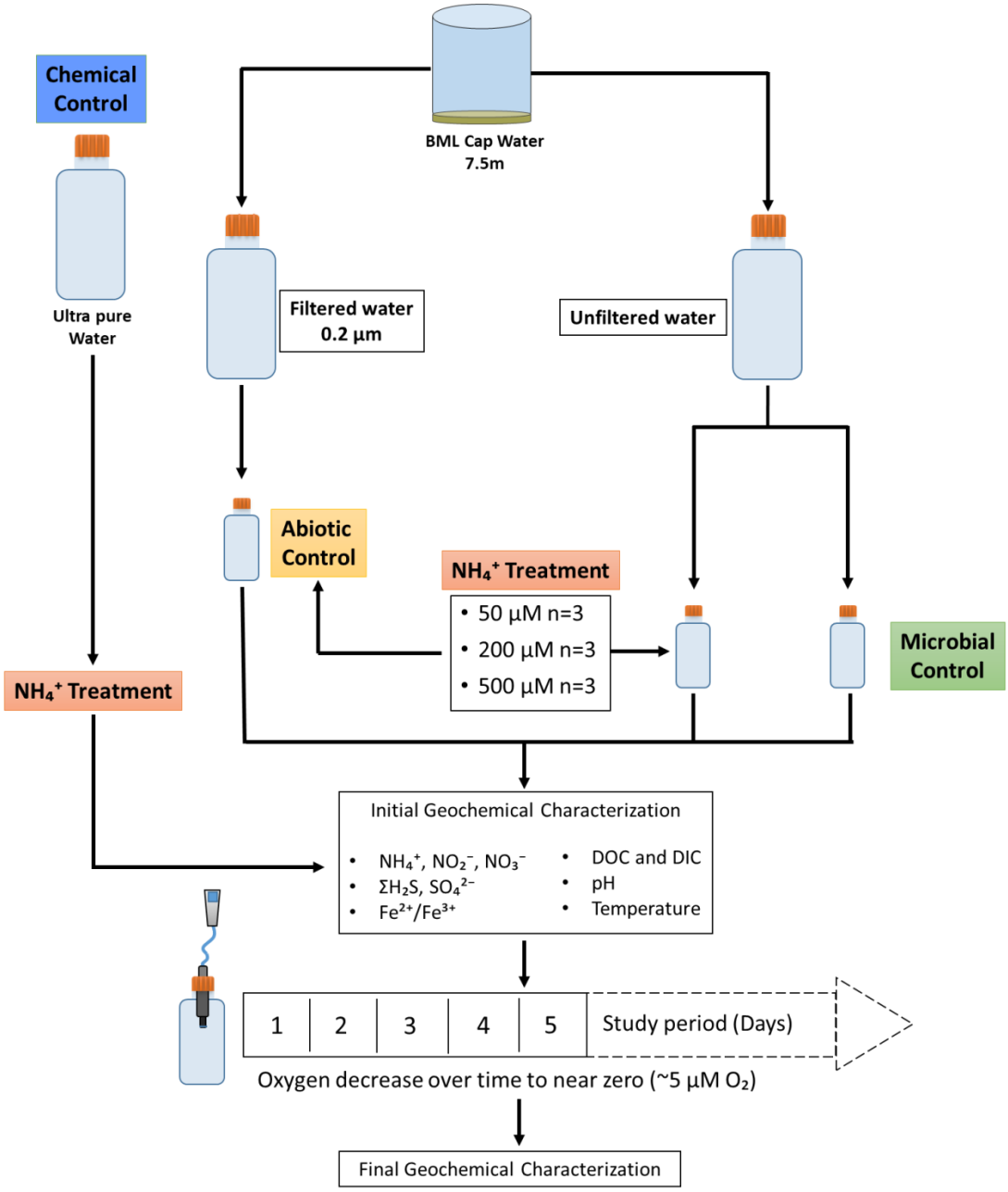

Figure 2.4 The experimental microcosm set-up and design including abiotic controls (0.2 um filtered but amended with the three concentrations of ammonia) and the microbial control (unamended BML water; endemic microbes present). The abiotic controls received the same NH_4^+ treatment additions while the microbial control received no NH_4^+

treatment additions. Both control groups ran in parallel with the three ammonia treatment additions.

For each ammonia treatment condition, replicates and the two controls the water were geochemically characterized at the initiation and the end of the experiment (determined by when the oxygen concentration within the microcosm decreased below 5 µM) for the suite of analytes identified. Chemical controls consisting of MQ water amended with the NH_4^+ stock solutions at the three different concentrations were also run to account for any stock solution impacts.

Workflow:

1. From the 2.5L sample water batch, water was thoroughly mixed and transferred equal sample water amount into 4x500mL media bottles.

2. Three (500mL) bottles received the stock solution treatment and were set up as replicates. A pre-test (500mL) bottle was filled with sample water (from the same 2.5L bottle) which received the same treatment and used to account for initial concentration for all suite of constituents, as described in the water sample characterization, and then discarded.

3. The fourth (500mL) bottle was unamended water (did not receive any treatment) and ran as untreated control. Sterilized (abiotic control) sample water was filled the fifth experimental bottle to run in parallel with treatments. An extra empty (500mL) bottle was filled with sterilized water and received the same treatment

concentration as in step 2. This bottle served to account for the initial concentration for all variables in the sterile control and then discarded.

4. All (5) bottles were closed (without leaving any headspace) with a customized lid with the oxygen sensor embedded that measured the oxygen concentration continuously inside each bottle. All bottles were then left until oxygen in the treatments bottles reached zero.

5. All treatment replicates were sampled for all variables simultaneously. Both control groups were also be sampled at the same time. 15mL falcon tubes were pre-spiked with the corresponding reagent beforehand to speed up the sampling. All sample analyses were be done immediately, following the corresponding HACH methods for ammonia, nitrate, and nitrite, sulfate and sulfide (section 2.2). A sample of 40mL was collected and frozen to be further analyzed for DOC and DIC.

2.3.3 NH_4^+ Incubation Time Series Chambers

Using the oxygen profile, measured during the O_2 consumption experiments, gradients were identified and used as sample points. Five incubation bottles were set up with the same NH_4^+ concentration (100 μM) simultaneously and sampled at specific oxygen concentrations (i.e. 85, 55, 40, 15, 5% oxygen saturation) to account for changes in the nitrogen species. An extra bottle served as the initial (pre-test) analysis for all the constituents. Every individual unit was sacrificed at the pre-determined oxygen level. Then, a full water geochemistry characterization was done for each bottle. At low O_2

concentrations, nitrification may be generating secondary intermediates species of nitrogen, developing different reaction rates. Water transfer, treatment setup, and water characterization follows the same workflow as in section 2.3.

2.3.4 Control Groups

In order to assess the precision and verifiability of the experiments, two control groups ran in parallel with each treatment. The first control group was unamended BML water which determined the response of the bulk water microbial community in the oxygen consumption. These results permitted discerning between the effect on the oxygen consumption of the nitrifying organisms and the effect on the oxygen consumption from the rest of the endemic community that will also use oxygen. The second control group (abiotic control) corresponded to filter sterilized sample water. Sample water was sterilized by filter sterilization (0.2 μm, (ASTM, 2005; Bowman et al., 1967; Cheryan, 1998; Jornitz et al., 2001; Segers et al., 1994)). From the 2.5L bottle batch, four bottles were sterilized and used for the abiotic control experiments. During the experiments, sterilized water received the same NH_4^+ concentration as the experimental treatment to verify the contribution in oxygen consumption related to abiotic processes in the water. Ultra-pure water MQ (18.2 MΩ·cm at 25 °C; 0.22 μm membrane filter) was amended with NH_4^+ to assess the effect of the stock solution to the oxygen consumption by replicating an incubation chamber experiment.

2.3.5 Oxygen Consumption Rate

Oxygen probe sensors (YIS ProODO) were attached to the lid of the media bottle (Figure 2.5). This allowed measuring oxygen continuously inside the bottles, once the bottle receives the addition of ammonium and closed. There were five oxygen sensors which limited the number of replicates for each experimental treatment. Oxygen uptake rates were calculated, by determining the slope of the change in oxygen concentration, when the oxygen levels were decreasing.

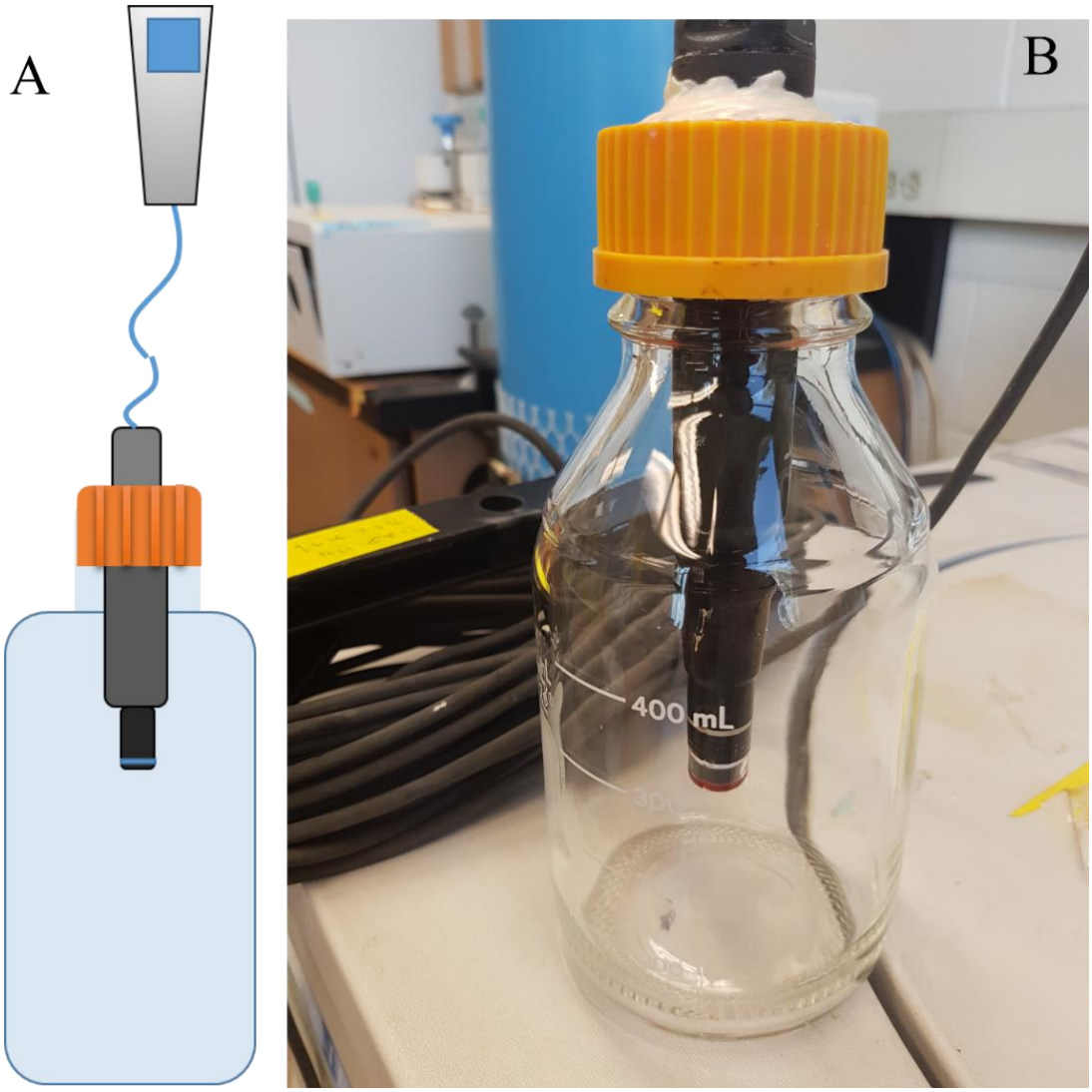

Figure 2.5 Nitrification microcosm bottle design. A) Schematic view of the microcosm oxygen consumption bottle, B) photographic view of the oxygen probe attached to the lid of a 500mL pyrex media bottle

All sample water was near oxygen saturation. Oxygen concentration decrease served as the proxy to delineate post-test analysis. The total oxygen consumption associated with nitrification was calculated by subtracting the abiotic consumption and consumption from the endemic control as follows:

Total oxygen consumption (nitrification) = NH_4^+ Treatment ΔO_2 – (abiotic ΔO_2 + untreated ΔO_2)

Every oxygen sensor probe was calibrated before each experiment according to manufacturer instruction. All customized bottles/lids were tested before the experiment, using oxygen depleted DI water, to check for oxygen diffusion (in and out).

2.3.6 Experiment Validity

Sample water was characterized for [NH_4^+], [NO_3^-] and [NO_2^-] to determine bulk water concentration before the beginning of each treatment experiment. Alkalinity and pH were measured before and after each experiment to monitor the changes in these two parameters. Alkalinity ranged between 500 to 700 mg/L CO_3^-, similar to what was previously reported (Allen, 2008, personal commun. Golder Corp 2013). Some physical aspects, such as temperature, light and pH, may affect the development of the proposed experiments. In order to control these aspects some considerations were adapted:

Temperature: Continuous monitoring of water sample temperature was controlled accordingly to maintain the same temperature during all the experiments.

Light: Nitrification, both ammonium and nitrite oxidation, is inhibited by strong light. Therefore, experimental water bottles were stored in a container and a cover was placed on top of it to eliminate the light effect.

Sterilization: All instruments and glass containers used to prepare solutions were acid washed and rinsed with ultrapure water to remove any trace metals and/or particulates. All 500mL bottles, which held the experiments, were steam sterilized to eliminate any microbial material.

Nitrogen species recovery: Standard curves were prepared for each constituent. Unamended water was mixed with a known concentration of either nitrogen species stock solution (i.e. ammonium, nitrate, or nitrite) and compared with measured concentration for the recovery of each nitrogen species

$$\%\ Recovery = \frac{measured\ concentration}{known\ added\ concentration} x100$$

2.4 Statistical analysis

Differences of geochemical properties between platforms for 2016 were tested using two-way ANOVAs to compare the means of each species individually, separated by zone. ANOVA's were also used to test for differences in mean CH_4, NH_4^+ and ΣH_2S concentration between layers. Fitting regression models were used to identify relationships between variables. Data were checked for a significance level of confidence (α=0.05). For chapter 4, one way ANOVA determined whether there are any statistically significant differences between the means of three experimental groups (amended,

unamended, and abiotic group) followed by Tukey HSD test to differentiate the significance of treatment means. Multiple linear regression models were used to identify relationships between variables. Dispersion was reported on each analysis as the standard deviation of the means. All statistical analyses (T-tests, ANOVA and models) and figures were produced using R studio (version 0.99.902, RStudio Team, 2015) working with R-base (version 3.3.2, R Development Core Team, 2008).

2.5 References

ASTM, 2005. ASTM F838-05, Standard Test Method for Determining Bacterial Retention of Membrane Filters Utilized for Liquid Filtration.

Bowman, F.W., Calhoun, M.P., White, M., 1967. Microbiological methods for quality control of membrane filters. J. Pharm. Sci. 56, 222–225.

Cheryan, M., 1998. Ultrafiltration and microfiltration handbook. CRC press.

Jornitz, M.W., Agalloco, J.P., Akers, J.E., Madsen, R.E., Meltzer, T.H., 2001. Filter Integrity Testing in Liquid Applications, Revisited. Pharm. Technol.

Reid, M.L., Warren, L.A., 2016. S reactivity of an oil sands composite tailings deposit undergoing reclamation wetland construction. J. Environ. Manage. 166, 321–329.

Segers, P., Vancanneyt, M., Pot, B., Torck, U., Hoste, B., Dewettinck, D., Falsen, E., Kersters, K., De Vos, P., 1994. Classification of Pseudomonas diminuta Leifson and Hugh 1954 and Pseudomonas vesicularis Büsing, Döll, and Freytag 1953 in Brevundimonas gen. nov. as Brevundimonas diminuta comb. nov. and Brevundimonas vesicularis comb. nov., respectively. Int. J. Syst. Evol. Microbiol. 44, 499–510.

Slater, G.F., Cowie, B.R., Harper, N., Droppo, I.G., 2008. Variation in PAH inputs and microbial community in surface sediments of Hamilton Harbour: implications to

remediation and monitoring. Environ. Pollut. 153, 60–70.

Viollier, E., Inglett, P.W., Hunter, K., Roychoudhury, A.N., Van Cappellen, P., 2000. The ferrozine method revisited: Fe (II)/Fe (III) determination in natural waters. Appl. geochemistry 15, 785–790.

Warren, L.A., Kendra, K.E., Brady, A.L., Slater, G.F., 2015. Sulfur biogeochemistry of an oil sands composite tailings deposit. Front. Microbiol. 6.

Westcott, F., Watson, L., 2005. End Pit Lakes technical guidance document. Clear. Environ. Consult. CEMA end Pit Lakes subgroup, Proj. 61.

Chapter 3: The precarious balance between physical transport and biogeochemical consumption in determining water cap oxygen concentrations in the first oil sands pit lake, Base Mine Lake.

Submitted by Arriaga D, Colenbrander Nelson T, Risacher FF, Morris PK, Corey Goad, Gregory Slater GF, and Warren LA to the Journal of Chemosphere, January 2018

3.1 Abstract

Bitumen extraction in the Athabasca oil sands region of Alberta Canada has resulted in 1 billion m^3 of tailings that require reclamation. Base Mine Lake (BML), the first commercial-scale end pit lake in the Alberta oil sands, is currently being assessed as a potential fluid fine tailings (FFT) reclamation strategy. To be successful, pit lakes require the development of an oxygenated portion of the water cap capable of supporting macrofauna. As this is the first oil sands pit lake, it is unknown to what extent oxygen-consuming constituents (OCC), such as methane, hydrogen sulfide and ammonia, all of which are elevated within FFT, will be mobilize into the water cap and impact oxygen concentrations. Results of this field-based study identify that high oxygen consumption rates (OCR) are driven by methane and ammonia at the FFT-water interface where concentrations of OCC are highest. These OCR values are within the range of highly productive eutrophic to hyper eutrophic lakes. Given the extensive mass of both methane and ammonia held within the FFT, as well as evidence of direct methanogenesis within

oil sands tailings ponds, biogeochemical redox cycling is anticipated to impact BML oxygen concentrations for decades. Vertical transport of oxygen through physical mixing is important to maintaining an oxic FFT-water interface, and in BML the oxygen influx slightly exceeds the mass consumed by biogeochemical redox cycling. The oxygen mass balance indicates that without the physical movement of oxygen into the hypolimnion, the OCR values currently observed would result in anoxia in the lower 3.5 meters of the BML water cap within 24 hours. The upwards migration of the oxic-anoxic boundary would enable generation of new OCC directly within the water cap through anaerobic redox transformations. For instance, the high levels of sulfate (~2 mM) in the BML water cap exceed water cap oxygen concentrations by three orders of magnitude, indicating that generation of $\sum H_2S$ would be a critical risk to the viability of this technology if anoxia were to establish within BML waters. Ultimately, the results here guide the development and application of water-capped tailings as a reclamation strategy for not only the oil sands industry, but also for other anthropogenically impacted or engineered systems with high oxygen demand.

3.2 Introduction

Alberta is one of the world's main producers of oil. The Athabasca Oil Sands region, (AOSR, Figure 3.1) in northern Alberta, has one of the largest oil reservoirs in the world (CAPP, 2018; GOA, 2012). Bitumen is extracted from oil sands by a warm water extraction process (Li et al., 2011), generating a mixture of solids and water called tailings. Once the sand settles out and some of the water is released, a fluid-like waste slurry known as fluid fine tailings (FFT) remains, consisting of fine clay and silt particles,

oil sands process-affected water (OSPW), and residual bitumen and solvents (i.e. naphtha). FFT is transferred to holding ponds to allow the fine particles to settle further by gravity densification. Dewatering and settling rates for FFT are normally greatest during the first year after deposition and slow every year afterward, requiring decades to fully consolidate (Dompierre and Barbour, 2016; Kasperski, 1992; Kasperski and Mikula, 2011; MacKinnon, 1989). Oil sands operators store all OSPW and tailings material on site until viable reclamation strategies are developed. Currently, over 1 billion cubic meters of FFT require reclamation in the AOSR (GOA, 2015). One of the current long-term reclamation strategies being investigated for FFT is water-capped tailings technology (WCTT) by the use of pit lakes. In WCTT, a freshwater cap is established over a layer of FFT typically within a mined-out surface pit, resulting in an artificial lake referred to as a pit lake (PL). Pit lakes have been widely used to reclaim coal and metal mine pits for more than 100 years (Castro and Moore, 2000). However, as oil sands FFT differ from coal and metal mine tailings physically in consolidation properties, geochemically in the types and concentrations of geochemically reactive constituents and microbiologically in the types and functionalities of the microbial communities that are associated, the viability of WCTT for oil sands tailings remains uncertain.

Syncrude Canada, Ltd. (Syncrude) is one of the biggest proponents for WCTT and PL within the AOSR, and has been performing small-scale field and laboratory testing for nearly four decades. However, certain aspects of WCTT and PL implementation can only be studied and confirmed at full scale (COSIA, 2012). Syncrude has built the first commercial demonstration of an oil sands pit lake, Base Mine Lake

(BML; Fort McMurray, AB Canada, Figure 1) and is currently monitoring and studying the development of the lake. One important feature of a pit lake is that oxygen levels within the upper water cap are high enough to support a self-sustaining ecosystem, including macrofauna (Soni et al., 2014). A variety of oxygen-consuming constituents (OCC), such as methane (i.e. ~1.4 mM), ammonia (~700 μM), and hydrogen sulfide (~86 μM) as well as active microbial communities are present within FFT (Allen, 2008; Chen et al., 2013; Holowenko et al., 2000) that will negatively impact the development and maintenance of an oxic zone with the water column and present considerable risk to the success of PL for FFT. Thus, it will be critical to identify how FFT and mobilized OCC impact the BML water column oxygen concentrations to inform the design of further pit lakes. As at least another ten PL are currently planned for the region, understanding the effect of FFT on the water column is critical for the success of these pit lakes across the whole industry.

Constituents within the FFT will almost certainly be mobilized into the BML water cap. These constituents include particulates (e.g. dissolved and particulate organic carbon: DOC and POC, Fe and S containing solids), gases (e.g. H_2S, CH_4) and dissolved ions (e.g. NH_4^+, HS^-, and Fe^{2+}; Allen, 2008; Quagraine et al., 2005; Siddique et al., 2014; Westcott, 2007). Diverse microbial communities capable of methanotrophy, methanogenesis, and sulfur reduction and oxidation exist within active within oil sands tailings ponds. Therefore, oxygen is likely being consumed by biogeochemical redox transformations of OCC mobilized from the FFT (Fedorak et al., 2003; Fedorak et al., 2002; Holowenko et al., 2000; Penner and Foght, 2010; Ramos-Padron et al., 2011;

Saidi-Mehrabad et al., 2013; Siddique et al., 2006; Siddique et al., 2007). Oil sands tailings ponds have been shown to be anoxic (Chen et al., 2013; Holowenko et al., 2000; Stasik et al., 2014), with typically <1 m oxic surface layer (Haveroen et al., 2005; Ramos Padron, 2013). Consequently, anaerobic Bacteria and Archaea tend to dominate these ecosystems (Fedorak et al., 2003; Fedorak et al., 2002; Holowenko et al., 2000; Siddique et al., 2006; Siddique et al., 2007). These tailings ponds have also changed biogeochemically as they have matured. Oxygen consumption within Syncrude's Mildred Lake Settling Basin (MLSB) has changed over the last three decades from primarily H_2S-driven oxygen consumption, to H_2S and CH_4 driven oxygen consumption, after methanogens began producing CH_4 *in situ* (Foght et al., 1985; Sobolewski, 1992, 1997). Since BML is the first demonstration AOSR pit lake, it is not known how much OCC will be mobilized from the FFT, and therefore how much oxygen will be consumed within the water cap. Thus, it is not known how long it will take for an oxic zone to be established in BML.

BML differs from tailings ponds in a number of physical and chemical aspects. The water cover in BML is ~10 m, which is twice as deep as the typical <5 m water depth of tailings ponds. Also, tailings are not added or removed from in BML, as would occur in a tailings pond, and the water cap of BML is a mixture of oil sands process water and freshwater, not just OSPW which would be present in tailings ponds. The first study assessing the water cap geochemistry of BML (Risacher et al., 2018) determined that 2015 summer water cap oxygen concentrations were impacted primarily by CH_4 mobilized from the FFT (3 years post-commissioning), but also by NH_4^+ mobilized from

the FFT in 2016. Interestingly, that study also identified that oxygen persisted to the FFT-water interface (FWI), albeit at low concentrations (i.e. 10 µM, < 5 % saturation), which is very different from the anoxic conditions observed in oil sands tailings ponds. Further, the maximum rate of decrease with depth measured in water column oxygen profiles in BML occurred in the metalimnetic region of the water cap, despite the highest concentrations of reductants occurring at the FWI, suggesting that other processes, not identified in that study, may also affect oxygen concentrations in BML. Here, the objectives of this study were to determine how oxygen consumption rate (OCR) changes with depth in the BML water cap, and identify which OCC is involved. Also, this study will determine the role of physical processes in the overall net O_2 profile of the water cap of BML.

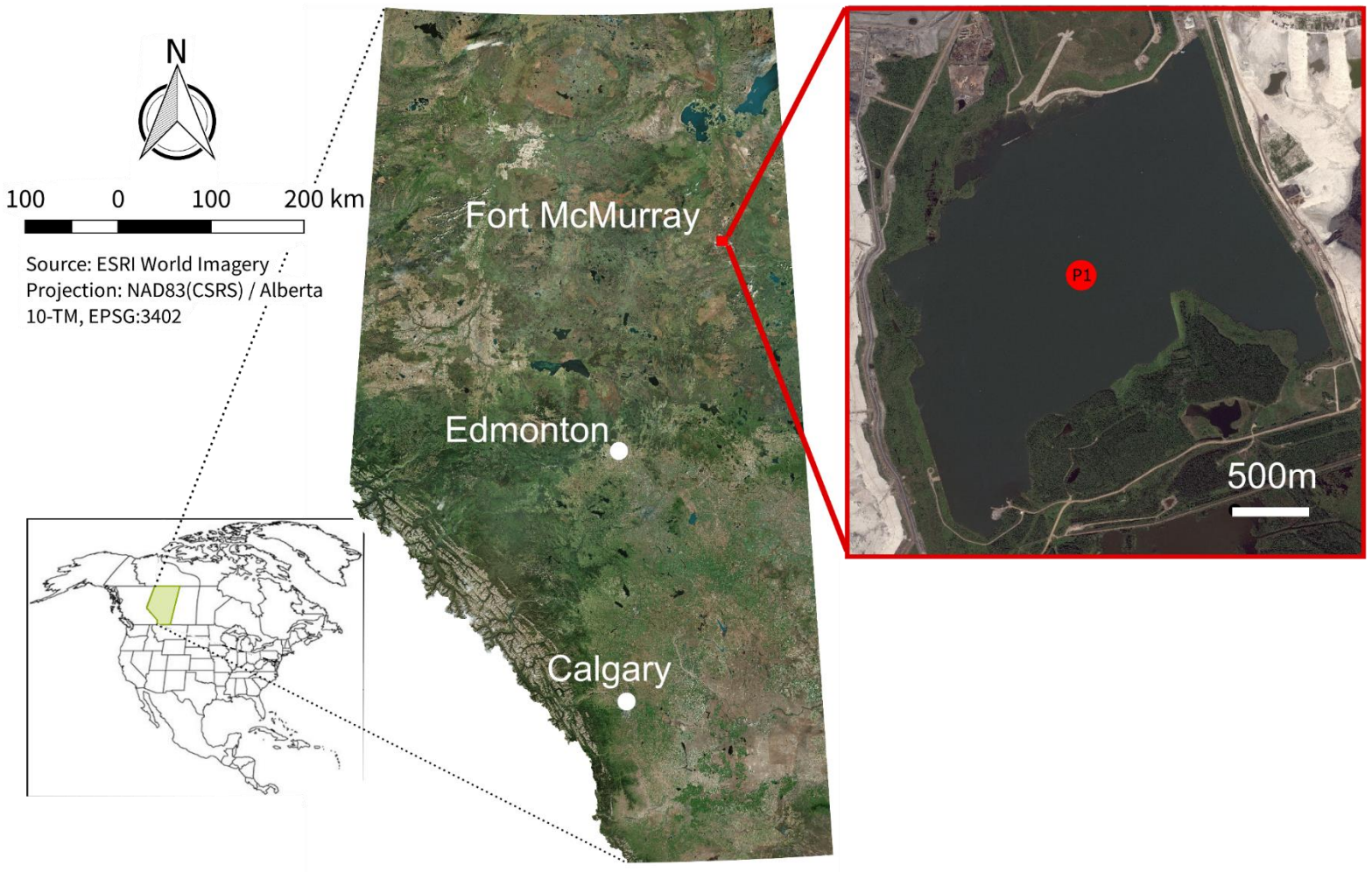

Figure 3.1 A) Location of the AOSR in northern Alberta, Canada. Base Mine Lake (inset), the first oil sand end pit lake, P1: platform 1

3.3 Materials and methods

3.3.1 Study Area

Base Mine Lake (Fort McMurray, AB; 57° 0' 38.88"N, 111° 37' 22.44"W) was commissioned in 2012 and consists of ~10 m of a mixed freshwater/OSPW water column over top of ~40 m of FFT material in an approximately 7 km^2 lake (Testa, 2010). Prior to commissioning, FFT was deposited at this site through a series of discharge pipes over 14 years, and the age of the FFT may vary from bottom to top depending on where the FFT was dredged from (e.g. MLSB). All surveying, sampling and geochemical analysis occurred at the central platform (P1) within BML (Figure 1). The survey, sampling and geochemical analyses are briefly summarized below, and full details are provided in Risacher et al. (2018).

3.3.2 OCR Experimental Campaign Design

OCR values were determined on seven different dates between July 14 and August 30, 2016 (July 14, July 26, July 27, August 3, August 10, August 17, and August 30). A total of six OCR experiments were conducted on each of these dates across multiple depths (3 to 6 depths were assessed simultaneously), including the FWI, the metalimnetic-hypolimnetic interface, the mid hypolimnion and upper epilimnion zones. The depths for OCR experiments were identified from the water column oxygen profile measured at the start of each experimental campaign. A water sample for each OCR experimental chamber was collected at the time of filling to provide the geochemical characteristics of the water prior to experimentation (Figure 3.2). The specific depths

chosen for OCR experiments over these seven sampling campaigns were selected to determine how OCR varies with depth (i.e. in each stratified layer: epilimnion, metalimnion, hypolimnion). OCR was measured at a greater depth resolution within the hypolimnion (close to the FWI and the underlying FFT, which is the source of potential OCC) and the metalimnion (which represents the largest decrease in oxygen concentrations within the water cap). Variability between individual OCR chambers was assessed by conducting duplicate experiments at same depth.

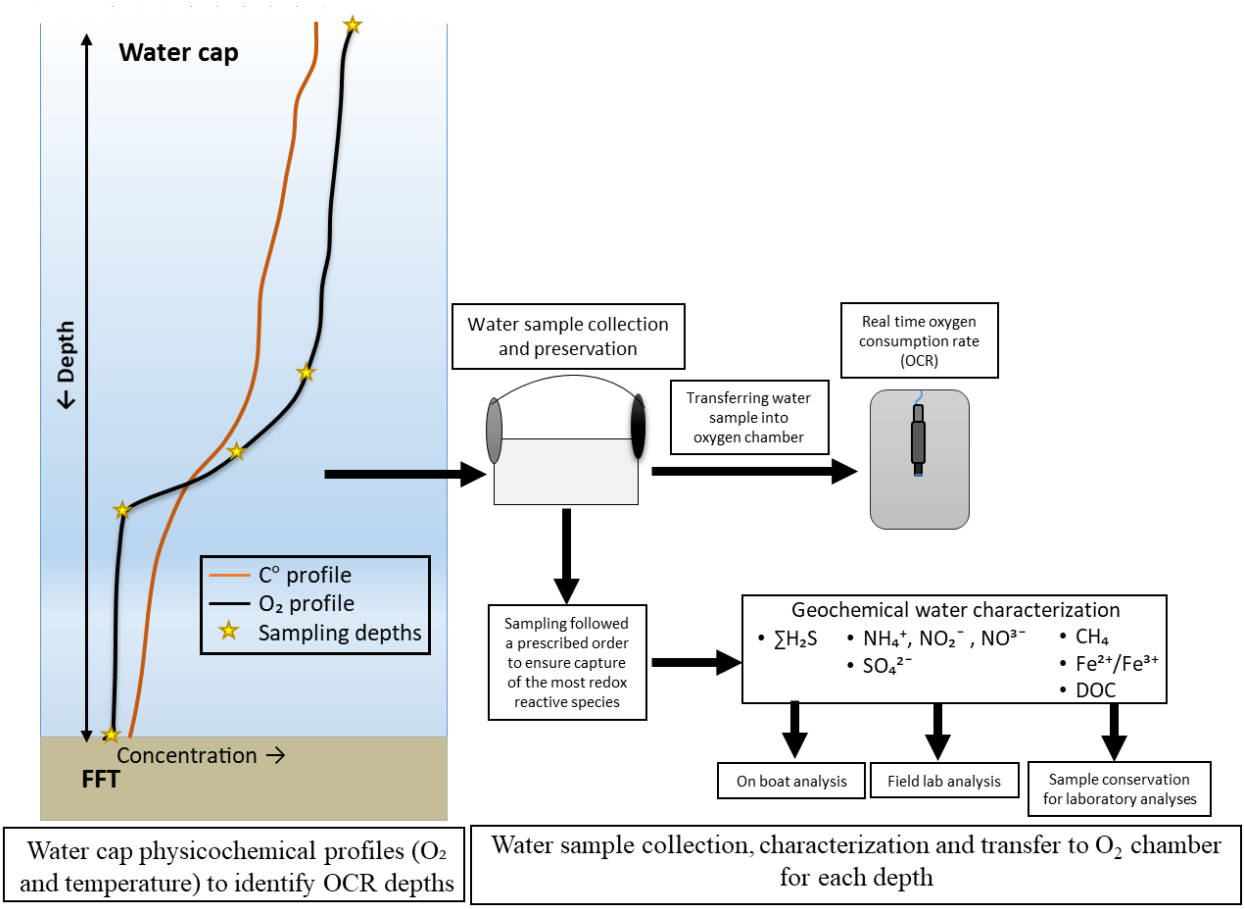

Figure 3.2 The depths at which samples were collected for OCR experimentation and geochemical characterization were determined from temperature and oxygen profiles. Depths selected for each campaign were chosen to capture gradients in oxygen concentration, and always included the FWI region, where OCC concentrations would be highest. Water was collected from each of the identified depths for each campaign (Table 3.1) to fill the experimental OCR chambers and for geochemical characterization following a prescribed order to ensure the preservation of redox-sensitive constituents (i.e. CH_4, $\sum H_2S$ and Fe^{2+}).

3.3.3 Water Physicochemistry Characterization

Physicochemical characteristics in the water column (pH, temperature, dissolved oxygen concentration and % saturation, specific conductivity, ORP, turbidity, salinity; YSI Professional Plus 6-Series Sonde, YSI Incorporated) were measured from the BML surface to the FWI at ~50 cm intervals. The depths for OCR experiments were determined from these profiles (Figure 3.2).

3.3.4 Geochemical Sample Collection and Preservation

All sampling equipment and sample containers were prepared by soaking in 5% (v/v) HCl for 12 h followed by seven rinses with ultrapure water (18.2Ωm cm-1, MilliQ, Millipore) (inorganic analytes). Bulk water was collected in a 9 L Van Dorn bottle (Wilco Model: E-411-19XX-H62) and samples were collected for measurement of CH_4, bulk carbon (DOC and POC), and dissolved (< 0.45 µm) aqueous species of Fe^{2+}/ Fe^{3+}, NH_4^+, NO_2^-, NO_3^-, ΣH_2S, and SO_4^{2-}.

Sampling followed a prescribed order so that the most redox reactive species (CH_4 and ΣH_2S) were measured first. Briefly, samples for CH_4 measurement were extracted immediately upon retrieval of the Van Dorn sampler on the boat, by syringing 30 mL of sample directly from the closed Van Dorn via the embedded sampling tube with a 3-way stop cock into a 60 mL plastic syringe. The water was then transferred by injection into a pre-evacuated 60 mL serum bottle (Wheaton) and crimp sealed with a 20 mm chlorobutyl stopper (Bellco glass). The chlorobutyl stoppers were pre-treated by boiling in 1 N NaOH for one hour prior to use. The serum bottles were pre-treated with

mercuric chloride to halt any microbial activity once the sample was introduced. Samples were refrigerated and analyzed upon return to McMaster University.

For $\sum H_2S$ analyses, water samples were collected into acid-washed plastic 60 mL syringes from the Van Dorn sampler and filtered directly through 0.45 μm sterile syringe filters (Supor membrane) into sample containers containing reagents to fix the $\sum H_2S$, and analyzed on the boat using the methylene blue method with a HACH portable spectrophotometer (HACH DR/2800 spectrophotometer, HACH Company, Loveland, CO, USA).

Samples for Fe (II) and Fe (III) were collected into acid-washed 15 mL polyethylene terephthalate centrifuge tubes and preserved by the addition of 2% v/v Optima-Grade hydrochloric acid and refrigerated until return to McMaster University for analysis. Water samples for measurement of organic and inorganic carbon were collected in carbon-clean amber glass 120 mL bottles. Bottles were cleaned with detergent, rinsed with MilliQ water, then ethanol, and placed in a 10% HCl bath for >8 hours. After seven rinses with MilliQ water, bottles were placed in a muffle furnace at 450°C for 8h to remove any residual carbon. Lids were rinsed with a 1:1:1 mixture of dichloromethane, hexane, and methanol and allowed to dry. In the field, each bottle was rinsed twice with sample before filling and then frozen at -20°C until filtration for measurement of dissolved organic carbon (DOC) in the laboratory.

A further water sample was collected into a 1 litre, acid-washed Nalgene bottle for SO_4^{2-}, NO_3^-, NO_2^- and NH_4^+ analyses and stored on ice until the end of the day. These

samples were refrigerated until they could be analyzed at the field laboratory, or upon return to McMaster University.

3.3.5 Geochemical Analyses

Three to seven replicates collected at the same time and from the same depth during filling of each OCR chamber were analyzed for all geochemical analytes. Field blanks (3; ultrapure water, filtered and preserved on site) and process blanks (3) were collected and analyzed for each analyte.

Samples for carbon analysis were thawed and filtered with a syringe-driven 0.7µm GF/F glass microfiber filter unit (13 mm, GE Life Sciences) immediately before analyses. The filtrate was analyzed in duplicate for total organic carbon (TOC) and total inorganic carbon (TIC) on a Shimadzu TOC-L Total Organic Carbon Analyzer with an autosampler ASI-L, using the 680°C combustion catalytic oxidation method as per manufacturer recommended protocols (Mandel Scientific). Total organic carbon values were obtained by subtracting the TIC values from the total carbon values. Dissolved inorganic carbon (DIC) and DOC were analyzed for each sample.

Methane was analyzed following the method described by Slater et al. (2008). Briefly, CH_4 was measured with an SRI GC (model 8610C) equipped with a 3' (1 m) silica gel column and a flame ionization detector at McMaster University.

Samples for Fe (II) and Fe (III) were analyzed colorimetrically by a modified ferrozine method from Viollier et al. (2000) at McMaster University. SO_4^{2-}, NO_3^-, NO_2^- and NH_4^+ were analyzed by spectrophotometry (Method 8051, Method 8171, Method

8507 and 8155; HACH DR/2800 spectrophotometer, HACH Company, Loveland, CO, USA) either in the on-site field laboratory or at McMaster University.

3.3.6 Oxygen Consumption Rate Experiments

A specialized experimental oxygen consumption chamber was constructed from customized pelican cases by embedding oxygen sensors and inlet and outlet ports so water could be introduced while expelling air from the outlet port (Figure 3.2). An optical oxygen sensor (YSI ProODO) was embedded directly inside the oxygen consumption case through a third port to continuously log oxygen concentrations (mg/L and % saturation; every minute), pressure (kPa) and temperature (°C) every minute within the sealed chamber via an external data logger (ProODO handheld). All ports were air- and water-sealed by a through-wall fitting and held in place with an industrial adhesive agent (3M Marine Adhesive Sealant 5200). All customized OCR experimental chambers were tested with O_2-depleted deionized water to ensure no oxygen could diffuse into the cases prior to experimental use. Oxygen diffusion into the cases over 24 hours was non-detectable (measured by the O_2 probe). The DO probes were calibrated prior to each use according to the manufacturer's instructions. To fill each OCR chamber, water was collected into a Van Dorn sampler from each of the desired depths and then transferred directly through the outlet sampling tube into the inlet port on the OCR chamber, which minimized exposure of the water sample to the atmosphere. At the same time, a duplicate water sample from the same depth was collected for geochemical characterization as described above. This water sample allowed for an initial, or baseline, geochemical characterization of the water for each OCR experiment. A total of 31 OCR experiments

were deployed throughout the water column during July and August of 2016 (Table 3.1). The experiments lasted from a few hours to a few days, depending on the starting oxygen concentration and oxygen demand. The OCR was determined by the least squares method of the change in oxygen concentration (e.g. HagMan and la Cour Jansen, 2007) after the oxygen concentration neared zero (~5 μM) inside the chamber. For three duplicate OCR experiments in the hypolimnetic zone duplicates varied between 10 and 15% from the mean. We attribute this difference to disturbance of the FFT during sampling, which unavoidably resuspends the FFT particles and creates variance in the duplicate OCR experiments.

3.3.7 Vertical oxygen mixing model

Water cap temperature and oxygen profiles were used to quantify the how much vertical transport of oxygen was occurring using the heat budget method (Benoit and Hemond, 1990; Heinz et al., 1990; Jassby and Powell, 1975). The profiles had a vertical resolution of 0.5 m, measured diurnally on four days (i.e. for July 26, July 27, August 3, and August 17) when a full water column characterization occurred. To account for vertical transport in the oxygen mass balance, vertical profiles of turbulent diffusivity K_z (m^2/d) were estimated from the temperatures measured in the water column profiles. K_z values were calculated from the change in heat content of the lake between the thermocline and the upper boundary of the hypolimnion (Cornett and Rigler, 1987; Foley et al., 2012; Kreling et al., 2017). This method associates the total change in heat content below the depth z_i with the diffusive heat flux at this depth, so the turbulent diffusivity K_z can be estimated as:

$$Kz = -\frac{\int_{z}^{z_i} dT/dt \cdot A \, dz}{A \cdot dT/dz} \qquad \text{Equation 1}$$

where dz (m) is the depth and dT (°C) is the temperature differences between lower metalimnion and the upper boundary in the hypolimnion; A (m^2) is the area at the upper hypolimnetic boundary. Because the heat balance underlying Eq. 1 does not consider warming by penetrating solar radiation, its application is restricted to depths exceeding the light penetration (estimated euphotic zone ~1m; supporting material Table S1).

The daily vertical transport of oxygen across the upper boundary of the hypolimnion (VT, mmol/m^2/d) was calculated as the product of the turbulent diffusivity coefficient (K_z) by the vertical gradient in oxygen concentration (dO_2/dz in mmol/m^3/m or mmol/m^4) calculated from the water cap oxygen profile versus depth data (Denkenberger et al., 2007; Kreling et al., 2017; Matthews and Effler, 2006):

$$VT = -Kz \cdot dO_2/dz \qquad \text{Equation 2}$$

The vertical gradient in oxygen concentration used in the calculations is the gradient across the depth delineating the upper boundary of the hypolimnion (below the depth of the maximum temperature gradient and where the temperature gradient between adjacent 1-meter strata was <0.5 °C/m), and is calculated from the water cap oxygen profile versus depth data. Gradients and fluxes are directional; positive vector magnitudes presented here indicate when oxygen is transported into the hypolimnion. The vertical transport method assumes that a lake is horizontally well-mixed, so horizontal water temperature and dissolved oxygen changes are small when compared to variations in the vertical direction (Burba, 2013; Charlton, 1980; Quay et al., 1980; Stauffer, 1985).

3.3.8 Statistical Analyses

All statistical analyses were performed and figures produced in R studio (version 3.2.2., RStudio Team, 2017) working with R-base (version 3.3.2, R Development Core Team, 2008). Significance for all statistical analyses was set at an alpha value of 0.05.

3.4 Results and Discussion

3.4.1 Water Column Physicochemical Characteristics

The BML water cap was thermally stratified for the first six sampling campaigns (July 14 to Aug 17), with a mean surface temperature of 21.5±0.6 °C and an FWI mean temperature of 13.6±0.6 °C (Figure 3.3; Table S2). Oxygen profiles also evidenced depth dependent concentrations; decreasing from mean epilimnetic oxygen values of 203 ±2.3 µM (6.5 mg/L; 73 % saturation) to 8.1±0.6 µM (≈0.3 mg/L; 2.5 % saturation) in the deepest hypolimnion waters just above the FWI (Figure 3.3). The greatest decrease in oxygen concentration was measured in the metalimnion, decreasing from 187 µM (67% saturation) at the top of the metalimnion (~4.5 m) within 3 meters to 10 µM (< 5% saturation) at the top of the hypolimnion (Figure 3.3). On August 30, fall turnover had occurred which resulted in a water cap temperature of 17°C and oxygen concentration of 140 µM (45 % saturation) from the BML water surface to the FWI (Figure 3.3). Conductivity and pH remained constant within the water column across the six stratified sampling campaigns with mean respective values of 2795±21 mS/cm and 8.2±0.1, until the FWI where conductivity increased and pH decreased (supporting material Table S2).

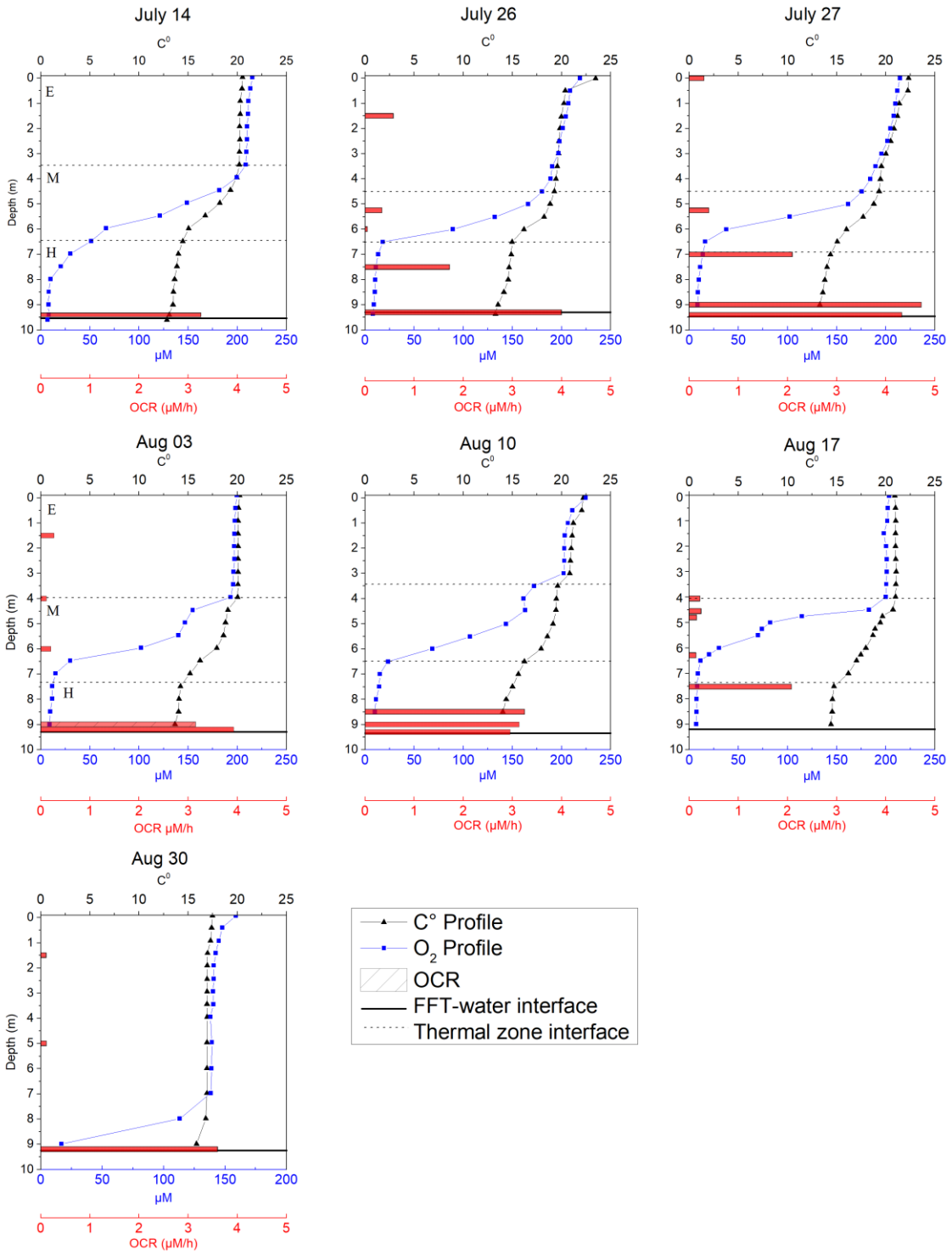

Figure 3.3 BML water cap oxygen and temperature profiles (July 14 to August 30, 2016) and experimentally determined OCR values. Note Aug 30th was post turnover. E: epilimnion, M: metalimnion and, H: hypolimnion.

3.4.2 Oxygen Consumption Rates

A total of 31 OCR experiments were carried out assessing oxygen consumption rates within the three thermal regions of the stratified BML water column, and at the FWI on the first three sampling campaigns (July 26, July 27 and August 03; Figure 3.3, Table 3.1). Additionally, OCR experiments at a higher depth resolution (0.5 m) focused on two zones of interest: the FWI (August 10) and across the metalimnetic-hypolimnetic interface (August 17).

The depth-dependent OCR values determined for each sampling date/depth indicate OCR values are highest (mean of 3.6 µM/h ±0.2; n=13) at the FWI and decrease moving upwards into the water column (Figure 3). These observations supported the hypotheses that OCR are depth-dependent and the FWI has the highest OCR values associated with the FFT as the source of OCC. Metalimnetic and epilimnetic OCR values were equivalent and an order of magnitude lower than those measured at the FWI, in the range of 0.2 µM/h±0.04 (n=14) despite much higher water cap oxygen concentrations (212 and 177 µM respectively; Figure 3.3). OCR values measured on August 30, post turnover, show no difference between those measured in the water column and at the FWI, and were lower than the values observed during summer stratification for the previous six experimental campaigns. The FWI OCR values determined here for BML are consistent with those measured in hypereutrophic systems (Gelda and Auer, 1996), while the measured epilimnetic and metalimnetic OCR values are below those reported for meso-eutrophic systems, closer to those associated with highly productive systems (Table 3.2).

Despite numerous studies on pit lakes within coal and metal mining (see Castendyk et al., 2015 for a complete list of publications) no published values on OCR in these contexts exist to compare the rates established here for BML. Thus to the best of our knowledge, these OCR represent the first values established for any pit lake and indicate that biogeochemical oxygen consumption is important in the consideration of the possible viability of WCTT. Further, our results provide an important biogeochemical baseline of possible oxygen consumption rates that can be expected for pit lakes containing methane and ammonia rich tailings that can help guide PL design.

Table 3.1 Oxygen consumption rate values (OCR; uM/hr) determined for different depths of the BML water cap in July and August 2016. (Temperature is the *in-situ* temperature value at the time of water collection for a given depth; FWI: FFT-water interface)

Depth (m)	Zone	Temperature °C	OCR uM/hr	Time elapsed (hours)
9.4	FWI	21.6	3.3	9.2
1.5	Epilimnion	22.1	0.6	11
5.3	Metalimnion	22.2	0.3	14
6.0	Metalimnion	21.2	0.1	11
7.5	Hypolimnion	17.5	1.7	15
9.4	FWI	16.0	4.0	12
9.4	FWI	16.2	4.0	14
0.0	Epilimnion	23.1	0.3	10
5.3	Metalimnion	22.6	0.4	6.0
7.0	Hypolimnion	16.9	2.1	10
9.0	Hypolimnion	17.4	4.7	8.7
9.4	FWI	17.4	4.3	7.0
1.5	Epilimnion	20.4	0.2	30
4.0	Metalimnion	20.5	0.1	13
6.0	Metalimnion	23.2	0.2	19
9.0	Hypolimnion	19.2	3.2	19
9.2	FWI	17.5	3.9	9.5
8.5	Hypolimnion	22.7	3.2	7.1
8.5	Hypolimnion	19.2	3.3	8.3
9.0	Hypolimnion	16.5	2.7	2.0
9.0	Hypolimnion	16.0	3.6	2.0
9.2	FWI	16.2	3.0	5.4
9.2	FWI	20.0	3.0	7.7
4.0	Metalimnion	17.8	0.2	16
4.5	Metalimnion	20.6	0.2	31
4.8	Metalimnion	17.6	0.1	22
6.3	Metalimnion	19.4	0.1	25
7.5	Hypolimnion	18.1	2.1	18
1.5	Epilimnion	16.9	0.1	24
5.0	Metalimnion	17.7	0.1	26
9.2	FWI	17.3	3.6	14

Table 3.2 Mean and standard deviation (±) summer 2016 BML OCR values (per area) determined across the seven sampling campaigns in each of the four water cap regions (epilimnion, metalimnion, hypolimnion and FWI) compared to literature values for systems spanning a range of trophic status
SOD: sediment oxygen demand; AHOD: aerial hypolimnetic oxygen demand; AHM aerial hypolimnetic mineralization

Site Location	Type of measurment	Environment	mM $O_2/m^2/d$	Reference	
BML Epilimnion	OCR	Oil sand Pit Lake	7.7 ±5.1		
BML Metalimnion	OCR	Oil sand Pit Lake	4.9 ±2.5		
BML Hypolimnion	OCR	Oil sand Pit Lake	66.9 ±5.9		
BML FFT-water	OCR	Oil sand Pit Lake	87.4 ±4.4		
Superior	AHOD	Great lakes	13	Charlton	1980
Lac d'Annecy	AHM	Mesoeutrophic lake	37	Masson et al	2001
Lake Mendota	AHOD	Eutrophic lake	30	Stewart	1976
Texoma	SOD	Eutrophic lake	53	Veenstra & Nolen	1991
Odongagoa	AHOD	Hypereutrophic lake	112	Matthews & Effler	2006

3.4.3 The linkage between OCR and OCC

Initial BML water chemistry for all OCR experiments shows increasing concentrations of potential OCC with depth: Fe^{2+}, $\sum H_2S$, CH_4, NH_4^+, and DOC (i.e. the highest concentrations were observed closest to the FFT; Table 3.3). Concentrations of Fe^{2+} (ANOVA, d.f. =18, $p>0.05$) and $\sum H_2S$ (ANOVA, d.f. =18, $p<0.05$) remained below 5 µM throughout the water column, indicating that their impacts on OCR would be constrained to the FWI region. DOC concentrations showed a nonsignificant trend of increasing concentrations with depth (ANOVA, d.f. =13, $p>0.05$). Aqueous dissolved methane (ANOVA, d.f. =19, $p<0.001$) concentrations decreased from a maximum of 120 µM at the FWI to <5 µM in the lower metalimnion. NH_4^+ (Figure 3.4; ANOVA, d.f. =18, $p<0.01$) was detected throughout the BML water cap (~10 µM in the epilimnion).

Table 3.3 Mean (± standard deviation) metalimnetic (n=7) and hypolimnetic (n=6) BML concentrations of important biogeochemical analytes across the experimental campaigns dates July 14 to Aug 30th, 2016; note epilimnetic geochemical analyses were only available for Aug 3rd

Constituent	Epilimnion	Metalimnion	Hypolimnion
CH_4 (µM)	0.28	2.2±1.3	91±6.2
$\sum H_2S$ (µM)	0.0*	0.04±0.0	2.1±0.66
SO_4^{2-} (mM)	1.8	2.0±0.17	2.1±0.12
NH_4^+ (µM)	11	11±1.9	41±3.9
NO_2^- (µM)	2.3	2.8±0.52	1.2±0.22
NO_3^- (µM)	46	31±2.7	16±2.9
DOC (mg/L)	46	53±1.6	54±1.7
Fe(II) (µM)	3.5	2.8±0.78	4.2±1.0
Fe(III) (µM)	9.4	5.9±1.2	8.5±1.3

* Below detection limits

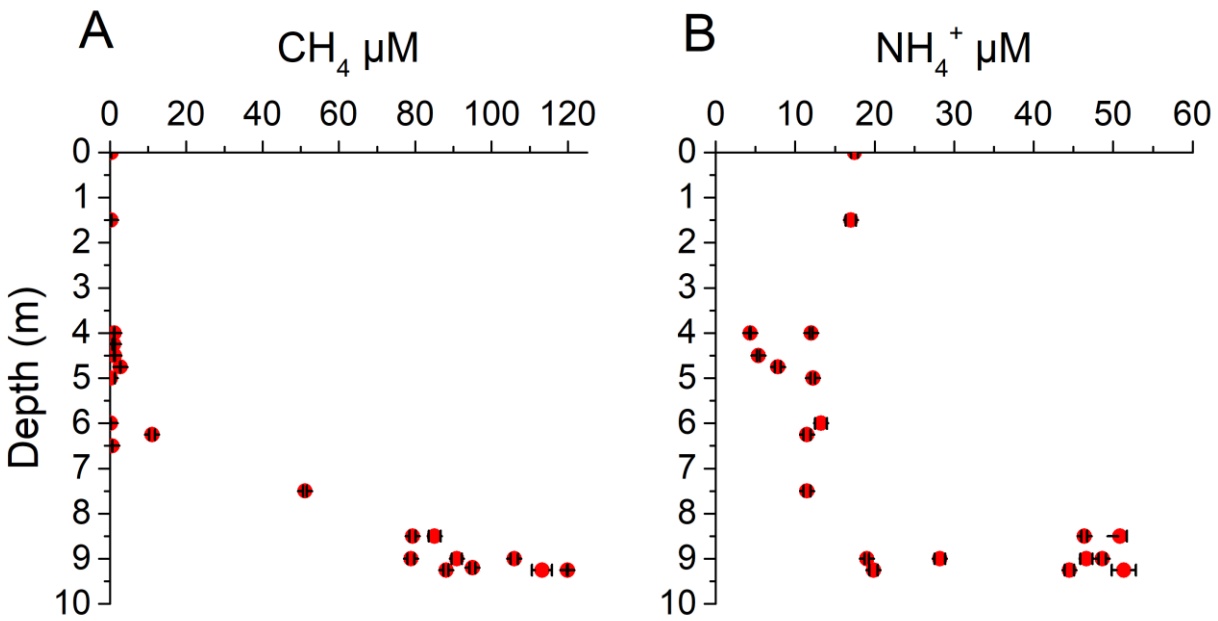

Figure 3.4 Mean BML water cap dissolved (a) methane and (b) ammonia concentrations compiled from all the depths analyzed across the six stratified experimental OCR campaigns, as a function of depth. Error bars represent standard error of triplicates.

Linear regression analyses indicated significant positive relationships between initial methane and ammonium concentrations and OCR values across the entire water cap (ANOVA, d.f. =17, $p<0.05$) and for the hypolimnion specifically (ANOVA, d.f.=9, $p<0.05$; Figure 3.5A-D). However, no significant relationships were observed between both methane or ammonium concentrations and OCR values for the epilimnion/metalimnion regions (ANOVA, d.f. =7, $p>0.05$; Figure 3.5E-F). In addition, the best fit models for methane explained a larger percentage of the variance in observed BML OCR values, both throughout the water cap (94%) and in the hypolimnion specifically (77%; Fig 3.5A, and Fig 3.5C) the best fit models for ammonium alone explained 86% and 55% of the variance in the water cap and hypolimnion OCR values, respectively (Figures 3.5 A and D). The combination of methane and ammonium in the epilimnion and metalimnion did not significantly affect variance in OCR values (Figures 3.5, ANOVA, d.f.=7, $p>0.05$) while in the hypolimnion, these constituents combined explained 79% of the variance (Figure 3.5H). While individually, both constituents can explain a large portion of the OCR, the overall combination of methane and ammonium throughout the water cap slightly increased the variance explained from 94% by methane alone to 97% of the variance in OCR explained, when both methane and ammonia were considered (Figures 3.5 A-I). Together, rather than individually, methane and ammonium concentrations showed to be driving the oxygen consumption throughout the water cap. Depth-dependent differences in concentrations changes for methane and ammonia reflect these differential influences on OCR. Methane concentrations decreased 98% from ~90 µM in the hypolimnion to ~2 µM in the metalimnion and to ~0.3 µM in the

epilimnion. In contrast, ammonia concentrations decreased only 73% from a hypolimnetic high of ~ 41 µM to 11 µM in both the metalimnion and epilimnion. In other words, the highest rates occurred at the highest concentrations of both methane and ammonia which is consistent with the mobilization of OCC from the FFT layer impacting oxygen concentrations, such that the highest concentrations of these two constituents and associated oxygen consumption occur at the FWI. These results support the hypothesis that methane, in addition to ammonium, is the primary OCC driving observed oxygen consumption in BML water cap. Other studies of a hypereutrophic lake report similar results, with CH_4 accounting for the largest portion (between 40 to 70%; lower than that observed here for BML) of the oxygen demand, followed by NH_4^+ and, in a secondary role, Fe^{+2} and $\sum H_2S$ (Adams et al., 1982; Brooks and Effler, 1990; Gelda and Auer, 1996; Sweerts et al., 1991).

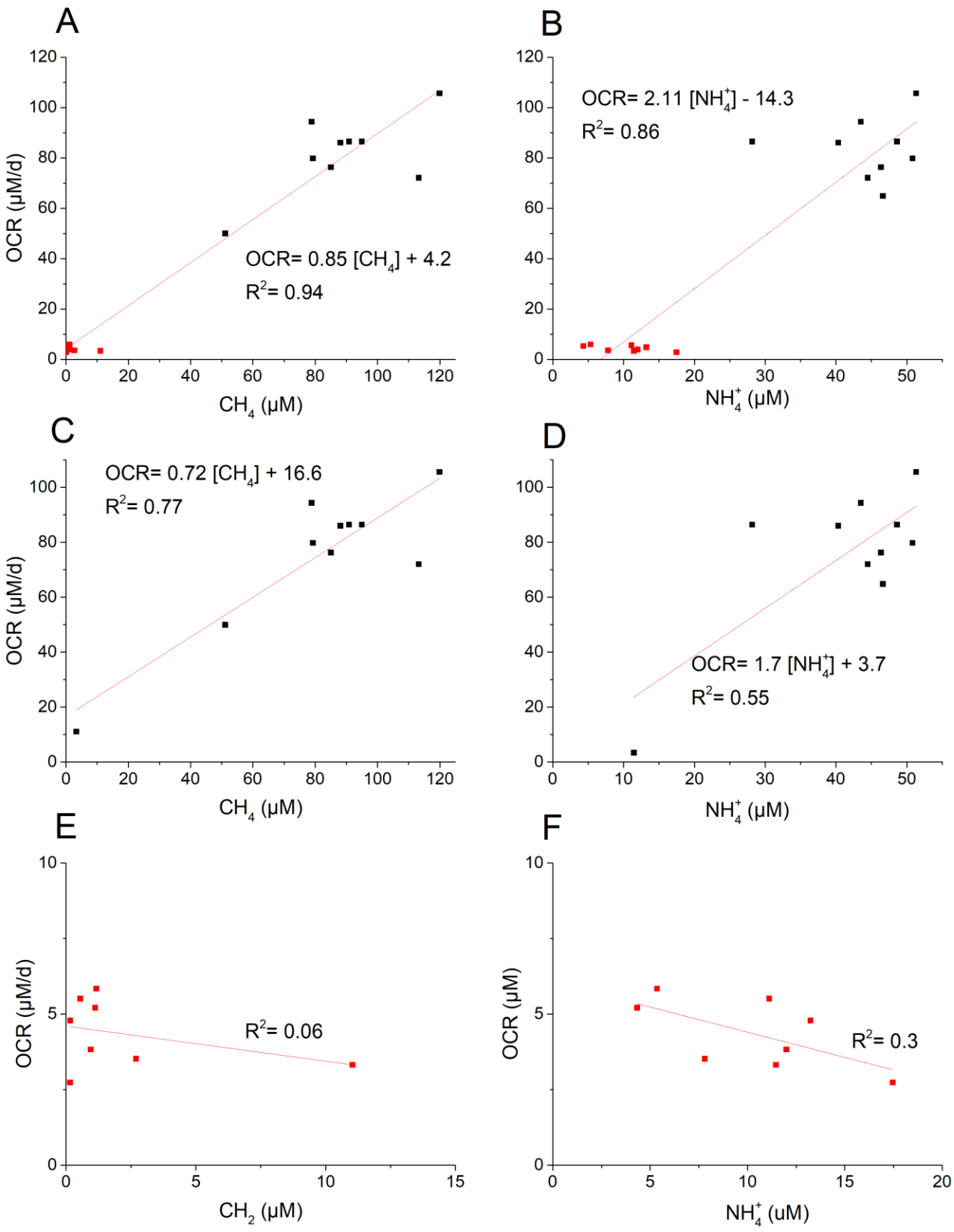
A
OCR (µM/d)
CH4 (µM)
OCR= 0.85 [CH4] + 4.2
R2= 0.94
B
OCR= 2.11 [NH4+] - 14.3
R2= 0.86
NH4+ (µM)
C
OCR= 0.72 [CH4] + 16.6
R2= 0.77
D
OCR= 1.7 [NH4+] + 3.7
R2= 0.55
E
R2= 0.06
CH2 (µM)
F
OCR (µM)
R2= 0.3

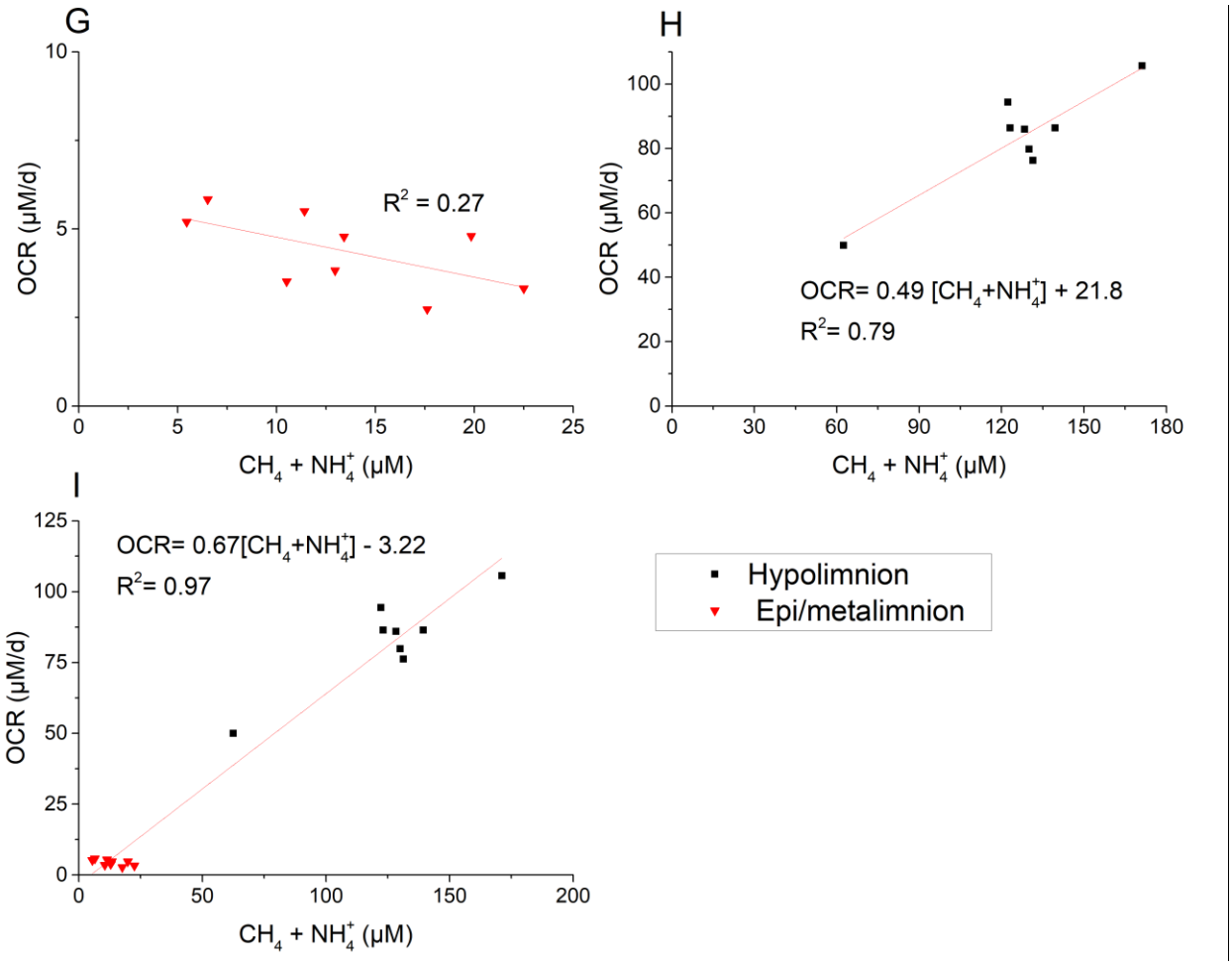

Figure 3.5 Linear regression modelling of BML water cap OCR values versus water cap concentrations of (A) CH4, (B) NH4+, (C-D) CH4 and NH4+in the hypolimnion, (E-F) CH4 and NH4+ in the epilimnion-metalimnion, the sum of [CH4] + [NH4+] concentrations in the epilimnion-metalimnion (G), hypolimnion (H) and throughout the water cap (I) determined for each of the date and depth-dependent OCR experiments. Triangle dots indicate measurements from the epilimnion and metalimnion, while square dots indicate hypolimnetic values.

3.4.4 BML water cap oxygen mass balance: the importance of both biogeochemical and physical processes in determining BML water cap oxygen profiles

Results shown in Figures 3.3 and 3.4 identify that the highest OCR values occur in proximity to the FWI, consistent with high biogeochemical consumption of FFT mobilized OCC. However, BML metalimnetic oxygen concentrations show the highest rate of decrease across the water cap (Figure 3.3), despite having much lower OCR values than those observed at the FWI (Figure 3.3, Table 3.1). These results indicate that physical processes must be involved in the overall observed BML water cap oxygen balance. And thus, any interpretation of the impact of biogeochemically linked oxygen consumption will have to be integrated with physical modelling in order to understand oxygen behaviour within BML.

In order to identify the relative importance of biogeochemical redox cycling in determining depth dependent net oxygen concentrations within the BML water cap, *observed oxygen loss* and *predicted oxygen loss* values were determined for each depth of experimentation for July 26th, July 27th, August 3rd, and August 17th. ***Observed oxygen loss*** values were calculated as the volume-weighted mass losses in oxygen (aerial-volumetric data; supporting material Table S3) based on the volume of each thermally defined zone in the entire BML volume and the oxygen concentrations measured in the water column using the YSI probe (described in section 3.3.3; supporting material Table S2). For each meter of the water cap, a volume-weighted mass of water (L) was multiplied by its associated oxygen deficit (µmol/L/d; calculated as the difference between YSI determined oxygen concentrations for every half meter) (Chapra, 2008).

The sum of these individual oxygen deficits determined the *observed oxygen loss* for each of the three thermal zones. *Predicted oxygen loss* was calculated as the product of the volume-weighted mass of water (L) and the oxygen deficit (µmol/L/d), predicted by experimentally derived OCR (µmol/L/d) values for each thermal zone.

Predicted oxygen loss values under predicted epilimnetic and metalimnetic oxygen losses and over predicted hypolimnetic *oxygen losses* (Figure 3.6, Table 3.4). The largest differences in oxygen losses occurred in the metalimnion, where predicted oxygen loss values accounted for only 3% of the observed oxygen losses, and in the hypolimnion where predicted oxygen loss values exceeded observed oxygen losses by 10- to 16-fold. In other words, the metalimnion should have much higher oxygen concentrations than observed, while the hypolimnion should be anoxic based on OCR values (Figure 3.6, Table 3.4). *The predicted oxygen loss* values are based on OCR, which means they reflect biogeochemical oxygen consumption. The large and contrary differences between the predicted and observed oxygen losses in the metalimnion and hypolimnion highlight that physical transport mechanisms are important and must be considered in order to develop an accurate conceptual model of oxygen dynamics within the BML water cap.

Turbulent processes generally dominate vertical mixing in lakes (Effler, 1996; Jassby and Powell, 1975; Martin and McCutcheon, 1998; Wodka et al., 1983). Thus, turbulent processes are well represented by heat flux calculations over the layers of interest (Martin and McCutcheon, 1998). A large oxygen gradient occurs in BML, typically at 6 m (Figure 3.3), where vertical oxygen fluxes were estimated by the use of the cross-gradient flux of oxygen with standard equations (Jassby and Powell, 1975). The

averaged calculated vertical transport of oxygen from the metalimnion to the hypolimnion was 81 mmol O_2/m^2/ d. The averaged OCR predicted upper hypolimnetic oxygen consumption of 78 mmol/m^2/d (Table 3.5). Applying this physical mechanism for loss of oxygen from the metalimnion and corresponding gain of oxygen to the hypolimnion brings volume-weighted *observed oxygen losses* and *predicted oxygen losses* values within 10% of each other for all experimental campaigns (Figure 3.6, Table 3.5). The overall net oxygen concentration in the water cap of BML reflected the interaction of both oxygen mass physical transport and in situ biogeochemical processes consuming oxygen, supporting the hypothesis proposed.

These results are consistent with the notion that system scale physical processes are also important in determining the observed oxygen concentrations observed at depth within BML (e.g. Dompierre et al., 2016; Lawrence et al., 2015). Other studies have also identified turbulent mixing to have played a key role by transferring oxygen from the surface to the hypolimnion, where a metalimnetic oxygen minima resulted in a locally enhanced in situ oxygen consumption (Kreling et al., 2017; Stauffer, 1987). Importantly, without this physical O_2 transport to the BML hypolimnion, the oxic-anoxic boundary would move up to a depth of 6 meters within one day (Figure 3.6), based on experimental hypolimnetic OCR values and the volume weighted oxygen mass. Reduced OCC constituents mobilized from the FFT layer would also be able to migrate higher up into the water cap and impact surface zone oxygen concentrations directly (Figure 3.6). Further, anaerobic redox transformations would then be possible within the BML water cap and would generate more OCC through sulfate, nitrate and iron reduction. The high

sulfate concentrations observed in the BML water cap (~ 2 mM, 1000x higher than O_2 concentrations; Risacher et al. 2018) indicate high levels of $\sum H_2S$ could be generated, which would pose a significant risk to the development of a stable surface oxic zone. Sulfate reduction has been identified as an important process which drives oxygen consumption and anoxia in oil sands tailings ponds (Chen et al., 2013; Stasik et al., 2014).

Studies in pit lakes (Stevens and Lawrence, 1997; von Rohden et al., 2009, 2007; von Rohden and Ilmberger, 2001) have demonstrated that physical mixing is important to assess the vertical exchange processes into the water cap of coal/metal tailings pit lakes. Our K_z values (10^{-5} m/s), were within the estimated range in the metalimnion and monimolimnion/hypolimnion of mine lakes (Karakas et al., 2003; von Rohden and Ilmberger, 2001; Winkler et al., 2012; Yeates and Imberger, 2003) and similar K_z to those found in natural lakes (Crowe et al., 2008; Katsev et al., 2010; Kreling et al., 2017; Stauffer, 1987). Thus, collectively results here and these other PL studies underscore that the design of PL should consider basin shape in order to facilitate or prevent mixing dependent on the desired outcomes of the PL strategy. However, to our knowledge, there are no studies of a pit lake that has combined both biogeochemical and physical mixing models to explain observed oxygen concentrations within the water cap. As identified earlier, this is the first report directly measuring oxygen consumption rates within any pit lake, and thus provides an important baseline for understanding the interactive biogeochemical and physical processes that collectively drive observed water column

oxygen levels that will be important to guide WCTT planning across extractive resource industries.

Table 3.4 Temporal, BML July-August 2016 volume-weighted observed (calculated using measured O_2 concentrations) and predicted oxygen loss (based on OCR) values by thermal zone

		10^3 moles			
	Time period	July 26, 2016	July 27, 2016	August 3, 2016	August 17, 2016
Thermal zone					
Epilimnion	*Observed oxygen loss*	87.4	49.5	25.1	10.1
	Predicted oxygen loss	50.8	25.8	19.7	18.9
Metalimnion	*Observed oxygen loss*	620	649	617	664
	Predicted oxygen loss	16.2	16.4	12.2	17.8
Hypolimnion	*Observed oxygen loss*	59.5	53.2	48.8	37.8
	Predicted oxygen loss	645	620	609	605

Table 3.5 Turbulent diffusivity coefficients oxygen gradient oxygen vertical transport and OCR predicted consumption across the upper boundary in the hypolimnion on four days during the 2016 summer

	Kz	dO_2/dz	Vertical Transport	OCR predicted demand
	m^2/d	$mmol/m^4$	mmol $O_2/m^2/d$	
26-Jul-16	-1.0	-76	76	80
27-Jul-16	-1.0	-87	85	79
3-Aug-16	-1.0	-87	87	78
17-Aug-16	-1.6	-50	78	76

3.5 Conclusions

This is the first report directly measuring oxygen consumption rates within any pit lake, and thus provides an important biogeochemical baseline of possible OCR that can be expected for pit lakes containing methane and ammonia rich tailings. Methanotrophy and nitrification were determined as key microbial processes driving the oxygen consumption within the BML water cap (Figure 3.6). Given the extensive mass of methane and ammonia within the FFT, as well as evidence of direct methanogenesis within oil sands tailings ponds, biogeochemical redox cycling is expected to impact BML oxygen concentrations for decades. However, dewatering and settling rates for FFT have slowed down every year since BML was decommissioned in 2012, which in turn will decelerate the OCC expression into the water cap and as consequence, the growth and activity of microbes are expected to decrease to levels observed in natural lakes. In addition, this is the first study to assess jointly biogeochemical redox cycling & physical mixing to interpret the water cap O_2 profile. Results of this study indicate that both biogeochemical and physical processes must be jointly considered to more fully inform the design of successful pit lakes across the whole oil industry. Determining these crucial aspects affecting the development of the oxic layer in BML reveals fundamental novel insights into the key biogeochemical players which will aid operators to predict whether certain operations will lead to desired (e.g. biodegradation/bioremediation of FFT chemicals) or undesired effects (e.g. gas emissions, anoxia). Results contribute to our understanding of fundamental controls of O_2 concentrations in a variety of systems, not only in pit lakes, in terms of the interactive biogeochemical and physical processes that

collectively drive observed water column oxygen levels to have a more accurate prediction of the O_2 dynamics and help guide pit lake design.

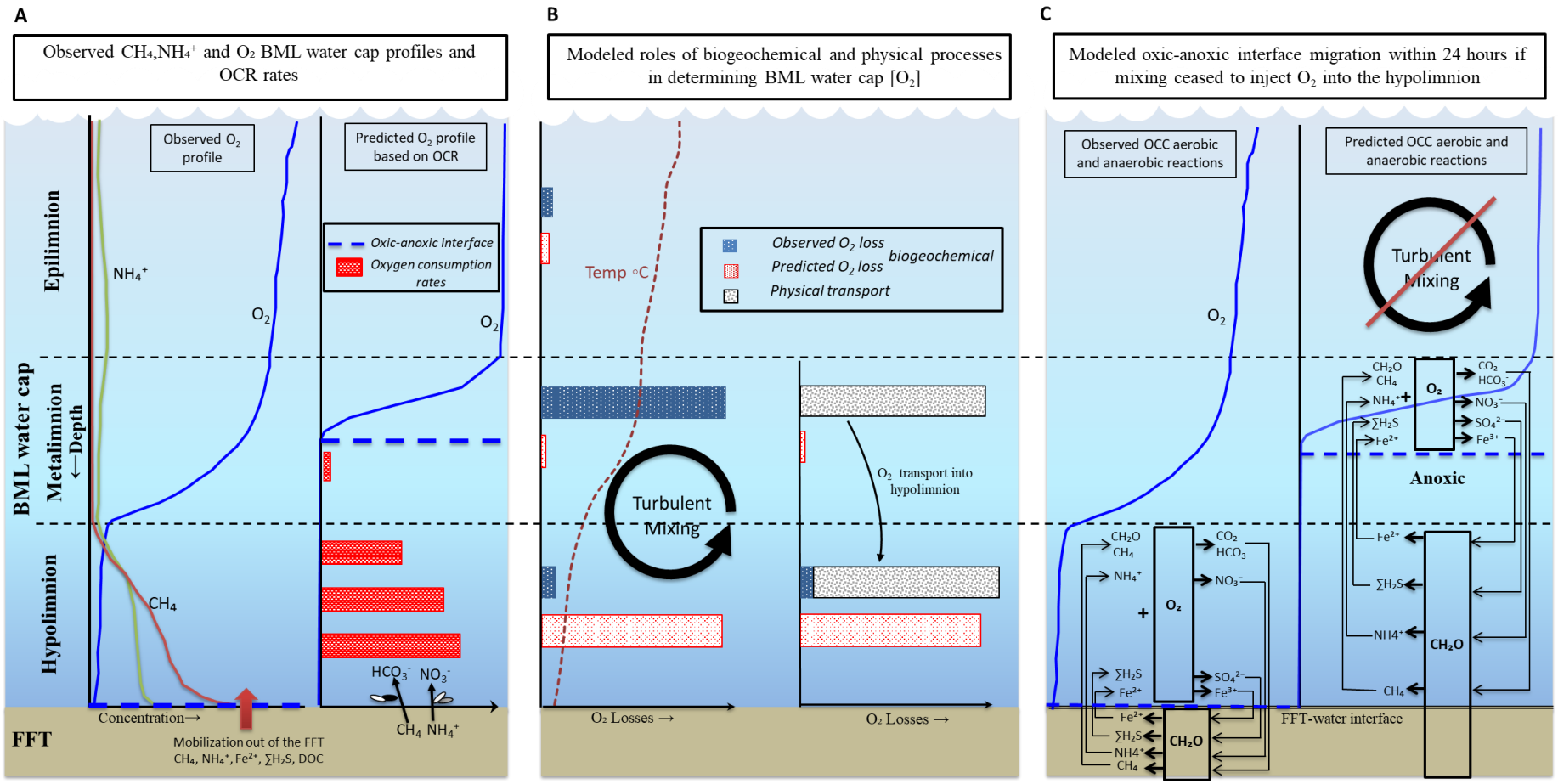

Figure 3.6 Processes determining the depth-dependent oxygen profile and concentrations within BML. Panel A: While oxygen concentrations decrease most rapidly through the metalimnion, the highest OCR values occur closest to the FFT, the source of possible OCC, where oxygen concentrations are the lowest (<5% saturation). Concentrations of CH_4 and NH_4^+ (highest at the FWI) are significantly positively correlated to OCR values consistent with their important role in determining oxygen concentrations, particularly within the hypolimnion.

Panel B: Observed and predicted volume-weighted O_2 mass losses, identifying the underpredicted losses in the metalimnion by predicted (based on OCR) oxygen losses and the overpredicted losses in the hypolimnion. The modelling of vertical oxygen transport across the metalimnetic–hypolimnetic interface identifies the mass of oxygen lost from the metalimnion and contributed to the hypolimnion through this physical mechanism is equivalent to the hypolimnetic O_2 difference between observed and predicted O_2 losses based on OCR values. Panel C. Without the O_2 injection from the metalimnion, the oxygen demand exerted at the FWI would exceed the available oxygen in the hypolimnion and as consequence, the oxic-anoxic boundary will move up and reduced OCC mobilized from the FFT layer would also be able to migrate higher up into the water cap and impacting the oxygen concentrations in the overlying layers. Note: X-axis not to scale, see text for corresponding values.

3.6 Acknowledgements

We would like to thank Syncrude Canada Limited, Mine Closure Research Group for field sampling support and especially Dallas Heisler and Carla Wytrykush for their inputs to the development of this manuscript. We would also like to acknowledge the help provided by boat operators Christopher Beierlin and Richard Kao, the BML coordinator Janna Lutz, the field laboratory manager Mohamed Salem and field leads Wendy Kline, John Arnold and Mike Arsenault on-site at Mildred Lake mine, Fort McMurray, AB. This research was funded by NSERC (CRDPJ 488301-15) and COSIA.

3.7 Supporting Material

Table S1 Nutrient (Chla) and estimated euphotic zone. Chla n=3 and n=6 for July and August respectively; secchi disk and estimated euphotic zone n=4 and n=7 for July and August respectively. Reference: Hartfield Consultants Syncrude 2017

	Depth (m)	Chlorophyll a (ug/L)	Secchi disk (m)	Estimated Euphotic Zone (m)
July	1.5	3.2 ±1.9	0.2 ±0.05	0.5 ±0.1
August	1.5	4.0 ±2.8	0.6 ±0.1	1.1 ±0.2

Table S2 Water column physicochemical profiles from the water surface to the top of the FFT (O_2, pH, turbidity, temperature and conductivity)

	14-Jul-16			26-Jul-16			27-Jul-16		
	Epilimnion	Metalimnion	Hypolimnion	Epilimnion	Metalimnion	Hypolimnion	Epilimnion	Metalimnion	Hypolimnion
Temperature ˚C	20.3 ± 0.1	16.8 ± 2	13.4 ± 0.4	20.2 ± 1.2	17.1 ± 1.8	14.2 ± 0.7	20.7 ± 1.1	16.4 ± 2.0	13.7 ± 0.3
Conductivity (mS/cm)	2776 ± 2.7	2807 ± 20.5	2841 ± 2.5	2811 ± 8.4	2843 ± 34.4	2892 ± 7.7	2814 ± 5.5	2854 ± 35.6	2905 ± 8.1
pH	8.3 ± 0.0	8.1 ± 0	7.9 ± 0.1	8.3 ± 0.0	8.1 ± 0.1	7.9 ± 0.1	8.3 ± 0.0	8.1 ± 0.1	7.9 ± 0.0
Turbidity NTU	70 ± 0.9	109 ± 31	331 ± 351	45.4 ± 2.4	71.8 ± 33.7	276 ± 261	42.2 ± 1.5	83.5 ± 47.6	202 ± 16.4
O_2 µmol/L	211 ± 2.2	114 ± 66	10.2 ± 5.1	200 ± 11.1	117 ± 65.5	10.3 ± 1.8	200 ± 12.9	84.6 ± 72.7	9.53 ± 1.3

	3-Aug-16			10-Aug-16			17-Aug-16		
	Epilimnion	Metalimnion	Hypolimnion	Epilimnion	Metalimnion	Hypolimnion	Epilimnion	Metalimnion	Hypolimnion
Temperature ˚C	20.1 ± 0.1	16.8 ± 1.9	13.9 ± 0.2	20.8 ± 1.0	17.1 ± 1.8	14.2 ± 0.7	21.0 ± 0.1	17.8 ± 1.8	14.5 ± 0.1
Conductivity (mS/cm)	2798 ± 1.0	2853.5 ± 37.2	2904.3 ± 4.0	2882 ± 6.7	2909 ± 37.4	2972.0 ± 12.3	2813 ± 0.6	2827.8 ± 24.5	2885.3 ± 1.5
pH	8.3 ± 0.00	8.1 ± 0.13	7.9 ± 0.02	8.3 ± 0.03	8.1 ± 0.14	7.9 ± 0.04	8.3 ± 0.04	8.1 ± 0.12	7.9 ± 0.01
Turbidity NTU	33.2 ± 0.21	75.0 ± 44.1	110.6 ± 20.2	25.0 ± 1.6	42.3 ± 17.0	58.6 ± 3.1	22.2 ± 0.16	30.1 ± 8.2	52.9 ± 9.8
O_2 µmol/L	196.9 ± 1.8	74.3 ± 62.9	10.1 ± 1.3	195.0 ± 21.6	75.8 ± 63.1	12.5 ± 2.4	199.1 ± 5.9	60.3 ± 56.8	7.4 ± 0.2

Table S3 BML water cap depth dependent volumes calculated for every 0.5 m (areal data from Geoff Halferdahl)

Depth (m)	Volume below (L)	Depth interval	Volume per 0.5m interval (L)	Area (m^2)
0.0	68140681874	0-0.5	4099475066	8241307
0.5	64041206809	0.5-1	4054153157	8156456
1.0	59987053651	1-1.5	3992493835	8056429
1.5	55994559817	1.5-2	3906153977	7904901
2.0	52088405840	2-2.5	3815950911	7721286
2.5	48272454929	2.5-3	3722010119	7526553
3.0	44550444810	3-3.5	3665590873	7378692
3.5	40884853937	3.5-4	3625449417	7290335
4.0	37259404521	4-4.5	3580193688	7208867
4.5	33679210833	4.5-5	3534283806	7111979
5.0	30144927027	5-5.5	3495227414	7027983
5.5	26649699613	5.5-6	3453866854	6951136
6.0	23195832759	6-6.5	3413517318	6862724
6.5	19782315441	6.5-7	3378936230	6791776
7.0	16403379210	7-7.5	3346270994	6724982
7.5	13057108216	7.5-8	3313610024	6659513
8.0	9743498192	8-8.5	3281144163	6594952
8.5	6462354029	8.5-9	3248016282	6528348
9.0	3214337747	9-9.5	3214337747	6463431

3.8 References

Adams, D.D., Matisoff, G., Snodgrass, W.J., 1982. Flux of reduced chemical constituents (Fe^{2+}, Mn^{2+}, NH_4^+ and CH_4) and sediment oxygen demand in Lake Erie. Hydrobiologia 91, 405–414.

Allen, E.W., 2008. Process water treatment in Canada's oil sands industry: I. Target pollutants and treatment objectives. J. Environ. Eng. Sci. 7, 123–138. https://doi.org/10.1139/s07-038

Benoit, G., Hemond, H.F., 1990. Polonium-210 and lead-210 remobilization from lake sediments in relation to iron and manganese cycling. Environ. Sci. Technol. 24, 1224–1234. https://doi.org/10.1021/es00078a010

Castendyk, D.N., Eary, L.E., Balistrieri, L.S., 2015. Modeling and management of pit lake water chemistry 1: Theory. Appl. Geochemistry 57, 267–288.

Crowe, S.A., O'Neill, A.H., Katsev, S., Hehanussa, P., Haffner, G.D., Sundby, B., Mucci, A., Fowle, D.A., 2008. The biogeochemistry of tropical lakes: A case study from Lake Matano, Indonesia. Limnol. Oceanogr. 53, 319–331.

Brooks, C.M., Effler, S.W., 1990. The distribution of nitrogen species in polluted Onondaga Lake, NY, USA. Water. Air. Soil Pollut. 52, 247–262. https://doi.org/10.1007/bf00229437

Burba, G., 2013. Eddy covariance method for scientific, industrial, agricultural and regulatory applications: A field book on measuring ecosystem gas exchange and areal emission rates. LI-Cor Biosciences.

CAPP, 2018. Canada's oil sands. Canadian Association of Petroleum Producers (CAPP) [WWW Document]. URL http://www.capp.ca/ Last visited on 24 April 2018

Castro, J.M., Moore, J.N., 2000. Pit lakes: their characteristics and the potential for their remediation. Environ. Geol. 39, 1254–1260. http://dx.doi.org/10.1007/s002549900100.

Chapra, S.C., 2008. Surface water-quality modeling. Waveland press.

Charlton, M.N., 1980. Hypolimnion oxygen consumption in lakes: discussion of productivity and morphometry effects. Can. J. Fish. Aquat. Sci. 37, 1531–1539. https://doi.org/10.1139/f80-198

Cornett, R.J., Rigler, F.H., 1987. Vertical transport of oxygen into the hypolimnion of lakes. Can. J. Fish. Aquat. Sci. 44, 852–858. https://doi.org/10.1139/f87-103

COSIA. Technical guide for fluid fine tailings management, 2012. http://www.cosia.ca/uploads/documents/id7/TechGuideFluidTailingsMgmtAug2012.pdf (21 January 2018, date last accessed).

Denkenberger, J.S., Driscoll, C.T., Effler, S.W., O'Donnell, D.M., Matthews, D.A., 2007. Comparison of an urban lake targeted for rehabilitation and a reference lake based on robotic monitoring. Lake Reserv. Manag. 23, 11–26. https://doi.org/10.1080/07438140709353906

Dompierre, K. A., & Barbour, S. L. (2016). Characterization of physical mass transport through oil sands fluid fine tailings in an end pit lake: a multi-tracer study. *Journal of contaminant hydrology*, *189*, 12-26.

Dompierre, K. A., Lindsay, M. B., Cruz-Hernández, P., & Halferdahl, G. M. (2016). Initial geochemical characteristics of fluid fine tailings in an oil sands end pit lake. *Science of the Total Environment*, *556*, 196-206.

Effler, S.W., 1996. Limnological and engineering analysis of a polluted urban lake: prelude to environmental management of Onondaga Lake, New York. Springer Science & Business Media. https://doi.org/10.1007/978-1-4612-2318-4

Fedorak, P.M., Coy, D.L., Dudas, M.J., Simpson, M.J., Renneberg, A.J., MacKinnon, M.D., 2003. Microbially-mediated fugitive gas production from oil sands tailings and increased tailings densification rates. J. Environ. Eng. Sci. 2, 199–211. https://doi.org/10.1139/s03-022

Fedorak, P.M., Coy, D.L., Salloum, M.J., Dudas, M.J., 2002. Methanogenic potential of tailings samples from oil sands extraction plants. Can J Microbiol 48, 21–33. https://doi.org/10.1139/w01-129

Foght, J.M., Fedorak, P.M., Westlake, D.W.S., Boerger, H.J., 1985. Microbial content and metabolic activities in the Syncrude tailings pond. AOSTRA J Res 1, 139–146.

Foley, B., Jones, I.D., Maberly, S.C., Rippey, B., 2012. Long-term changes in oxygen depletion in a small temperate lake: effects of climate change and eutrophication. Freshw. Biol. 57, 278–289.

Gelda, R.K., Auer, M.T., 1996. Development and testing of a dissolved oxygen model for a hypereutrophic lake. Lake Reserv. Manag. 12, 165–179.

GOA, 2012. Oil sands information portal. Government of Alberta (GOA) [WWW Document]. URL http://environment.alberta.ca/apps/osip/ Last visited on 24 April 2018

GOA, 2015. Lower Athabasca Region – Tailings Management Framework for the Mineable Athabasca Oil Sands.

HagMan, M., la Cour Jansen, J., 2007. Oxygen uptake rate measurements for application at wastewater treatment plants. Vatten 63, 131.

Haveroen, M.E., MacKinnon, M.D., Fedorak, P.M., 2005. Polyacrylamide added as a nitrogen source stimulates methanogenesis in consortia from various wastewaters. Water Res. 39, 3333–3341.

Heinz, G., Ilmberger, J., Schimmele, M., 1990. Vertical mixing in Überlinger See, western part of Lake Constance. Aquat. Sci. 52, 256–268.

Holowenko, F.M., MacKinnon, M.D., Fedorak, P.M., 2000. Methanogens and sulfate-reducing bacteria in oil sands fine tailings waste. Can J Microbiol 46, 927–937.

Jassby, A., Powell, T., 1975. Vertical patterns of eddy diffusion during stratification in Castle Lake, California. Limnol. Oceanogr. 20, 530–543.

Karakas, G., Brookland, I., Boehrer, B., 2003. Physical characteristics of acidic mining lake 111. Aquat. Sci. 65, 297–307.

Kasperski, K.L., 1992. A review of properties and treatment of oil sands tailings. AOSTRA J. Res. 8, 11.

Kasperski, K.L., Mikula, R.J., 2011. Waste streams of mined oil sands: characteristics and remediation. Elements 7, 387–392.

Katsev, S., Crowe, S.A., Mucci, A., Sundby, B., Nomosatryo, S., Douglas Haffner, G., Fowle, D.A., 2010. Mixing and its effects on biogeochemistry in the persistently stratified, deep, tropical Lake Matano, Indonesia. Limnol. Oceanogr. 55, 763–776.

Kreling, J., Bravidor, J., Engelhardt, C., Hupfer, M., Koschorreck, M., Lorke, A., 2017. The importance of physical transport and oxygen consumption for the development of a metalimnetic oxygen minimum in a lake. Limnol. Oceanogr. 62, 348–363.

Lawrence, G.A., Tedford, E.W., Pieters, R., 2015. Suspended solids in an end pit lake: potential mixing mechanisms. Can. J. Civ. Eng. 43, 211–217.

Li, X., Sun, W., Wu, G., He, L., Li, H., Sui, H., 2011. Ionic liquid enhanced solvent extraction for bitumen recovery from oil sands. Energy & Fuels 25, 5224–5231.

MacKinnon, M.D., 1989. Development of the tailings pond at Syncrude's oil sands plant: 1978–1987. AOSTRA J. Res 5, 109–133.

Martin, J.L., McCutcheon, S.C., 1998. Hydrodynamics and transport for water quality modeling. CRC Press.

Masson, S., Angeli, N., Guillard, J., Pinel-Alloul, B., 2001. Diel vertical and horizontal distribution of crustacean zooplankton and young of the year fish in a sub-alpine lake: an approach based on high frequency sampling. J. Plankton Res. 23, 1041–1060.

Matthews, D.A., Effler, S.W., 2006. Assessment of long-term trends in the oxygen resources of a recovering urban lake, Onondaga Lake, New York. Lake Reserv. Manag. 22, 19–32.

Peng, Y.Z., Chen, Y., Peng, C.Y., Liu, M., Wang, S.Y., Song, X.Q., Cui, Y.W., 2004. Nitrite accumulation by aeration controlled in sequencing batch reactors treating domestic wastewater. Water Sci. Technol. 50, 35–43.

Penner, T.J., Foght, J.M., 2010. Mature fine tailings from oil sands processing harbour diverse methanogenic communities. Can J Microbiol 56, 459–470. https://doi.org/10.1139/w10-029

Quagraine, E.K., Peterson, H.G., Headley, J. V, 2005. In situ bioremediation of naphthenic acids contaminated tailing pond waters in the Athabasca oil sands region—demonstrated field studies and plausible options: a review. J. Environ. Sci. Heal. 40, 685–722.

Quay, P.D., Broecker, W.S., Hesslein, R.H., Schindler, D.W., 1980. Vertical diffusion rates determined by tritium tracer experiments in the thermocline and hypolimnion of two lakes. Limnol. Oceanogr. 25, 201–218.

Ramos-Padron, E., Bordenave, S., Lin, S., Bhaskar, I.M., Dong, X., Sensen, C.W., Fournier, J., Voordouw, G., Gieg, L.M., 2011. Carbon and sulfur cycling by microbial communities in a gypsum-treated oil sands tailings pond. Env. Sci Technol 45, 439–446. https://doi.org/10.1021/es1028487

Ramos Padron, E., 2013. Physiology and Molecular Characterization of Microbial Communities in Oil Sands Tailings Ponds. University of Calgary.

Risacher, F.F., Morris, P.K., Arriaga, D., Goad, C., Nelson, T.C., Slater, G.F., Warren, L.A., 2018. The interplay of methane and ammonia as key oxygen consuming constituents in early stage development of Base Mine Lake, the first demonstration oil sands pit lake. Appl. Geochemistry 93. https://doi.org/10.1016/j.apgeochem.2018.03.013

Saidi-Mehrabad, A., He, Z., Tamas, I., Sharp, C.E., Brady, A.L., Rochman, F.F., Bodrossy, L., Abell, G.C., Penner, T., Dong, X., Sensen, C.W., Dunfield, P.F., 2013. Methanotrophic bacteria in oilsands tailings ponds of northern Alberta. ISME J 7, 908–921. https://doi.org/10.1038/ismej.2012.163

Siddique, T., Fedorak, P.M., Foght, J.M., 2006. Biodegradation of short-chain n-alkanes in oil sands tailings under methanogenic conditions. Env. Sci Technol 40, 5459–5464.

Siddique, T., Fedorak, P.M., MacKinnon, M.D., Foght, J.M., 2007. Metabolism of BTEX and naphtha compounds to methane in oil sands tailings. Env. Sci Technol 41, 2350–2356.

Siddique, T., Kuznetsov, P., Kuznetsova, A., Arkell, N., Young, R., Li, C., Guigard, S., Underwood, E., Foght, J.M., 2014. Microbially-accelerated consolidation of oil sands tailings. Pathway I: changes in porewater chemistry. Front Microbiol 5, 106. https://doi.org/10.3389/fmicb.2014.00106

Slater, G.F., Cowie, B.R., Harper, N., Droppo, I.G., 2008. Variation in PAH inputs and microbial community in surface sediments of Hamilton Harbour: implications to remediation and monitoring. Environ. Pollut. 153, 60–70.

Sobolewski, A., 1997. Microbial distributions in process-affected aquatic ecosystems. Draft Rep. Submitt. to Syncrude Res. Ltd.

Sobolewski, A., 1992. The microbial characteristics of oil sands tailings sludge. Prep. AOSTRA by EVS Consult.

Soni, A., Mishra, B., & Singh, S. (2014). Pit lakes as an end use of mining: A review. *Journal of Mining and Environment*, *5*(2), 99-111.

Stasik, S., Loick, N., Knöller, K., Weisener, C., Wendt-Potthoff, K., 2014. Understanding biogeochemical gradients of sulfur, iron and carbon in an oil sands tailings pond. Chem. Geol. 382, 44–53.

Stauffer, R.E., 1987. Effects of oxygen transport on the areal hypolimnetic oxygen deficit. Water Resour. Res. 23, 1887–1892.

Stauffer, R.E., 1985. Nutrient internal cycling and the trophic regulation of Green Lake, Wisconsin. Limnol. Oceanogr. 30, 347–363.

Stevens, C.L., Lawrence, G.A., 1997. The effect of sub-aqueous disposal of mine tailings in standing waters. J. Hydraul. Res. 35, 147–159.

Stewart, K.M., 1976. Oxygen deficits, clarity, and eutrophication in some Madison lakes. Int. Rev. Hydrobiol. 61, 563–579.

Sweerts, J.-P.R.A., Baer-Gilissen, M., Cornelese, A.A., Cappenberg, T.E., 1991. Oxygen-consuming processes at the profundal and littoral sediment-water interface of a small meso-eutrophic lake(Lake Vechten, The Netherlands). Limnol. Oceanogr. 36, 1124–1133.

Testa, B.M., 2010. RECLAIMING: ALBERTA'S OIL SANDS MINES. Earth 55, 44–55.

Todd, M.J., Vellidis, G., Lowrance, R.R., Pringle, C.M., 2007. Measurement of water residence time, flowpath and sediment oxygen demand in seasonally inundated floodplain swamps of the Georgia Coastal Plain, in: Watershed Management to Meet Water Quality Standards and TMDLS (Total Maximum Daily Load) Proceedings of the 10-14 March 2007, San Antonio, Texas. American Society of Agricultural and Biological Engineers, p. 140.

Veenstra Nolen, S. L., J.N., 1991. In-situ sediment oxygen demand in five Southwestern US Lakes. Water Res. 25, 351–354.

Viollier, E., Inglett, P.W., Hunter, K., Roychoudhury, A.N., Van Cappellen, P., 2000. The ferrozine method revisited: Fe (II)/Fe (III) determination in natural waters. Appl. geochemistry 15, 785–790.

von Rohden, C., Ilmberger, J., 2001. Tracer experiment with sulfur hexafluoride to quantify the vertical transport in a meromictic pit lake. Aquat. Sci. 63, 417–431.

von Rohden, C., Ilmberger, J., Boehrer, B., 2009. Assessing groundwater coupling and vertical exchange in a meromictic mining lake with an SF6-tracer experiment. J. Hydrol. 372, 102–108.

von Rohden, C., Wunderle, K., Ilmberger, J., 2007. Parameterisation of the vertical transport in a small thermally stratified lake. Aquat. Sci. 69, 129–137.

Westcott, F., Watson, L., 2005. End Pit Lakes technical guidance document. Clear. Environ. Consult. CEMA end Pit Lakes subgroup, Proj. 61.

Winkler, M.K.H., Yang, J., Kleerebezem, R., Plaza, E., Trela, J., Hultman, B., van Loosdrecht, M.C.M., 2012. Nitrate reduction by organotrophic Anammox bacteria in a nitritation/anammox granular sludge and a moving bed biofilm reactor. Bioresour. Technol. 114, 217–223.

Wodka, M.C., Effler, S.W., Driscoll, C.T., Field, S.D., Devan, S.P., 1983. Diffusivity-based flux of phosphorus in Onondaga Lake. J. Environ. Eng. 109, 1403–1415.

Yeates, P.S., Imberger, J., 2003. Pseudo two-dimensional simulations of internal and boundary fluxes in stratified lakes and reservoirs. Int. J. River Basin Manag. 1, 297–319.

Chapter 4: Nitrification in BML, the first oil sands pit lake: Investigating the effects of NH_4^+ on the oxygen consumption

4.1 Introduction

The extraction and processing of bitumen from oil sands of the Athabasca region in north-eastern Alberta (Canada) have produced over 1 billion m^3 of tailings stored in settling impoundments (Alberta Government, 2017). Tailings slurry consists of 55 wt % solids (silts, clays and sands), and contain ~1% residual bitumen (Chalaturnyk et al., 2002), which are pumped into large settling basins known as tailings ponds, where the solids are allowed to settle out, forming semi-consolidated fluid fine tailings (FFT). Because of the acute toxicity of certain substances (e.g., naphthenic acids) to aquatic organisms (Headley et al., 2011) and the slow densification rate of FFT (Eckert et al., 1996), the oil sands industry faces environmental and operational challenges for a sustainable pond management and safe containment of FFT.

One of the current long-term reclamation strategies being investigated for FFT is water capped tailings technology (WCTT) by the use of pit lakes. In WCTT, vacant mine pits will be filled with both highly consolidated tailings capped with a mix of processed water and freshwater inputs, aiding in the efficiency of natural reclamation and ecosystem sustainability. Base Mine Lake (BML, Syncrude Canada) is the first large-scale demonstration of this technology in the Athabasca oil sands region. BML was commisioned in 2013 and consists of circa 40 m depth of FFT overlain by 10 m of a mix of processed-water and freshwater cap. The goal is to establish a self-sustaining

ecosystem with a stable oxic zone occurring within the surface water cap that provides long-term, stable containment for FFT as part of the closure landscape for a mine. This outcome requires that oxygen inputs from atmospheric diffusion, watershed and rain inputs and any *in situ* photosynthetic production exceed oxygen consumption driven by FFT constituents, enabling some portion of the surface water cap to remain oxygenated. The concern for the success of WCTT as an FFT reclamation strategy is that mobilization of reductants (e.g., CH_4, NH_4^+, H_2S) from the underlying FFT may be sufficiently large to prevent the development of an oxic portion of the water cap.

Initial physical and geochemical assessment of BML (Dompierre et al., 2016) showed it behaved similarly to oil sands tailing ponds (Stasik et al., 2014) with respect to oxygen consumption. The high production of CH_4 and $\sum H_2S$, produced anaerobically within the FFT, exerted a high oxygen demand, which results in anoxic conditions within the first meter of tailing ponds (Chen et al., 2013; Holowenko et al., 2000; Penner and Foght, 2010). Field sampling over two years, 2015–2016, characterized the geochemistry of the BML water cap from the FFT–water interface (FWI) to the surface (Risacher et al., 2018). In 2015, CH_4 was the only identified variable significantly negatively related to BML water cap oxygen concentrations. However, in 2016, NH_4^+ emerged as an important OCC negatively related to water cap oxygen concentrations in addition to CH_4. A lack of nitrifying microbes within the legacy FFT, as well as competition with methanotrophs at deeper water depths associated with oxygen limitations, were hypothesized to have delayed the establishment of nitrification in BML. Interestingly, nitrate (NO_3^-) and nitrite (NO_2^-) ion concentrations have been observed to be below

detection levels in oil sands tailing ponds (Stasik et al., 2014) but the presence of nitrate reducers (10^9 cells/g dry weight tailings) suggests that denitrification may be occurring in these systems (Foght et al., 2017), which could geochemically obscure the activity of nitrifying bacteria given the low oxygen status of oil sands tailings ponds. A recent field-based investigation of oxygen consumption rates (OCR) in BML identified both CH_4 and NH_4^+ were important to oxygen consumption, consistent with the results of Risacher et al. 2017, and providing further support for active nitrification occurring within BML (Arriaga et al., 2018).

Nitrification is the microbially mediated oxidation of ammonium to nitrite and the further oxidation of nitrite to nitrate; and a major pathway in the overall nitrogen (N) cycle of freshwater systems (Curtis et al., 1975; Harris, 2012; Sprent, 1987; Wetzel, 1983). The complete aerobic oxidation of ammonium to nitrate is a two-step process conducted generally by ammonium-oxidizing organisms (oxidation of ammonia to nitrite, equation 1) and nitrite-oxidizing organisms (oxidation of nitrite to nitrate, equation 2).

$$NH_4^+ + 1.5O_2 \rightarrow NO_2^- + H_2O + 2H^+$$ Equation 1

$$NO_2^- + 0.5O_2 \rightarrow NO_3^-$$ Equation 2

$$NH_4^+ + 2O_2 \rightarrow NO_3^- + H_2O + 2H^+$$ Equation 3; overall nitrification

Ammonium concentration is rarely above 5 uM in pit lakes (Johnson and Castendyk, 2012; http://pitlakesdatabase.org). Therefore, nitrification has not been an important process in any pit lake, especially acidic lakes where nitrification will be strongly limited. As nitrification has not been shown to be an important process affecting

oil sands tailings ponds' geochemical status, the impacts of nitrification relative to the other potential oxygen-consuming processes such as methanotrophy and sulfur oxidation in the BML water cap are not known. As pore water ammonia concentrations within FFT are on the order of 200 to 300 µM (Risacher et al. 2018), the emergence of active nitrification could play a major and on-going role in determining future end pit lake water column oxygen concentrations. The objectives of this study were to experimentally quantify the impacts of nitrification on BML oxygen concentrations in batch OCR experiments using BML hypolimnetic water depleted in methane and amended with varying ammonia concentrations and assess if nitrification rates are ammonia concentration-dependent. Also, this laboratory-study aimed to establish the O_2 consumption contributions of laboratory-determined nitrification to potential BML water ammonium oxidation.

4.2 Methods

4.2.1 Site Description and Sample Collection

Base Mine Lake (Fort McMurray, AB, coordinates: 57° 0′ 38.88″N, 111° 37′ 22.44″W) consists of a mixture of fresh water and oil sands process water cap of approximately 10 m in depth, in a 7 km^2 lake (Figure 2.1). BML water was collected on August 4th, 2017 from a depth of 7.5 meters within the water cap. This depth was identified for sample collection based on a physico-chemical profile of the water cap determined at 50 cm intervals from the BML surface to the FWI at a central sampling site for pH, temperature, dissolved oxygen, specific conductivity, oxidation-reduction

potential (ORP), turbidity (Nephelometric Turbidity Units; NTU) and salinity (Practical Salinity Unit; PSU) (YSI Professional Plus 6-Series Sonde, YSI Incorporated). Physicochemical and geochemical parameters (analyzed on-site) for this date are shown in Table 4.1 and Table 4.2. The sampling depth of 7.5m was chosen as it was the upper boundary and thus where the highest oxygen concentrations within the hypolimnetic zone occurred and where nitrifiers were thought to be most active as reported in Risacher et al 2018.

4.2.2 Microcosm Water Sample Collection and Preservation

The water sample (20L) was collected to overflowing using a 6.2 L sampling van dorn bottle (WaterMark, Forestry supplies). All sampling equipment and sample containers were prepared by soaking in 5% (v/v) HCl for about 12 h followed by seven rinses with ultra-pure water (18.2Ωm cm-1, Milli-Q, Millipore) (inorganic analytes). Samples were collected to characterize important aqueous and particulate constituents, such as the bulk carbon (dissolved organic carbon), and dissolved (<0.45 µM) aqueous species, such as Fe^{2+}/Fe^{3+}, ΣH_2S and SO_4^{2-}, to verify for other potential oxygen-consuming constituents (OCC).

For $\sum H_2S$ analyses, water samples were collected into sample containers containing reagents to fix the $\sum H_2S$ and analyzed via the methylene blue method directly on the boat with a HACH portable spectrophotometer (Hach DR/2800 spectrophotometer, HACH Company, Loveland, CO, USA).

Samples for Fe (II) and Fe (III) were collected into acid washed 15 mL tubes and preserved by the addition of 2% v/v Optima-Grade hydrochloric acid and stored refrigerated until analysis. Organic and inorganic carbon water samples were collected, in duplicate, in carbon-clean amber borosilicate glass 40mL vials. Bottles were cleaned with detergent, rinsed with Milli Q, then ethanol, and placed in a 10% HCl bath for >8 hours. After seven rinses with MilliQ water, vials were placed in a muffle furnace at 450°C for 8h to remove any residual carbon. Lids were rinsed with a 1:1:1 mixture of dichloromethane, hexane, and methanol and allowed to evaporate. Three to five replicates water samples were prepared by pipetting from the microcosm into pre-spiked tubes containing reagents to fix for SO_4^{2-}, NO_3^-, NO_2^- and NH_4^+ analyses.

The goal of sample collection was to provide a BML sample that contained viable endemic nitrifying bacteria, not to maintain the geochemical conditions at the time of collection. Thus the sample was subsequently stored at room temperature and shipped back to McMaster University for subsequent experimentation within 14 days of collection. The BML water was characterized immediately prior to initiation of the experiment, as discussed subsequently to establish the geochemical conditions of the water and confirm the loss of any methane within the original water sample, which would remove confounding influences of methanotrophy on experimental OCR values.

Table 4.1
Physicochemical parameters in the water cap of BML on August 4th, 2017

Depth (m)	Temperature (˚C)	Specific Conductivity (mS/cm)	pH	ORP	Turbidity (NTU)	Salinity (PSU)	DO (µmol/L)
0.0	21.0	2787	8.3	194	4	1.5	237
1.0	21.1	2789	8.3	192	4	1.9	237
1.5	21.0	2788	8.3	190	4	1.9	236
2.0	21.0	2788	8.3	189	4	1.9	237
3.0	21.0	2789	8.3	187	4	1.9	236
4.0	20.9	2791	8.3	186	4.2	1.9	235
4.5	20.6	2774	8.3	184	4.3	1.9	235
5.0	20.3	2778	8.3	183	4.7	1.9	221
5.5	17.7	2790	8.3	182	6.2	1.9	165
6.0	16.8	2801	8.2	182	8.5	1.9	107
6.5	16.5	2809	8.1	183	9.5	1.9	70.3
7.0	16.5	2809	8.1	183	10.7	1.9	48.8
7.5	15.9	2799	8.1	184	10.9	1.9	23.1
8.0	14.9	2797	8.0	178	19.1	1.9	0.9
8.5	14.7	2796	8.0	151	23.1	1.9	0.6
9.0	14.3	2804	8.0	-50	34.2	1.9	0.0
9.5	14.0	2803	8.0	-93	40.5	1.9	0.0

Table 4.2
Geochemical analytes measured in the water cap of BML on August 4th, 2017

Depth (m)	$\sum H_2S$ µM	SO_4^{2-} mM	NH_4^+ µM	NO_2^- µM	NO_3^- µM	CH_4 µM
0.0	BD	2.6	16.4	3.9	62.8	0.2
1.5	BD	2.7	13.0	4.1	57.0	0.3
4.5	BD	2.6	17.2	4.1	65.8	0.3
5.5	BD	2.7	16.5	4.0	60.2	0.4
6.5	BD	2.6	25.4	3.3	40.0	0.3
7.5	BD	2.5	31.3	2.7	19.9	0.4
7.8	BD	2.3	33.2	2.5	11.0	1.2
8.0	BD	2.6	22.6	0.9	0.0	7.4
9.8	BD	2.6	40.2	2.8	16.7	27.3

BD: Below detection limit 5 µM

4.2.3 Experimental Design

The experiments were designed to quantify the effect of varying ammonia concentrations on oxygen consumption by endemic BML microbes that excluded the possibility of methanotrophy by allowing for the loss of any methane from the original water sample collected from BML (Figure 2.4). Three treatment levels of NH_4^+ concentration on OCR values were assessed: 50, 200 and 500 µM (Figure 2.4). These concentrations were selected as they reflect the maximum bulk water concentration observed in the upper BML water cap (50 µM) and maximum NH_4^+ observed in the FFT (~200 µM; Risacher et al. 2018, Morris, 2018), as well as the typical concentrations observed in oil sands tailing ponds (<500 µM; Allen, 2008; Stasik et al., 2014).

Microbial and abiotic control microcosms were also included to account for any background microbial and/or abiotic processes that could influence observed OCR values or nitrogen species transformations (Figure 2.4). The microbial control consisted of unamended BML water, (i.e. endemic microbes and background ammonia concentrations present) and the abiotic control consisted of filtered sterilized BML water that would exclude microbes (cellulose nitrate filter towers (0.2 µm pore size, Thermo Scientific) (ASTM, 2005; Bowman et al., 1967; Cheryan, 1998; Jornitz et al., 2001; Segers et al., 1994) and amended with the three ammonia concentrations to establish any influences on oxygen consumption contributed by abiotic processes. Only one abiotic control experiment was conducted per treatment. In addition, chemical controls consisting of ultra-pure water MQ (18.2 MΩ·cm at 25 °C; 0.22 µm membrane filter) amended with the NH_4^+ stock solutions at the three different concentrations used for the experiments, were

conducted to determine any potential effects of the stock solution on oxygen consumption (Figure 2.4).

Each ammonia treatment experiment consisted of triplicate bottles examined simultaneously with one microbial and one abiotic control microcosm bottle. For each ammonia concentration treatment level, the BML water was first analyzed to determine initial nitrogen species concentrations and thus determine the ammonia amendment required to create the three treatment concentrations of 50, 200 and 500 μM. Experimental microcosms were set up in 500 mL borosilicate media bottles to which an oxygen probe sensor (YSI ProODO) had been attached to the lid and held in place with an industrial adhesive agent (3M Marine Adhesive Sealant 5200). The embedded oxygen probe enabled continuous measurement of oxygen concentrations (collected every 60 seconds) directly *in situ* within undisturbed microcosm bottles (Figure 2.5). Each microcosm bottle was allowed for water to overflow once the lid was closed to avoid any headspace. Each NH_4^+ treatment replicate experiment was terminated when the oxygen levels within the bottle reached near zero (≤5 μM) for approximately 10 days in general. Control microcosms were terminated at the same time as the replicates. Initial and final oxygen, pH, temperature and geochemical analytes (Fe^{2+}/Fe^{3+}, ΣH_2S and SO_4^{2-}, DOC, NO_3^-, NO_2^- and NH_4^+) were measured for each NH_4^+ treatment microcosm replicate and control microcosms (Table 4.1). NH_4^+ and NO_2^- oxidation rates were measured by the NH_4^+ disappearance and NO_3^- and NO_2^- production in the water with a time of incubation. OCR values were calculated for each microcosm by the least squares method of the change in oxygen concentration. The total OCR associated with nitrification was

calculated by subtracting any abiotic consumption and microbial consumption from the unamended control:

$$\text{OCR (nitrification)} = NH_4^+ \text{ Treatment } \Delta O_2 - (\text{abiotic } \Delta O_2 + \text{unamended } \Delta O_2)$$

As these experiments identified changes in OCR over the experimental time course, a subsequent experiment was carried out in which sampling occurred at these inflection points to assess any possible changes in geochemistry and gain greater insights into the possible processes driving oxygen consumption. Following the same methodology as the microcosm experiments described above, five replicate bottles containing an amended ammonium concentration of 100 μM were set up simultaneously and run in parallel. One bottle was sacrificed at the following percent oxygen saturation values that were associated with changes in OCR values in the previous experiments (85, 55, 40, 15 and 5% oxygen saturation) for geochemical characterization.

4.2.4 Geochemical Analyses

The geochemical analyses are briefly summarized subsequently, as full details are provided in Chapter 2. For all sampling time points (T= 0 and T=E for 3 levels of ammonium microcosms amendments and T= 100, T= 85, T= 55, T= 40, T= 20 and T= 5 O_2% microcosms), concentrations of nitrogen species, NH_4^+, NO_2^-, and NO_3^- and SO_4^{2-} concentration were determined by spectrophotometry (N species: methods 8171, 8155 and8507; sulfate (Method 8051); Hach DR/2800 spectrophotometer, HACH Company, Loveland, CO, USA). Three to five replicates were done per analyte. ΣH_2S analyses were done in five replicates using the methylene blue method (Method 8131). All samples

were collected by pipetting 10 mL of sample directly from the microcosm using a 10mL pipette (Eppendorf™ Fisher Scientific). Samples were syringed into 15mL tubes containing reagents to fix the analyte.

Samples for carbon analysis were immediately filtered with a syringe-driven 0.7µm GF/F glass microfiber filter unit (13mm, GE Life Sciences) and the filtrate was then analyzed in duplicate for dissolved organic carbon and dissolved inorganic carbon (DOC/DIC respectively) on a Shimadzu TOC-L Total Organic Carbon Analyzer with an autosampler ASI-L by the use of the 680°C combustion catalytic oxidation method as per manufacturer recommended protocols (Mandel Scientific). Organic carbon values were obtained by subtracting the inorganic C values from the total C values. Samples for ferrous and ferric iron were analyzed colorimetrically by a modified ferrozine method from Viollier et al (2000).

4.2.5 Nitrification Kinetics Cell Growth

The kinetic model was applied to describe quantitatively the nitrification cell growth. The double substrate-limiting Monod expression (Bae and Rittmann, 1996; Bungay, 1994; Wu et al., 2007) describe the combined effect of dissolved oxygen and NH_4^+-N on the growth rate as follows:

$$\mu = u_{max} \frac{S_{NH_4^+}}{K_{NH_4^+} + S_{NH_4^+}} * \frac{S_{O_2}}{K_{O_2} + S_{O_2}} - K_d \qquad (4)$$

Here, µ is the specific cell growth rate (mg-NH_4^+-N/g-cell d), μ_{max} is the maximum cell growth rate (d^{-1}), S_{O_2, NH_4^+} are the limiting substrates (mg/L), K_{O_2, NH_4^+} are

the half-saturation constant for oxygen and ammonium, respectively (mg/L) and, K_d is the endogenous decay coefficient (d^{-1}).

Using specific values for temperature, pH, initial ammonium and oxygen concentration, a kinetic expression results by combining several limiting factors of nitrification process on the biological growth as a product of a Monod-type expression (USEPA, 1975):

$$\mu_{Nit} = 0.47 * \left(e^{0.098*(T-15)}\right) * \left(1 - 0.833(7.2 - pH)\right) * \frac{S_{NH_4^+}}{10^{0.051*(T-1.1)}} * \frac{S_{O_2}}{S_{O_2}+1.3} \quad (5)$$

Where μ_{Nit} is the specific cell growth rate for nitrification (mg-NH_4^+-N/g-cell d) and T is the time-averaged temperature. The biokinetic parameters describing the appropriate nitrogen oxidation step, μ_{max} and K_S, were estimated by minimizing the sum of the squared errors using the SOLVER utility in MS Excel.

4.2.6 Statistical Analyses

ANOVA was used to statistically determine if significant differences in OCR occurred across ammonia treatment levels in the first set of experiments and with time in the second experiment. A multiple linear model was created to highlight trends in oxygen consumption by using the natural logarithm of the oxygen consumption rate as y and the natural logarithm of the concentration of NH_4^+ x. All statistical analyses (ANOVA) were performed and figures produced using R statistical software, (version 3.2.2., R Studio Team, 2017) working with R-base (version 3.3.2, R Development Core Team, 2008). Significance for all statistical analyses was set at an alpha value of 0.05.

4.3 Results and Discussion

4.3.1 Experimental Nitrification OCR

Linear OCR values (µM/h) were observed for each of the three ammonium treatment concentrations in both controls (Figure 4.1). Across the three NH_4^+ treatments, abiotic control OCR values ranged from 0.1 to 0.4 µM/h, most likely reflecting oxidation of other constituents within the BML water matrix, e.g. hydrocarbons, chlorates, hypochlorites and non-ferrous metals (Allen, 2008), while biotic control (e.g., bulk microbial respiration) OCR values ranged between 0.4 and 0.5 µM/h in the same range as those observed in a field-based investigation of OCR in the upper waters of BML where no evident methanotrophy or nitrification were occurring (Arriaga et al. 2018). Abiotic OCR decline as ammonium treatment concentration increase was attributed to the dilution of BML water with the stock solution and as consequence a decrease in the matrix effect. While abiotic chemical oxidation is an important oxygen-consuming process in pit lakes (e.g. H_2S or FeS_2 oxidation), the hydrocarbon nature of BML has produced a water matrix constituents that are uncommon in pit lakes or natural lakes, thus this is a unique process consuming oxygen in BML which should be accounted during the PL design.

In contrast to the linear loss of oxygen in the two control treatments, variable and increasing negative O_2 losses with time occurred in the three NH_4^+ treatments (Figure 4.1). During the first 4-5 days of the experiments, OCR values equaled the total of the mean abiotic and biotic control OCR values (0.6 µM/h; microbial control mean OCR

value 0.4 µM/h and abiotic control mean OCR value 0.2 µM/h) for all three ammonia treatment concentrations (Figure 3). However, after day 5 in each treatment, OCR values increased above the sum of the two controls to ~0.8 uM/d, followed by a progressive increase in OCR after a further 3-4 days to 1.2, 1.5 and 1.3 uM/d respectively until zero oxygen concentration was reached (Figure 4.1). In the 500 NH_4^+ treatment a further increase in OCR (1.7 uM/d) was observed on the last day (Figure 4.1).

The ~ 5 day lag in a differentiated response in oxygen consumption over and above the combined abiotic and biotic controls for all NH_4^+ amended treatments suggests that growth and/or activity levels of ammonium- and nitrite-oxidizer organisms had first to occur as has been noted in other studies (i.e., Bollmann et al., 2002; Van Loosdrecht and Henze, 1999). The recovery from ammonium starvation has been reported to be coupled to cell growth of a few survivor cells, which was argued to take days or even weeks (Laanbroek & Bar-Gilissen, 2002; Tappe et al., 1999; Van Loosdrecht and Henze, 1999; Wilhelm et al., 1998).

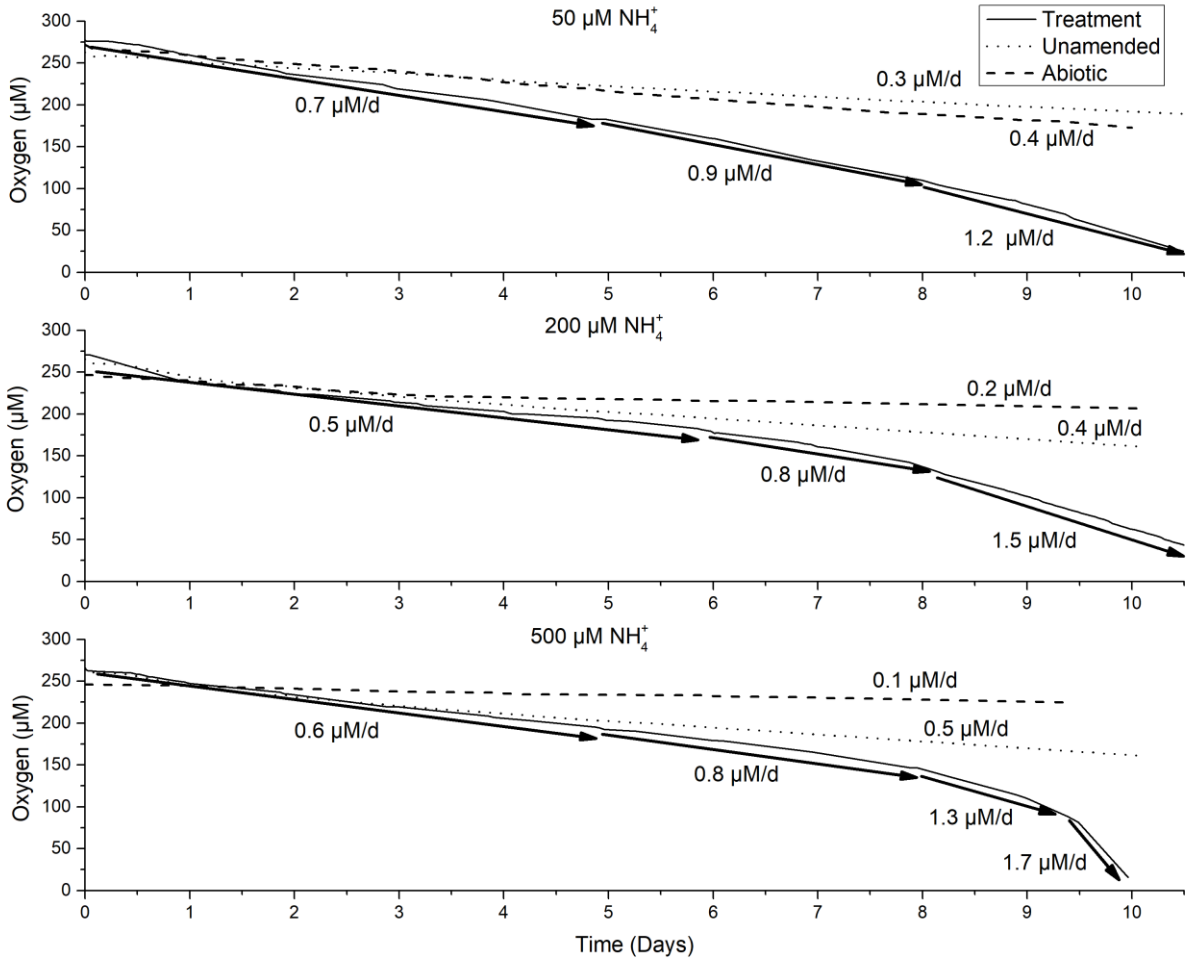

Figure 4.1 Oxygen concentrations versus time and time-dependent rates of OCR (µM/h) for each of the three NH_4^+ amended treatments. Abiotic and biotic controls are also indicated.

For all three NH_4^+ treatments, initial microcosm water temperature and pH values were 21 ± 1.2 °C and 8.4 ± 0.1, respectively (Table 4.3). Slight temperature variations (<1°C) occurred daily, and small pH decreases of 0.2 to 0.4 units in the NH_4^+ treatment experiments and less than 0.1 units in the abiotic and microbial controls occurred (Table 4.3). Microcosm water geochemical characterization at the start of the experiments for both NH_4^+ amended and control microcosms show negligible concentrations for other potential oxygen-consuming constituents (i.e. Fe^{2+} or $\sum H_2S$) (Table 4.3). Further, ammonium loss corresponded to increases in nitrite and nitrate, consistent with microbial nitrification (Figure 4.2). The loss of NH_4^+ for each of the three amendment concentrations (50 µM, 200 µM, 500 µM) was 45 ± 2.4 µM (82% loss), 60 ± 3.1 µM (31% loss), and 91 ± 2.8 µM (18% loss) respectively (Figure 4.2). The predicted oxygen consumption due to nitrification was calculated for each treatment, based on equations 1 and 2 (Both et al., 1992; Laanbroek et al., 1994) and measured concentrations of the three nitrogen species at T=0 and T=E (Figure 4.3) and taking into account the combined effects of abiotic consumption and microbial aerobic respiration. Predicted oxygen consumption due to nitrification accounts for 95% of the observed oxygen loss in the three treatments (Figure 4.3).

The rate of disappearance $(\Delta C/\Delta t)$ (RD) for $NH_4^+$and O_2 (Figure 4.4A) identifies a stoichiometric relationship of 1.8 moles of O_2 per mole of NH_4^+ very close to the 2 moles predicted by equations 1 and 2. This result is in agreement with the experimentally determined cell growth rate of oxygen consumption for nitrifiers (Grady Jr et al., 2011; Gujer and Jenkins, 1975). The maximum OCRs measured for each amended treatment

showed a linear relationship as a function of concentration (Figure 4.4B), indicating that the nitrification rates were enhanced by the ammonium concentration, supporting the hypothesis that nitrificationion and associated consumption of oxygen rates will be ammonium concentration dependent. At the end point (T=E) for all NH_4^+ treatments, nitrite accounted for ~65%, or ~ 2/3 of the NH_4^+ converted. Our results are consistent with the literature which shows that ammonia oxidation to nitrite (nitritation; equation 1) is the rate-determing step controlling the overall nitrification process (Grady et al. 2011; Wong-Chong and Loher, 1975). Further, in a balanced nitrifying system the modeled biomass ratio of ammonium-oxidizing bacteria (AOB) to nitrite-oxidizing bacteria (NOB) should be 2:1 according to thermodynamics and electron transfer (Arciero et al., 1991; Hooper et al., 1997; Winkler et al., 2012). In line with these predictions, growth experiments (Philips et al. 2002) providing optimal conditions for both ammonium-oxidizing bacteria (AOB) and nitrite-oxidizing bacteria (NOB) show that AOB grow faster than NOB. The minimum doubling time of AOB is 7-8 hours while the minimum doubling time of NOB is 10-13 hours. If AOB grow more quickly than NOB, and the ammonium oxidizing rate is higher than nithe trite oxidizing rate, nitrite as an intermediate will accumulate until the growth rate of NOB reaches an optimal state.

To the best of our knowledge, no measurements of nitrification rates in pit lakes have been published to compare with our data and provides an important geochemical baseline for any PL containing ammonia-rich tailings. In comparison with other natural environments, the NH_4^+ oxidation rates (0.7 uM/h) established here were higher than oxygen minimum zones (nM/h) and similar to to those observed in estuarine waters

(Bianchi et al., 1994a, 1994b; Grundle and Juniper, 2011; Iriarte et al., 1996). In general, other environments (e.g. eutrophic lakes or rivers) showed rates five to more than 100 times higher than those observed in BML water amended with ammonium. This could be caused by the difference in nitrification strategy. Studies have shown that "K-strategist" nitrifiers can grow slowly and survive long periods of starvation or under low O_2 and NH_4^+ conditions at a high growth rate (Dytczak et al 2008; Peng and Zhu; 2006). The other type of nitrifiers, "R-strategists", are better adapted to high NH_4^+ concentrations and thus render higher rates of ammonium oxidation. From the literature (Table 4.4), the systems with high ammonium concentration (> 150 μM NH_4^+) showed higher rates than those with low ammonium concentrations (nM to >20 μM NH_4^+). It is hypothesized that the nitrifying microbial community of BML should reflect the growth pattern of nitrifiers adapted to low ammonium concentrations (see more details below).

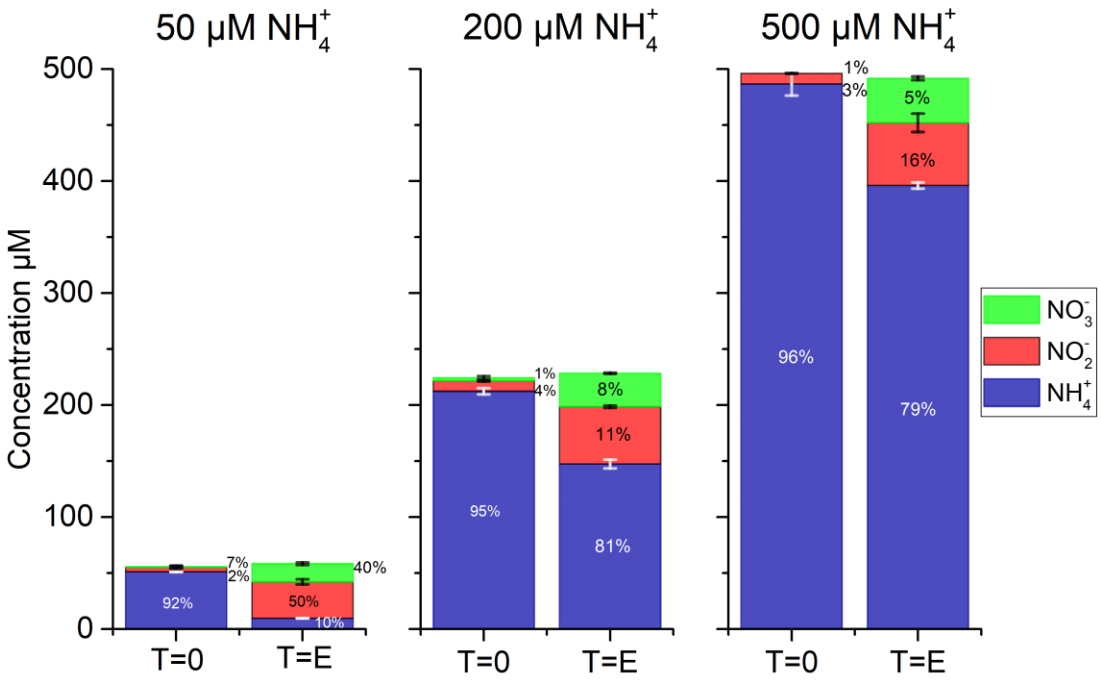

Figure 4.2 Nitrogen species mass balance per treatment for initial (T = 0, 100% oxygen saturation) and final (T = E, 0% oxygen saturation) for each of the three NH_4^+ treatment concentrations. The relative proportion of each N redox species is also identified. Vertical error bars indicate standard deviation (n = 3)

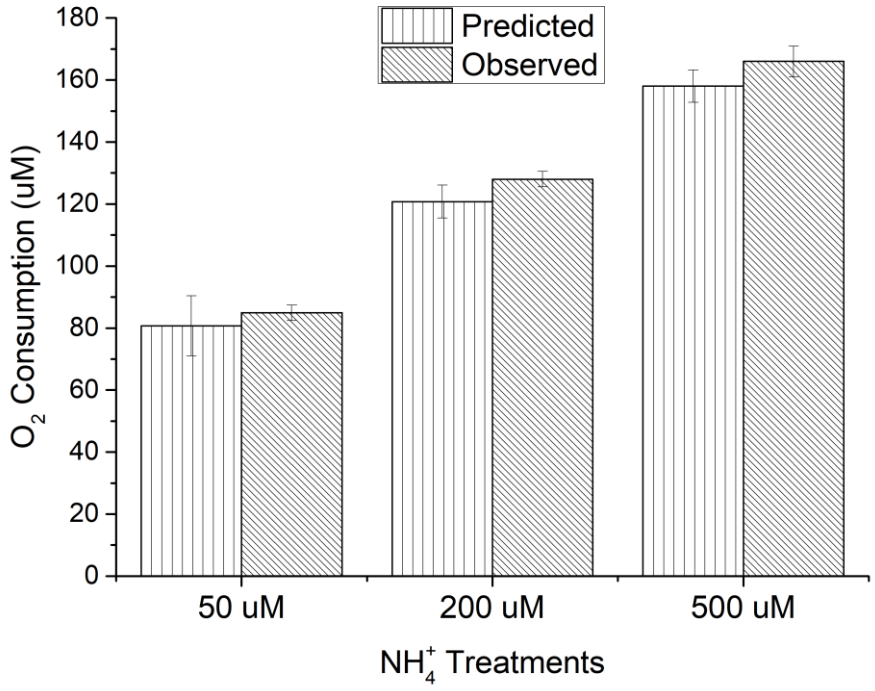

Figure 4.3 Observed and predicted oxygen consumption due to nitrification for the three amended ammonium concentration treatments. Predicted oxygen consumption was determined using equations 1 and 2 and T=E observed concentrations of NH_4^+, NO_2^- and NO_3^-. Bar plots represent the mean and standard deviation (n = 3)

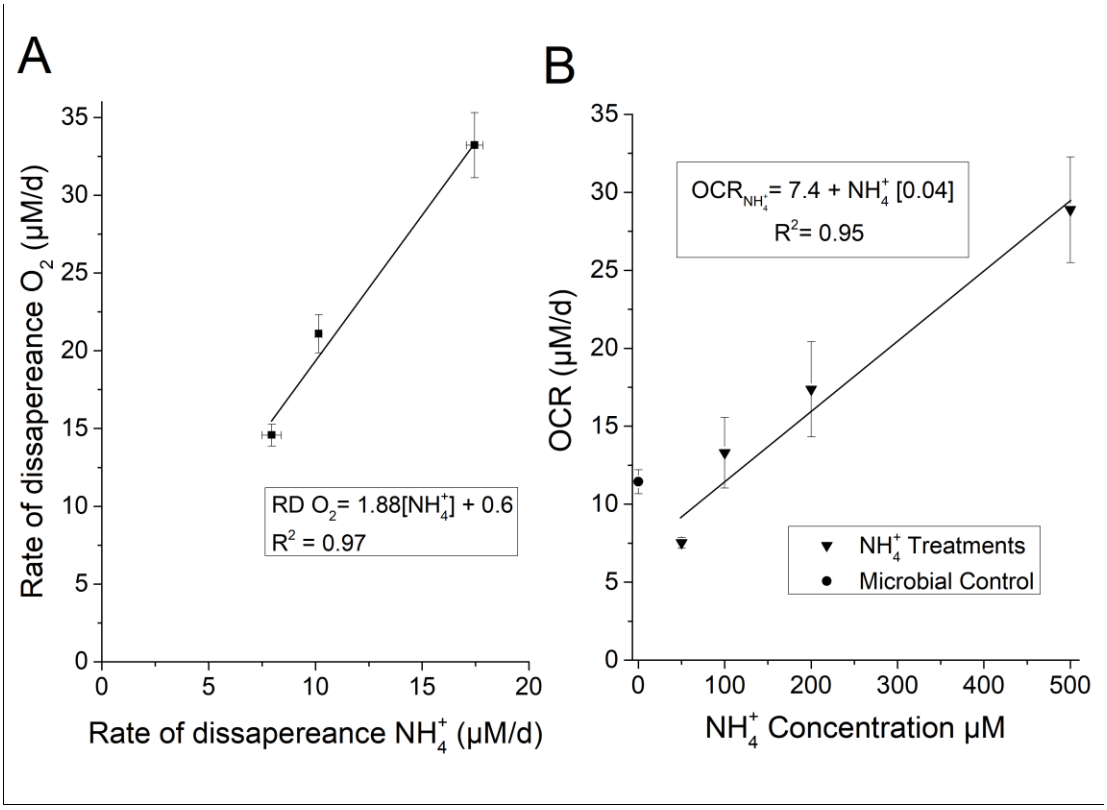

Figure 4.4 Ammonium concentration effect on oxygen concentration and OCR in BML water. A) The rate of disappearance of O_2 to NH_4^+ and, B) linear regression model of OCR per amended treatment after subtracting the contribution from the abiotic and microbial controls. Vertical and horizontal error bars indicate standard deviation (n = 3). Note: figure B include the 100 µM amended treatment (see next section).

Table 4.3 Mean (± standard deviation) concentrations of the biogeochemical analytes and physicochemical parameters across the experimental treatments and control groups. Note: abiotic controls and T=E for 100 µM treatment consisted of only 1 replicate

	NH_4^+ Treatments							
	50 µM		100 µM		200 µM		500 µM	
µM	T=0	T=E	T=0	T=E	T=0	T=E	T=0	T=E
SO_4^{2-} (mM)	2.7 ± 0.03	2.6 ± 0.03	2.7 ± 0.02	2.7	2.4 ± 0.04	2 ± 0.03	2 ± 0.03	3 ± 0.03
$\sum H_2S$	BD	BD	BD		BD	BD	BD	BD
Fe^{2+}	3.5 ± 0.18	3.0 ± 0.11	3.9 ± 0.1	3.4	3.2 ± 0.3	3.1 ± 0.1	2.0 ± 0.1	2.3 ± 0.3
Fe^{3+}	2.6 ± 0.10	1.6 ± 0.19	2.1 ± 0.3	3.5	2.0 ± 0.3	3.2 ± 0.2	2.7 ± 0.3	2.0 ± 0.2
DOC (mg/L)	70 ± 2.6	68 ± 2.9	65 ± 4.1	66	65 ± 2.2	69 ± 3.5	70 ± 3.7	69 ± 2.5
Temp	21 ± 0.24	19 ± 0.26	21 ± 0.3	23	21 ± 0.4	20 ± 0.6	23 ± 0.1	20 ± 0.2
pH	8.6 ± 0.09	8.2 ± 0.05	8.5 ± 0.12	8.2	8.3 ± 0.11	8.1 ± 0.07	8.5 ± 0.09	8.1 ± 0.07

	Abiotic Control						Microbial Control	
	50 µM		200 µM		500 µM			
µM	T=0	T=E	T=0	T=E	T=0	T=E	T=0	T=E
SO_4^{2-} (mM)	2.7	2.6	2.9	2.6	2.8	2.8	2.3 ± 0.22	2.6 ± 0.08
$\sum H_2S$	BD	BD	BD	BD	BD	BD	BD	BD
Fe^{2+}	1.4	1.3	1.7	3.1	1.7	2.1	1.5 ± 0.27	1.5 ± 0.21
Fe^{3+}	2.0	2.6	1.9	2.2	3.0	2.0	3.0 ± 0.35	3.1 ± 0.30
DOC (mg/L)	26	24	27	24	27	26	27 ± 2.4	24 ± 2.7
Temp	21	20	22	20	22	20	21 ± 0.74	20 ± 0.40
pH	8.4	8.3	8.4	8.5	8.4	8.4	8.5 ± 0.12	8.4 ± 0.13

BD: Below detection limit

Table 4.4 Comparison of the NH_4^+ oxidation rates in BML water and other natural systems.

Location	Nitrification Rate (uM NH_4^+/h)	Initial NH_4^+ Concentration (uM)	Type of Environment	Method	Reference
BML water	0.3 - 0.71	17	Hypolimion of an Oil sands Pit Lake	Microcosm incubations	This study
Scheldt estuary	0 - 1	5 -150	Eutrophic estuary	Incubation bottles	Andersson et al 2006
Chilean OMZ	0 - 0.06	< 20	Marine	$^5NH_4^+$ Tracer and incubators	Bristow et al 2016; Molina et al 2005; Ward et al. 1989, Lipschultz et al. 1990
Hamilton Harbour	33	570- 3600	Natural embayment	Incubation in dark bottles	Roy and Knowles, 1994
Rhône River estuary	9.6 - 89.6 mM/h	578	Eutrophic river	Incubation in dark bottles	Feliatra & Bianchi 1993
Seneca River	3.7	170	Eutrophic river	Sediment microcosm experiments	Pauer and Auer 2000
Lake Odongaga	3.5	150	Eutrophic Lake	Sediment microcosm experiments	Pauer and Auer 2000
Multiple	0 - 5.4	NG	Epilimnion of lakes	Incubation bottles	Hall 1986
Multiple	0 - 65	NG	Hypolimnion of lakes	Incubation bottles	Hall 1986

OMZ: Oxygen Minimum zones

NG: not given

The highest OCR (~1.7 uM/h) observed in these experiments was measured at a similar NH_4^+ concentration (>500 µM), to those observed in oil sands active tailing ponds where no nitrification has been detected to date. The results presented here indicate that nitrifiers are present within BML and can utilize NH_4^+ efficiently at high NH_4^+ concentrations in dilute oil sands process water (OSPW) matrices. The BML water cap is a mixture of OSPW and freshwater, which dilutes the naphthenic acids (NA) concentrations to 39 compared to 60 to 120 mg/L observed in tailings ponds (Allen, 2008; Risacher et al. 2018). It has been suggested that concentrations of NA of 40-120mg/L are sufficient to inhibit nitrifiers (Headley & McMartin, 2004; Quagraine et al., 2005; Rogers et al., 2002), providing a possible explanation for why their activity has not been detected to date in active oil sands tailings ponds (Misiti et al., 2013).

Similarly, the NH_4^+ conversion to nitrite, and further to nitrate, and the oxygen consumption observed for the 200 µM NH_4^+ treatment suggest nitrification near the FFT is a possibility, where there are high levels of NH_4^+ and oxygen is available. OCR field-based results for BML in the summer of 2016 (Arriaga et al. 2018; Chapter 3) indicate an overall OCR value of 3.6 uM/h at the FFT-water interface, approximately double the highest OCR rate determined herein experiments that exclude the possibility of methanotrophy. The field determined OCR would include all active chemical and biological processes. Using the experimental OCR values determined here, the potential role of nitrification in oxygen consumption in these field results was estimated by first subtracting the combined experimentally determined biotic and abiotic control rates (~0.6 uM/h) and the estimated contribution of methanotrophy (Table 4.5). As identified in

Risacher et al. 2018, methanotrophy plays a substantial role in BML water cap oxygen consumption. Indeed, methanotrophy was identified to account for 50 to 60% of the field based overall OCR oxygen demand (Arriaga et al. 2018), which translates to ~2.1 uM/h. The predicted contribution to OCR due to nitrification alone ranges between 0.9 and 1.1 uM/h (Table 5) for the BML FFT water interface closest to the experimental OCR values observed for the 200 uM NH_4^+ amendment experiment (0.9 ± 0.1 uM/h), a 2.5x higher concentration than that observed *in situ* of 40 uM (Table 1). However, *in situ*, the BML FFT water interface exhibits very low oxygen conditions (i.e. <5% saturation) and methanotrophs appear to outcompete nitrifiers under these conditions (Risacher et al. 2018).

Table 4.5 Mean and standard deviation (±) OCR values for the microcosm experiments compared to 2016 BML OCR

	OCR μM/h	Reference
NH_4^+ Treatment		
50 μM*	0.4 ± 0.0	This Study
200 μM*	0.9 ± 0.1	This Study
500 μM*	1.2 ± 0.1	This Study
Abiotic Control		
50 μM	0.3	
200 μM	0.2	
500 μM	0.1	
Microbial Control	0.4 ± 0.03	
Epilimnion & Metalimnion	0.3 ± 0.1	Arriaga et al 2018
Top Hypolimnion	2.0 ± 0.2	Arriaga et al 2018
Bottom Hypolimnion	3.4 ± 0.3	Arriaga et al 2018
FWI	3.6 ± 0.5	Arriaga et al 2018

* Nitrification OCR only

4.3.2 Time-dependent NH_4^+ driven oxygen consumption

In order to evaluate the hypothesis that nitrification is associated to the oxygen and ammonium consumption, a series of microcosms amended with the same NH_4^+concentration (100 μM), were serially assessed for the three nitrogen species concentrations at six different time points, corresponding to six oxygen saturation levels: 100, 85, 55, 40, 15 and, 5% O_2 saturation (Figure 4.5). At 85% O_2 saturation, no apparent ammonium consumption occurred (Fig. 4.5A). At 55% O_2, which occurred after day 5, detectable conversion of NH_4^+ to NO_2^- and NO_3^- was evident (Fig. 4.5B) i.e. consistent with the hypothesized start of nitrification for the three different ammonium concentration amendment microcosms (Figure 4.1). With progressive sampling, as $\%O_2$ decreased to 5%, (day 10) NO_2^- increased to 22 uM, NO_3^- to 47 uM and a total of 69 uM of NH_4^+ were converted.

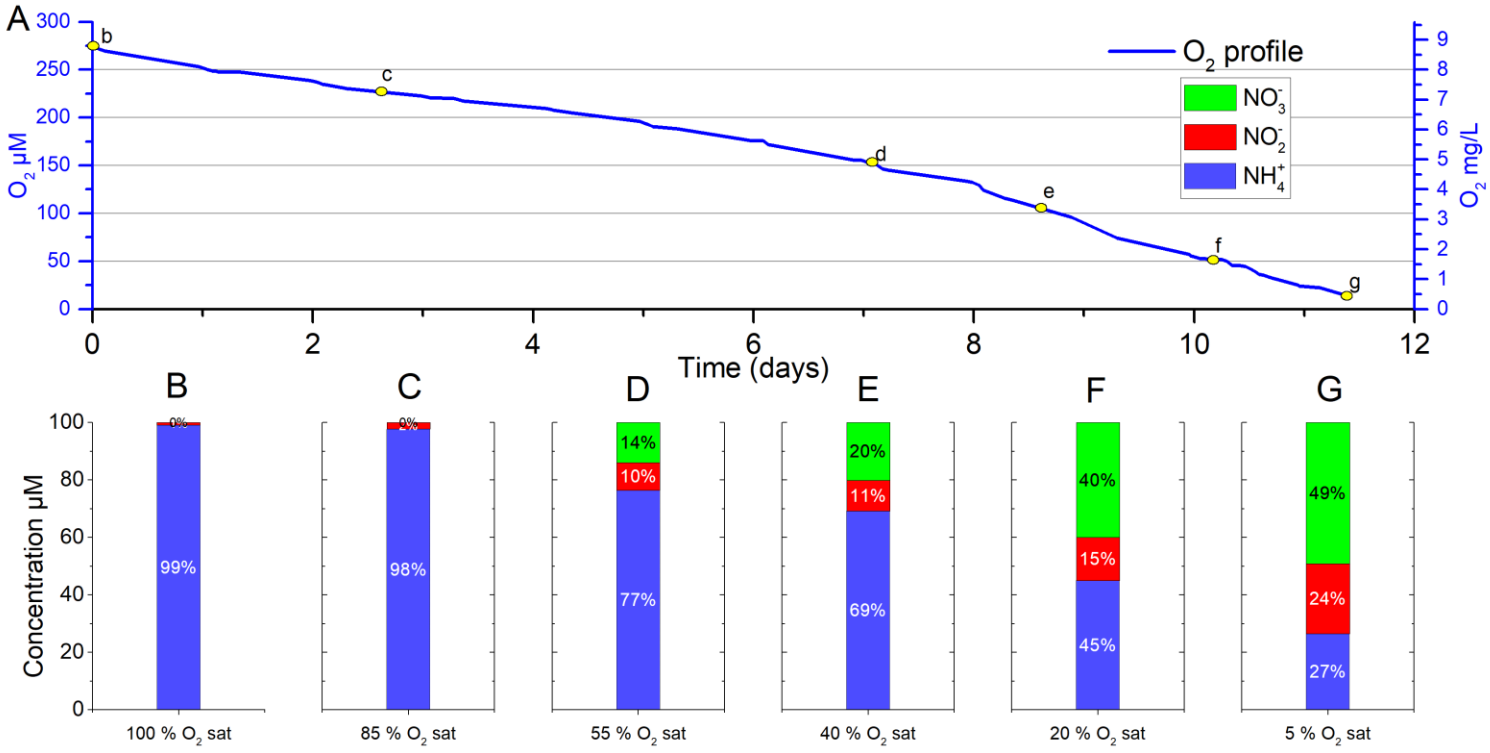

Figure 4.5 Oxygen and nitrogen species (NH_4^+, NO_2^-, NO_3^-) concentrations at six sampling points corresponding to 85, 55, 40, 20, 5 % O_2 saturation in a 100 µM NH_4^+ treatment microcosm experiment. A) Oxygen concentration over time (11 days); left and right y-axes (blue) indicate the oxygen concentration (µM and mg/L, respectively). B–G concentrations of the three nitrogen species concentration measured at the six oxygen saturation levels (yellow circles and small letters b–g). The bottom axis is the oxygen percent saturation at the time of sampling. Percentage indicates the relative nitrogen species abundance per assay

The relative oxygen consumption per O_2% saturation level was calculated, as above, subtracting the microbial and abiotic control OCR values from the total O_2 loss. The remaining O_2 loss, assumed to be due to nitrification, was compared with the predicted O_2 consumption derived from the conversion of NH_4^+ to NO_2^- and to NO_3^- following a stoichiometry of 1.8 moles of O_2 per mole of NH_4^+ (Figure 4.6A). The initial microbial and abiotic control O_2 consumption accounted for 95% of total oxygen loss (85% saturation on day 3) indicating little nitrification was occurring at this point in the experiment. The conversion of NH_4^+ to NO_2^- and to NO_3^- accounts for an increasing ~52% of the overall O_2 loss by the experimental endpoint (5% O_2; day 11).

Given that the energetics of the first step of nitrification is favoured, the NH_4^+ oxidation percentage and the nitrite oxidation percentage were calculated to assess the influence of oxygen saturation. The oxidation rates were calculated as suggested in Hanaki *et al*., 1990., using NH_4^+ oxidation% $= \Delta NO_2^- + \Delta NO_3^- / NH_4^+{}_i$ and NO_2^- oxidation% $= \Delta NO_2^- / NH_4^+{}_i$ where $NH_4^+{}_i$ is the initial ammonium concentration of 100 µM (Figure 4.6A). These indices directly indicate the percentage of progress for the ammonium oxidation and the nitrite oxidation steps in overall nitrification (Figure 4.5). An increase in oxidation rate was observed over the time course of the experiment for both NH_4^+ and NO_2^- oxidation steps. However, the NH_4^+ oxidation rate was always higher and both rates substantially increased (34 and 25% for NH_4^+ and NO_2^- respectively) once oxygen concentrations dropped below 20% O_2 (day 10) contrasting the observed field results determined *in situ*. These experimental results emphasize that the rapid establishment of nitrifying activity is possible under low oxygen conditions and that

both steps are possible when methanotrophs are absent and aerobic heterotrophy is limited by low concentrations of labile organic carbon. These results support the hypothesis that nitrification activity in BML water was associated to oxygen and ammonia consumption and nitrate and nitrite production.

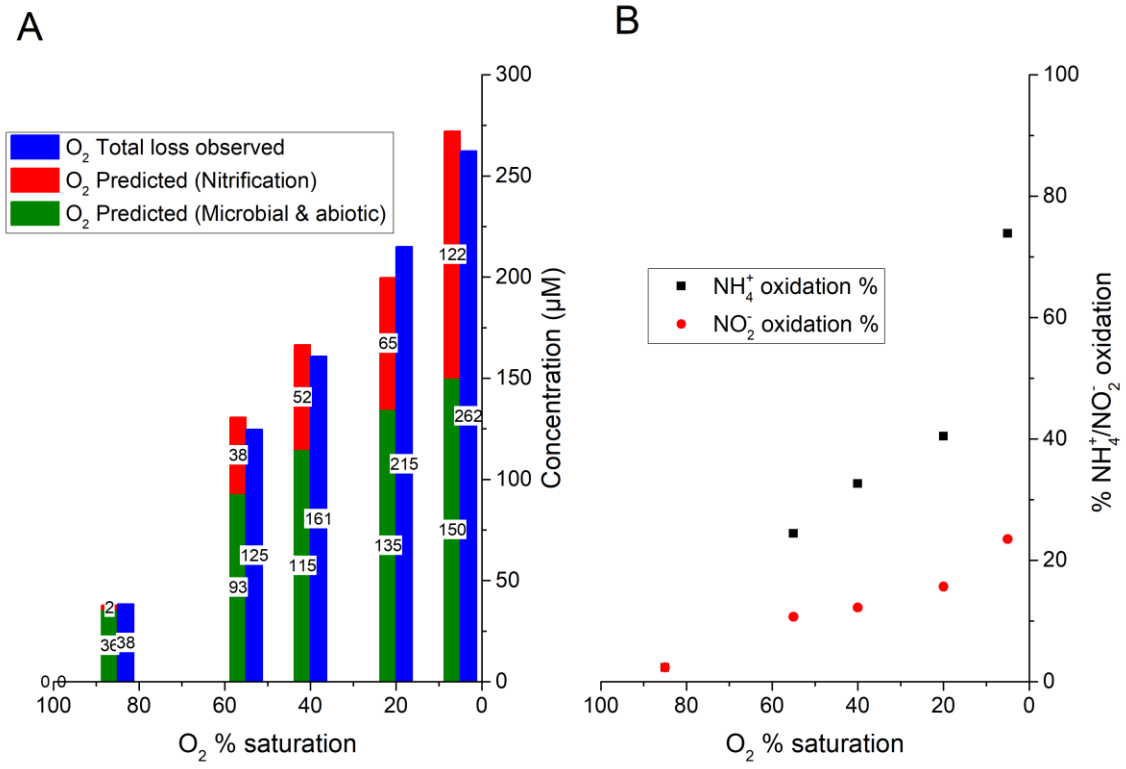

Figure 4.6 Predicted nitrification and NH_4^+/NO_2^- oxidation rates in microcosm experiments. A) The relative contributions of microbial and abiotic controls and predicted nitrification to oxygen consumption measured at different bulk oxygen % saturation levels for the 100 uM NH_4^+ amended experiment. Predicted nitrification values were determined by the relative change of NH_4^+, NO_2^- and NO_3^- using the experimental value determined here of 1.8. Microbial and abiotic contribution values determined in the previous experiments were applied here. B) NH_4^+ and NO_2^- oxidation rates as a function of O_2% saturation level. The oxidation rate was calculated as suggested in Hanaki et al., 1990. NH_4^+ oxidation % $= \Delta(NO_2^- + \Delta NO_3^-)/NH_4^+{}_i$; NO_2^- oxidation % $= \Delta NO_2^-/NH_4^+{}_i$ where $NH_4^+{}_i$ is the initial ammonium concentration (100 μM)

The kinetics of NH_4^+ to NO_2^- oxidation were estimated by fitting the numerical solutions of Eqs. (4) and (5) (Figure 4.7). Microbial nitrification in BML water shows Michaelis-Menten kinetics and it follows a first-order reaction, meaning the growth of nitrifying organism (or nitrification rate) is proportional to the ammonium concentration. Our K_s value for NH_4^+ of 1.01 (Table 4.6) is consistent with the results reported for pure batch nitrifying cultures of 1.0 (Loveless and Painter, 1968), 1.1 (Knowles et al, 1965), 1.0 (Sharma and Ahlert, 1977) and in activated sludge 0.99 (Chandran and Smeets, 2000). However, K_s reported in lab-scale reactors and bio-reactors are at least double in magnitude (Surmacz-Gorska et al., 1996; Dytczak et al, 2008; Taylor and Bottomley 2006). Nitrifying activity presented here is in agreement with other studies (Chen et al., 2006; Easter et al., 1994; Surampalli and Baumann, 1989; Watanabe et al., 1981) were at a low substrate concentration, the relationship becomes linear, following a first-order reaction. At a sufficiently high substrate concentration (> 6 mg/L; Dytczak et al., 2008; Laanbroek and Gerards, 1993; Sharma and Ahlert, 1977), nitrification rate becomes a zero-order expression, meaning the reaction rate does no longer increase with respect to substrate concentration. Cell growth due to nitrification indicates that rates of nitrification within BML are partially controlled by ammonia limitation as nitrification is ammonium-concentration dependent (Figure 6). In BML, the bulk water NH_4^+ concentration decrease from 40 μM in the FWI to close to 15 μM in the surface (Table 4.2; Risacher et al. 2018), reducing the nitrification rate lower than the bulk microbial respiration (Figure 4.4B). Results here build on the observed field based trends identified in Risacher et al 2018 and Arriaga et al. 2018 indicating that nitrifying organisms are present in BML waters and

will transform NH_4^+ in the water of BML. However, the limited ammonia concentration and competition with methanotrophs and potentially other aerobic heterotrophs under the limited O_2 conditions (i.e. <15 μM) observed *in situ* at the BML FFT water interface and within the hypolimnion, appears to hamper their ability to grow more efficiently. It was hypothesized that the nitrifying microbial community of BML should reflect a growth pattern adapted to low NH_4^+ and O_2 conditions. Our specific growth rate value falls within those values reported in similar NH_4^+ conditions (Martens-Habbena et al 2009) but it is below those reported in other studies where the NH_4^+ concentrations were not limited (i.e. >100uM) (Charley et al 1980; Kits et al 2017). Therefore, nitrifiers in BML will grow slowly but they can tolerate periods of starvation and the suboxic conditions in the hypolimnion.

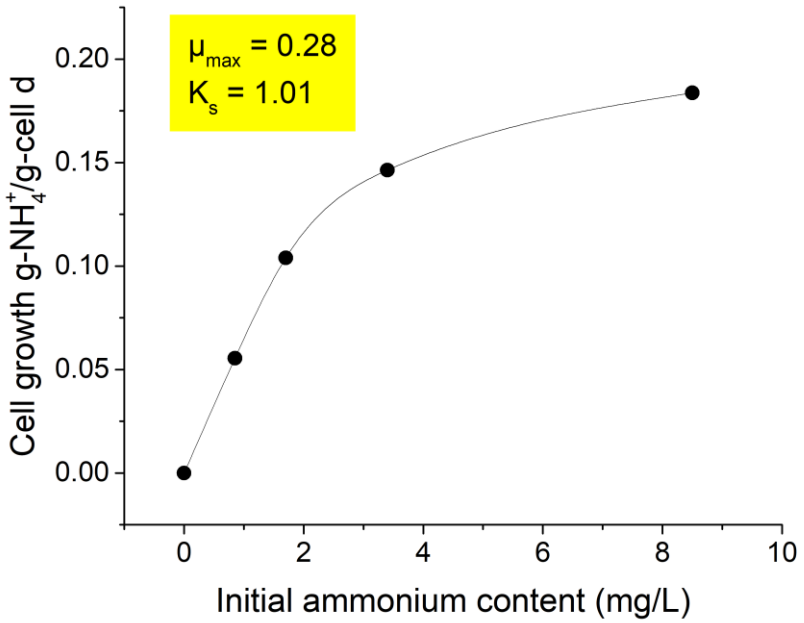

Figure 4.7 Cell growth (g-NH_4^+/g-cells d) as a function of NH_4^+ concentration. The black line represents the best fit.

Table 4.6 Reported K_s and u_{max} values for different systems

μ_{max} (1/h)	K_s mg NH_4^+-N/L	Reference
0.28	1.01 at 21°C	This Study
0.94	1.1 at 22°C	Knowles et al 1965
NR	1 at 20°C	Loveless and Painter 1968
0.66	1.0 at 25°C	Sharma and Ahlert, 1977
0.74	0.99	Chandran and Smeets, 2000
52	1.9	Surmacz-Gorska et al., 1996
NR	1.96	Taylor and Bottomley 2006
NR	2.92	Dytczak et al, 2008

NR: no reported

4.3.3 Link between Field and Experimental Nitrification

The OCR due to nitrification (Figure 4.4B) were plotted against field results, obtained from Arriaga et al. (2018), to compare the contribution of nitrification to the oxygen consumption in water cap of BML (Figure 4.7A). While the BML hypolimnetic OCRs represent the absolute contribution from all potential oxygen-consuming constituents (i.e. methane, ammonium, DOC, Fe^{2+} and $\sum H_2S$), results from Risacher et al 2018 and Arriaga et al 2018 indicate methane and ammonium accounted for most of the oxygen consumption observed in the BML water cap. To distinguish the relative contributions from each of these two processes, we obtained the difference between the linear models of methane and ammonium presented in Arriaga et al. 2018 by algebraic subtraction. Then, the difference obtained was deducted from the field NH_4^+ linear model, and compared against the laboratory NH_4^+ linear model, which included the microbial (respiration) control (Figure 4.7B).

The multivariate linear model (Figure 4.7B) shows that field and laboratory data fitted within the same trend and both are statistically significant (ANOVA, d.f. =17, $p<0.05$), explaining 77% of the variance. Using this model, we calculated the oxygen demand by nitrification alone in the hypolimnion of BML. To account for the oxygen consumption in BML, high-spatial resolution sampling (0.1 m; Morris, 2017) in the hypolimnetic zone permitted the calculation of a volume-weighted for ammonium concentration in the bulk water that can be utilized to calculate the oxygen demand. Adopting our nitrification model, the hypolimnetic oxygen demand by nitrification only is approximately 219 $x10^3$ moles.

Similarly, the volume-weighted concentration for the three N species (i.e. NH_4^+, NO_2^-, and NO_3^-) in BML was calculated using the geochemical data from August 7th (Table 4.2) for the surface (i.e. epilimnion and metalimnion) and hypolimnion zones (Table 4.6). The combined O_2 demand for NH_4^+ and NO_2^-, assuming a 1.7 NH_4^+ to NO_3^- conversion (Risacher et al. 2018), requires approximately 1309 $x10^3$ moles which is almost 6 times larger than our predicted value. This result does not support our hypothesis, as the experimentally determined nitrification O_2 consumption model underpredicted to the expected O_2 consumed by bulk water ammonia concentration of BML. Under the circumstances presented above, we hypothesize that nitrifiers will allocate in a more advantageous location such as the metalimnion-hypolimnion interface (e.g. Hernandez-Aviles et al., 2012). The total N mass in the surface layers is 4.5 larger than in the hypolimnion, indicating either 1) nitrification in the hypolimnion is partially suppressed mobilizing N into the surface layers and/or 2) nitrification is allocated in the metalimnion where N species are not contained. Interestingly, the surface layers contain double the amount of $NH_4^+$and 17 times more NO_3^- than in the hypolimnion, indicating that partial nitrification, caused by competition for oxygen with heterotrophs and the NH_4^+ limitation, occurs in the hypolimnion, where the highest concentration of ammonium occur, but most of the ammonium conversion to nitrate occurs in the metalimnion-hypolimnion interface.

In freshwater environments, nitrification is contained in the bottom water, occurring at the oxic-anoxic interface typically at the sediment-water interface, where nitrate can rapidly be reduced under anaerobic conditions. The N accumulation in the

water cap is a concern for the environmental sustainability of BML as it can stimulate primary productivity also known as harmful algal/cyanobacterial blooms (Anderson et al. 2002; Conley et al. 2009; Heisler et al. 2008). Besides, increased ammonium and nitrite concentrations in the water column are highly toxic to aquatic organisms, producing elevated levels of methemoglobin which have shown to cause anoxia in fish (Tilak et al. 2007; Romano and Zeng, 2013). Thus, further research should be focused to assess the N cycling and its potential outcomes for the water quality of BML.

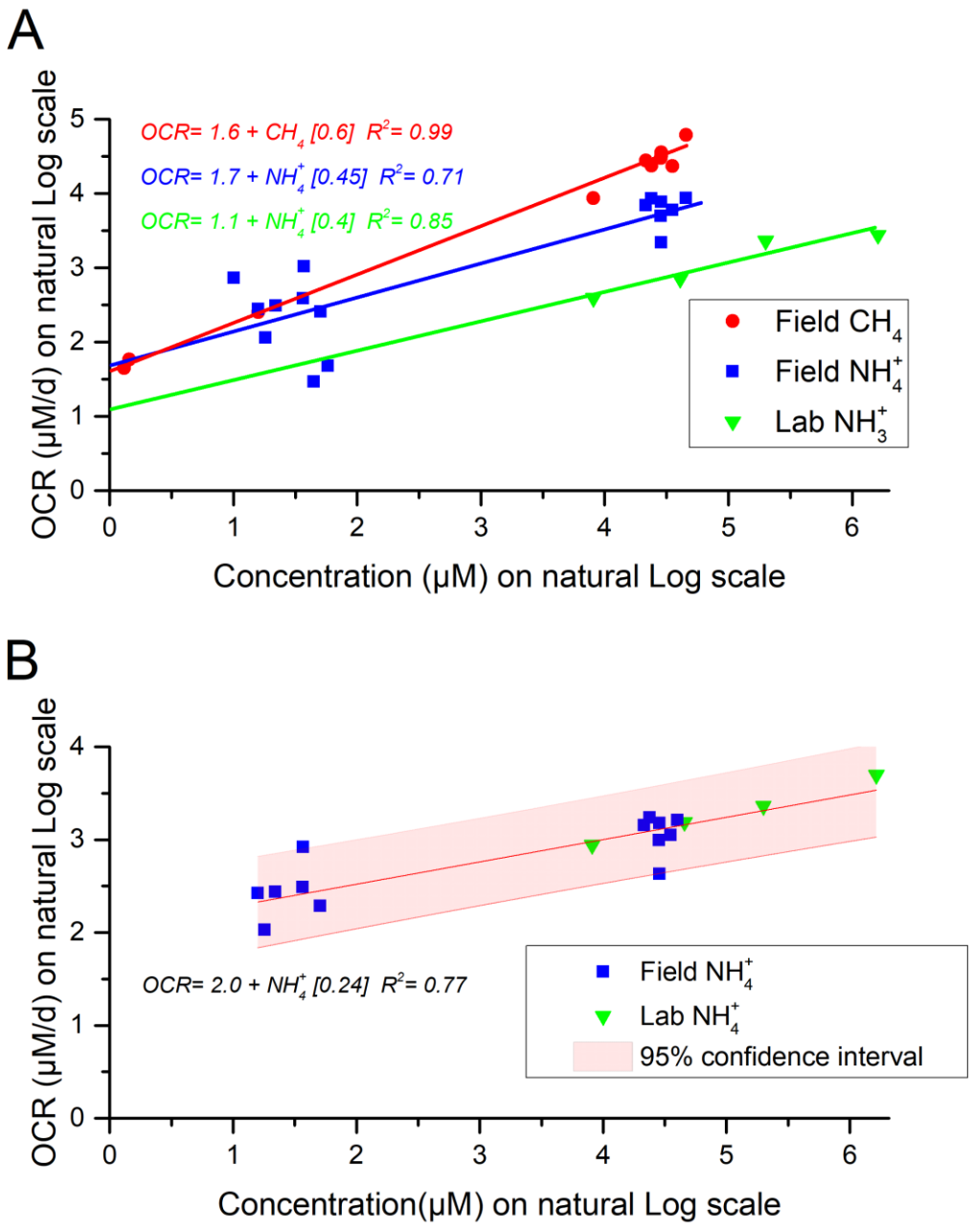

Figure 4.7 Nitrification relationship models. A) Linear models between field data for CH_4 and NH_4^+ and, laboratory NH_4^+ and OCR B) calculated field NH_4^+ only versus OCR for the BML water cap determined by algebraic subtraction of the field CH_4 contribution to

observed field OCR values and laboratory ammonium concentrations versus OCR. The red indicates a 97.5 % confidence interval.

Table 4.7 N species mass balance in BML from August 4th, 2017

	x10³ moles		
	Total NH_4^+	Total NO_2^-	Total NO_3^-
Surface	1061	308	2871
Hypolimnion	467	303	163

4.4 Conclusions

Nitrification emergence, as one of the main oxygen-consuming mechanisms within the first five years of BML decommission, provides evidence for the natural reclamation processes taking place over time. This research aimed at investigating nitrification and OCR under different ammonium treatments and O_2 aerobic stages. The main findings from this study are as follows:

- This is the first report directly measuring oxygen consumption rates related to nitrification within any pit lake, and thus provides an important biogeochemical baseline of possible nitrification rates that can be expected for pit lakes containing ammonia rich tailings.
- BML water amended with ammonia showed that nitrification activity was ammonium concentration-dependent proportional with oxygen and ammonia consumption and nitrate and nitrite production.

- Nitrification in the hypolimnion of BML is partially inhibited by the NH_4^+ concentration limitations and the competition for O_2 conditions providing evidence of the contribution to the excess of N species to the water cap that can affect the environmental sustainability of BML.

The findings presented here have significantly enhanced our understanding of nitrogen cycling within pit lakes containing ammonia rich tailings, and our observation linking laboratory and field data related to nitrification provides further evidence of the interplay of in situ biogeochemical processes that play a pivotal role in the oxygen consumption within the water cap. It is of significant relevance across extractive resource industries to create new guidelines on reclamation strategies but also for other anthropogenically impacted or engineered systems with high oxygen demand associated with ammonium.

4.5 References

Alberta Government, 2017. Oil Sands Information Portal [WWW Document]. Oil sands Inf. portal. URL http://osip.alberta.ca/map/ (accessed 1.31.18).

Allen, E.W., 2008. Process water treatment in Canada's oil sands industry: I. Target pollutants and treatment objectives. J. Environ. Eng. Sci. 7, 123–138. https://doi.org/10.1139/s07-038

Anderson, D.M., Glibert, P.M., Burkholder, J.M., 2002. Harmful algal blooms and eutrophication: nutrient sources, composition, and consequences. Estuaries 25, 704–726.

Arciero, D.M., Balny, C., Hooper, A.B., 1991. Spectroscopic and rapid kinetic studies of reduction of cytochrome c554 by hydroxylamine oxidoreductase from Nitrosomonas europaea. Biochemistry 30, 11466–11472.

Arriaga, D., Risacher, F.F., Morris, P.K., Goad, C., Nelson, T.C., Slater, G.F., Warren, L.A., 2018. The precarious balance between physical transport and biogeochemical consumption in determining water cap oxygen concentrations in the first oil sands pit lake, Base Mine Lake. Chemosphere.

ASTM, 2005. ASTM F838-05, Standard Test Method for Determining Bacterial Retention of Membrane Filters Utilized for Liquid Filtration.

Bae, W., Rittmann, B.E., 1996. A structured model of dual-limitation kinetics. Biotechnol. Bioeng. 49, 683–689.

Bianchi, M., Bonin, P., Feliatra, 1994. Bacterial nitrification and denitrification rates in the Rhone River plume (northwestern Mediterranean Sea). Mar. Ecol. Prog. Ser. 197–202.

Bianchi, M., Morin, P., Le Corre, P., 1994. Nitrification rates, nitrite and nitrate distribution in the Almeria-Oran frontal systems (eastern Alboran Sea). J. Mar. Syst. 5, 327–342.

Bollmann, A., Bär-Gilissen, M.-J., Laanbroek, H.J., 2002. Growth at low ammonium concentrations and starvation response as potential factors involved in niche differentiation among ammonia-oxidizing bacteria. Appl. Environ. Microbiol. 68, 4751–4757.

Both, G.J., Gerards, S., Laanbroek, H.J., 1992. Kinetics of nitrite oxidation in two Nitrobacter species grown in nitrite-limited chemostats. Arch. Microbiol. 157, 436–441.

Bowman, F.W., Calhoun, M.P., White, M., 1967. Microbiological methods for quality control of membrane filters. J. Pharm. Sci. 56, 222–225.

Bungay, H.R., 1994. Growth rate expressions for two substrates one of which is inhibitory. J. Biotechnol. 34, 97–100.

Chalaturnyk, R.J., Don Scott, J., Özüm, B., 2002. Management of oil sands tailings. Pet.

Sci. Technol. 20, 1025–1046.

Chandran, K., Smets, B.F., 2005. Optimizing experimental design to estimate ammonia and nitrite oxidation biokinetic parameters from batch respirograms. Water Res. 39, 4969–4978.

Charley, R.C., Hooper, D.G., McLee, A.G., 1980. Nitrification kinetics in activated sludge at various temperatures and dissolved oxygen concentrations. Water Res. 14, 1387–1396.

Chen, M., Walshe, G., Fru, E.C., Ciborowski, J.J.H., Weisener, C.G., 2013. Microcosm assessment of the biogeochemical development of sulfur and oxygen in oil sands fluid fine tailings. Appl. geochemistry 37, 1–11. https://doi.org/10.1016/j.apgeochem.2013.06.007

Chen, S., Ling, J., Blancheton, J.-P., 2006. Nitrification kinetics of biofilm as affected by water quality factors. Aquac. Eng. 34, 179–197.

Cheryan, M., 1998. Ultrafiltration and microfiltration handbook. CRC press.

Conley, D.J., Paerl, H.W., Howarth, R.W., Boesch, D.F., Seitzinger, S.P., Havens, K.E., Lancelot, C., Likens, G.E., 2009. Controlling eutrophication: nitrogen and phosphorus. Science (80-.). 323, 1014–1015.

Curtis, E.J.C., Durrant, K., Harman, M.M.I., 1975. Nitrification in rivers in the Trent Basin. Water Res. 9, 255–268.

Dompierre, K.A., Lindsay, M.B., Cruz-Hernandez, P., Halferdahl, G.M., 2016. Initial geochemical characteristics of fluid fine tailings in an oil sands end pit lake. Sci Total Env. 556, 196–206. https://doi.org/10.1016/j.scitotenv.2016.03.002

Dytczak, M.A., Londry, K.L., Oleszkiewicz, J.A., 2008. Activated sludge operational regime has significant impact on the type of nitrifying community and its nitrification rates. Water Res. 42, 2320–2328.

Easter, C.C., Novak, J.T., Libey, G.S., Boardman, G.R., 1994. Rotating biological

contactor performance in recirculating aquaculture systems. Orig. not available Exam.

Eckert, W.F., Masliyah, J.H., Gray, M.R., Fedorak, P.M., 1996. Prediction of sedimentation and consolidation of fine tails. AIChE J. 42, 960–972.

Foght, J.M., Gieg, L.M., Siddique, T., 2017. The microbiology of oil sands tailings: past, present, future. FEMS Microbiol. Ecol. 93.

Grady Jr, C.P.L., Daigger, G.T., Love, N.G., Filipe, C.D.M., 2011. Biological wastewater treatment. CRC press.

Grundle, D.S., Juniper, S.K., 2011. Nitrification from the lower euphotic zone to the sub-oxic waters of a highly productive British Columbia fjord. Mar. Chem. 126, 173–181.

Gujer, W., Jenkins, D., 1975. The contact stabilization activated sludge process—oxygen utilization, sludge production and efficiency. Water Res. 9, 553–560.

Hanaki, K., Wantawin, C., Ohgaki, S., 1990. Nitrification at low levels of dissolved oxygen with and without organic loading in a suspended-growth reactor. Water Res. 24, 297–302.

Harris, G., 2012. Phytoplankton ecology: structure, function and fluctuation. Springer Science & Business Media.

Headley, J. V, Barrow, M.P., Peru, K.M., Fahlman, B., Frank, R.A., Bickerton, G., McMaster, M.E., Parrott, J., Hewitt, L.M., 2011. Preliminary fingerprinting of Athabasca oil sands polar organics in environmental samples using electrospray ionization Fourier transform ion cyclotron resonance mass spectrometry. Rapid Commun. Mass Spectrom. 25, 1899–1909.

Headley, J. V, McMartin, D.W., 2004. A review of the occurrence and fate of naphthenic acids in aquatic environments. J. Environ. Sci. Heal. Part A 39, 1989–2010.

Heisler, J., Glibert, P.M., Burkholder, J.M., Anderson, D.M., Cochlan, W., Dennison,

W.C., Dortch, Q., Gobler, C.J., Heil, C.A., Humphries, E., 2008. Eutrophication and harmful algal blooms: a scientific consensus. Harmful Algae 8, 3–13.

Hernandez-Aviles, J.S., Bertoni, R., Macek, M., Callieri, C., 2012. Why bacteria are smaller in the epilimnion than in the hypolimnion? A hypothesis comparing temperate and tropical lakes. J. Limnol. 71, 10.

Holowenko, F.M., MacKinnon, M.D., Fedorak, P.M., 2000. Methanogens and sulfate-reducing bacteria in oil sands fine tailings waste. Can J Microbiol 46, 927–937.

Hooper, A.B., Vannelli, T., Bergmann, D.J., Arciero, D.M., 1997. Enzymology of the oxidation of ammonia to nitrite by bacteria. Antonie Van Leeuwenhoek 71, 59–67.

Iriarte, A., de Madariaga, I., Diez-Garagarza, F., Revilla, M., Orive, E., 1997. Primary plankton production, respiration and nitrification in a shallow temperate estuary during summer. J. Exp. Mar. Bio. Ecol. 208, 127–151.

Johnson, E., Castendyk, D.N., 2012. The INAP Pit Lakes Database: A novel tool for the evaluation of predicted pit lake water quality, in: Proceedings of the 9th International Conference on Acid Rock Drainage: Ottawa, Canada. pp. 1–12.

Jornitz, M.W., Agalloco, J.P., Akers, J.E., Madsen, R.E., Meltzer, T.H., 2001. Filter Integrity Testing in Liquid Applications, Revisited. Pharm. Technol.

Kits, K.D., Sedlacek, C.J., Lebedeva, E. V, Han, P., Bulaev, A., Pjevac, P., Daebeler, A., Romano, S., Albertsen, M., Stein, L.Y., 2017. Kinetic analysis of a complete nitrifier reveals an oligotrophic lifestyle. Nature 549, 269.

Knowles, G., Downing, A.L., Barrett, M.J., 1965. Determination of kinetic constants for nitrifying bacteria in mixed culture, with the aid of an electronic computer. Microbiology 38, 263–278.

Laanbroek, H.J., Bär-Gilissen, M.-J., Hoogveld, H.L., 2002. Nitrite as a stimulus for ammonia-starved Nitrosomonas europaea. Appl. Environ. Microbiol. 68, 1454–1457.

Laanbroek, H.J., Bodelier, P.L.E., Gerards, S., 1994. Oxygen consumption kinetics of Nitrosomonas europaea and Nitrobacter hamburgensis grown in mixed continuous cultures at different oxygen concentrations. Arch. Microbiol. 161, 156–162.

Laanbroek, H.J., Gerards, S., 1993. Competition for limiting amounts of oxygen between Nitrosomonas europaea and Nitrobacter winogradskyi grown in mixed continuous cultures. Arch. Microbiol. 159, 453–459.

Loveless, J.E., Painter, H.A., 1968. The influence of metal ion concentrations and pH value on the growth of a Nitrosomonas strain isolated from activated sludge. Microbiology 52, 1–14.

Martens-Habbena, W., Berube, P.M., Urakawa, H., José, R., Stahl, D.A., 2009. Ammonia oxidation kinetics determine niche separation of nitrifying Archaea and Bacteria. Nature 461, 976.

Misiti, T., Tandukar, M., Tezel, U., Pavlostathis, S.G., 2013. Inhibition and biotransformation potential of naphthenic acids under different electron accepting conditions. Water Res. 47, 406–418. https://doi.org/10.1016/j.watres.2012.10.019

Morris, P., 2018. Depth Dependent Roles of Methane, Ammonia and Hydrogen Sulfide in the Oxygen Consumption of Base Mine Lake, the pilot Athabasca Oil Sands Pit Lake.

Peng, Y., Zhu, G., 2006. Biological nitrogen removal with nitrification and denitrification via nitrite pathway. Appl. Microbiol. Biotechnol. 73, 15–26.

Penner, T.J., Foght, J.M., 2010. Mature fine tailings from oil sands processing harbour diverse methanogenic communities. Can J Microbiol 56, 459–470. https://doi.org/10.1139/w10-029

Philips, S., Wyffels, S., Sprengers, R., Verstraete, W., 2002. Oxygen-limited autotrophic nitrification/denitrification by ammonia oxidisers enables upward motion towards more favourable conditions. Appl. Microbiol. Biotechnol. 59, 557–566.

Quagraine, E.K., Peterson, H.G., Headley, J. V, 2005. In situ bioremediation of naphthenic acids contaminated tailing pond waters in the Athabasca oil sands region—demonstrated field studies and plausible options: a review. J. Environ. Sci. Heal. 40, 685–722.

Risacher, F.F., Morris, P.K., Arriaga, D., Goad, C., Nelson, T.C., Slater, G.F., Warren, L.A., 2018. The interplay of methane and ammonia as key oxygen consuming constituents in early stage development of Base Mine Lake, the first demonstration oil sands pit lake. Appl. Geochemistry 93, 49–59. https://doi.org/10.1016/j.apgeochem.2018.03.013

Rogers, V. V, Liber, K., MacKinnon, M.D., 2002. Isolation and characterization of naphthenic acids from Athabasca oil sands tailings pond water. Chemosphere 48, 519–527.

Romano, N., Zeng, C., 2013. Toxic effects of ammonia, nitrite, and nitrate to decapod crustaceans: a review on factors influencing their toxicity, physiological consequences, and coping mechanisms. Rev. Fish. Sci. 21, 1–21.

Segers, P., Vancanneyt, M., Pot, B., Torck, U., Hoste, B., Dewettinck, D., Falsen, E., Kersters, K., De Vos, P., 1994. Classification of Pseudomonas diminuta Leifson and Hugh 1954 and Pseudomonas vesicularis Büsing, Döll, and Freytag 1953 in Brevundimonas gen. nov. as Brevundimonas diminuta comb. nov. and Brevundimonas vesicularis comb. nov., respectively. Int. J. Syst. Evol. Microbiol. 44, 499–510.

Sharma, B., Ahlert, R.C., 1977. Nitrification and nitrogen removal. Water Res. 11, 897–925.

Sprent, J.I., 1987. The ecology of the nitrogen cycle. Cambridge University Press.

Stasik, S., Loick, N., Knöller, K., Weisener, C., Wendt-Potthoff, K., 2014. Understanding biogeochemical gradients of sulfur, iron and carbon in an oil sands tailings pond. Chem. Geol. 382, 44–53.

Surampalli, R.Y., Baumann, E.R., 1989. Supplemental aeration enhanced nitrification in a secondary RBC plant. J. (Water Pollut. Control Fed. 200–207.

Surmacz-Gorska, J., Gernaey, K., Demuynck, C., Vanrolleghem, P., Verstraete, W., 1996. Nitrification monitoring in activated sludge by oxygen uptake rate (OUR) measurements. Water Res. 30, 1228–1236.

Tappe, W., Laverman, A., Bohland, M., Braster, M., Rittershaus, S., Groeneweg, J. v, Van Verseveld, H.W., 1999. Maintenance energy demand and starvation recovery dynamics of Nitrosomonas europaea and Nitrobacter winogradskyi cultivated in a retentostat with complete biomass retention. Appl. Environ. Microbiol. 65, 2471–2477.

Taylor, A.E., Bottomley, P.J., 2006. Nitrite production by Nitrosomonas europaea and Nitrosospira sp. AV in soils at different solution concentrations of ammonium. Soil Biol. Biochem. 38, 828–836.

Tilak, K.S., Veeraiah, K., Raju, J.M.P., 2007. Effects of ammonia, nitrite and nitrate on hemoglobin content and oxygen consumption of freshwater fish, Cyprinus carpio (Linnaeus). J. Environ. Biol. 28, 45–47.

Transfer, U.S.E.P.A.O. of T., Parker, D.S., 1975. Process design manual for nitrogen control.

Van Loosdrecht, M.C.M., Henze, M., 1999. Maintenance, endogeneous respiration, lysis, decay and predation. Water Sci. Technol. 39, 107–117.

Viollier, E., Inglett, P.W., Hunter, K., Roychoudhury, A.N., Van Cappellen, P., 2000. The ferrozine method revisited: Fe (II)/Fe (III) determination in natural waters. Appl. geochemistry 15, 785–790.

Watanabe, Y., Ishiguro, M., Nishidome, K., 1981. Nitrification kinetics in a rotating biological disk reactor, in: Water Pollution Research and Development. Elsevier, pp. 233–251.

Wetzel, R.G., 1983. Limnology (2nd edn). Saunders Coll. Publ. Philadelphia 767, R81pp.

Wilhelm, R., Abeliovich, A., Nejidat, A., 1998. Effect of long-term ammonia starvation on the oxidation of ammonia and hydroxylamine by Nitrosomonas europaea. J. Biochem. 124, 811–815.

Winkler, M.K.H., Yang, J., Kleerebezem, R., Plaza, E., Trela, J., Hultman, B., van Loosdrecht, M.C.M., 2012. Nitrate reduction by organotrophic Anammox bacteria in a nitritation/anammox granular sludge and a moving bed biofilm reactor. Bioresour. Technol. 114, 217–223.

Wong-Chong, G.M., Loehr, R.C., 1975. The kinetics of microbial nitrification. Water Res. 9, 1099–1106.

Wu, S.-C., Shih, S.-H., Liu, H.-S., 2007. Dynamic behavior of double-substrate interactive model. J. Chinese Inst. Chem. Eng. 38, 107–115.

Chapter 5: Concluding Statements

5.1 Summary

This thesis set out to explain the interaction between biogeochemical redox cycling and physical processes influencing the oxygen dynamics across the water column of BML, the first oil sands pit lake. A field-based study examined the physicochemical and geochemical aspects throughout the water cap determined the oxygen consumption rates (OCR) and the link between the main oxygen-consuming constituents (OCC). OCR experimentation occurred during summer stratification in temporal and spatial scales at specific O_2 gradients and zones of interest such as the FFT-water interface (FWI). BML OCRs were depth-dependent associated with the Fluid Fine Tailings (FFT) as the source of OCC. Field results identified high OCR driven by methane and ammonia, within the range of highly productive eutrophic to hyper eutrophic lakes, at the FFT water interface, i.e. where concentrations of OCC are highest which is consistent with the mobilization of OCC from the FFT layer impacting oxygen concentrations, such that the highest concentrations of these two constituents and associated oxygen consumption occur at the FWI. Despite the observed high hypolimnetic OCR values, oxygen was detectable at the FFT interface, albeit at low concentrations, contrasting the anoxic lower waters typically observed in highly productive systems. A vertical O_2 transport model was implemented to gain insight into how both, biogeochemical and physical mixing, collectively describe the O_2 dynamics. Physical transport modelling revealed vertical entrainment of oxygen from the metalimnetic region into the hypolimnion currently exceeds hypolimnetic biogeochemical oxygen consumption by a small amount, explaining the persistence of

low levels of oxygen to the FFT water interface. BML O_2 transport modeling identified that physical processes at the system-scale play a key role in determining the oxygen distribution and concentrations observed at depth within a lake system.

The field observed emergence of nitrification as an important oxygen consumption mechanism within the BML water cap was assessed experimentally to gain insights into the projected impact to the future of BML. This study assessed the effect of varying ammonium concentration addition on OCR values and compared laboratory OCR values to field derived OCR in BML water in well-constrained experimental microcosms. Nitrification activity showed evidence to be ammonium-concentration dependent associated with oxygen and ammonia consumption and nitrate and nitrite production. OCRs linked to nitrification affirmed to be directly proportional to the ammonium concentration, confirming that nitrification is active in BML water. Microbial nitrification in BML water shows Michaelis-Menten kinetics following a first-order reaction, meaning the growth of nitrifying organism (or nitrification rate) is proportional to the ammonium concentration. The collective results presented here indicate that nitrification in the hypolimnion of BML was limited by extant ammonia concentrations (< 0.7 mg NH_4^+/L) and competition for O_2 with other heterotrophic organisms as observed in other N-rich environments. A comparison of experimental oxygen consumption due to nitrification nit results versus results from the field where other oxygen consuming processes are possible identify that field based nitrification rates are six times lower than the experimental oxygen consumption observed. These results highlight the competition for oxygen by multiple processes within BML will be an important control on biogeochemical cycling.

5.2 Knowledge Advancement

The results of this doctoral work contributes to our understanding of the fundamental controls of O_2 concentrations in a variety of systems, not only in pit lakes, in terms of the interactive biogeochemical and physical processes that collectively drive observed water column oxygen levels to have a more accurate prediction of the O_2 dynamics and help guide pit lake design. Determining the interplay of physical mixing and biogeochemical affecting the development of the oxic layer in BML reveals fundamental novel insights that inform design of future pit lakes. These new insights delineate the potential effects of mobilized reduced constituents in the water cap from FFT and processes that may mitigate or exacerbate these impacts.

This Ph.D. study is the first report directly measuring OCR within any pit lake. Thus, it provides an important geochemical baseline for an understanding of the expected oxygen consumption rates in pit lakes containing ammonia- and methane-rich tailings. In addition, the OCR values measured in BML water cap indicate that biogeochemical oxygen consumption is important in the consideration of the possible viability of WCTT. Results will guide the development and application of WCTT as a reclamation strategy for not only the oil sands industry, but also for other natural environments impacted by industrial and domestic contamination.

The uniqueness of this experimental aquatic oil sand pit lake environment creates a complex and dynamic system governed by physical, biological and chemical aspects. One of the goals of this doctoral work was to grasp a better understanding of the different

biogeochemical mechanisms occurring in the water cap and use this information to provide management strategies for future pit lakes. The OCRs assessed the water cap O_2 controls throughout the water cap and link those rates to the main oxygen-consuming constituents to deepen our understanding of the biogeochemical processes in this water system. For instance, the results identify that the FFT dissolved, particulate and gaseous compounds were mobilized up into the water cap, affecting the biogeochemical cycling of the water column. For the first time in an oil sands pit lake, this doctoral study identified a direct relationship between the OCR and associated OCC in BML water cap (Chapter 3). Also, the results of this thesis highlight the importance to understand the different factors affecting the oxygen consumption such as the aerobic respiration and the physical mixing. Without an O_2 injection into the hypolimnetic zone, the large O_2 demand can rapidly deplete the oxygen, moving up anaerobic processes, which in turn exacerbate the release of OCC and as consequence the oxygen demand. Results detailed in Chapters 3 and 4 also highlight important principles of geomicrobiology. For example, findings from this doctoral research identify important ecological niches where geochemical trends (i.e. ammonia and methane concentration were directly proportional to OCR) begin to identify the controls on these processes that will inform management strategies. Importantly, the results presented in Chapter 4 demonstrate that nitrification may be an important process affecting oxygen concentrations within oil sands pit lakes to grasp a better understanding of the fate and evolution of the N redox cycling. Overall, the results presented here have significant implications for developing effective strategies to manage of future oil sands Pit lakes and can be extrapolated to model and predict the

behaviour of other anaerobic soft sediments, such as contaminated harbour and estuary sediments. The results should also affect evaluation criteria for construction of pit lakes, which are proposed reclamation options for managing existing tailings ponds. Thus, the collective results from this doctoral work are of broad relevance to both the oil sands industry as well as other anthropogenically impacted or engineered systems with high oxygen demand.

5.3 Future Research Directions

The potential effects of the FFT compounds mobilized into the water column require further investigation, as outside of this thesis they remain poorly understood. In particular, those OCC discussed here since they were shown to be driving the fate of oxygen in the water column. Continuous monitoring of these compounds and seasonal assessment will provide a short and long-term evolution. Moreover, a complete understanding of physical and chemical parameters that can affect the water in BML should be incorporated into the geochemical monitoring. Hydrodynamics aspects, in particular, can provide a better understanding of the different mixing events that play an important role in the oxygen flux of BML. In addition, the FFT layer geochemical and physical aspects should be combined with the observations from the water cap to provide a general mechanism impacting oxygen in BML.

With respect to possible future research efforts concerning oxygen dynamics, an oxygen budget model will expand the results identified in this thesis work. A complete assessment of the different inputs (e.g. freshwater addition, precipitation, atmospheric

oxygen diffusion) and outputs (eg. evaporation, biological and chemical uptake) can provide a better understanding of the oxygen flux through the water column. Also, zones of intense redox cycling, such as the FWI and the metalimnion-hypolimnion interface, should be the focus of micro-scale oxygen measurements. Utilization of novel methods (e.g. oxygen microelectrodes or sediment traps) have been used for a long time in marine systems to obtain information about the oxygen dynamics and all the different parameters controlling it. For example, oxygen microelectrodes permit to measure in real time, *in-situ* and in small scale the water-sediment interface to identify distribution and utilization of oxygen, which can be expanded to measure different associated parameters (e.g. Fe^{+2}/Fe^{+3}, CH_4, NH_4, H_2S) simultaneously. A combination of in-situ methods and identification of microbial communities can assist to link important biogeochemical process occurring at a micro-scale.

Metagenomic DNA and RNA sequencing using next-generation methods could be employed to better distinguish the composition and functional characteristics of and differences between microbial communities linked to the oxygen-consuming processes discussed in this thesis, as well as to characterize the presence and expression of genes indicative of specific functions (e.g. aerobic mineralization, methanotrophy, and nitrification). Complimenting a comprehensive investigation of water column microbial community genetic information, microscopic imaging based on the use of electrons or X-rays (i.e. environmental scanning electron microscopy equipped with energy dispersive X-ray spectroscopy, scanning transmission X-ray microscopy) could be employed to better understand how communities (i.e. biofilms and flocs) are physically structured. All

these methods can be incorporated to provide a seasonal and annual distribution of the microbial community that can complement the geochemical trends observed in this thesis.

5.4 References

Powter, C., K. Biggar, M. Silva, G. McKenna, and E. Scordo, 2011, Review of oil sands tailings technology options: Tailings and Mine Waste.

Risacher, F. F., Morris, P. K., Arriaga, D., Goad, C., Nelson, T. C., Slater, G. F., & Warren, L. A. (2018). The interplay of methane and ammonia as key oxygen consuming constituents in early stage development of Base Mine Lake, the first demonstration oil sands pit lake. *Applied Geochemistry*, *93*, 49-59.

Siddique, T., T. Penner, J. Klassen, C. Nesbø, and J. M. Foght, 2012, Microbial communities involved in methane production from hydrocarbons in oil sands tailings: Environmental science & technology, v. 46, p. 9802-9810.

Stumm, W., and J. J. Morgan, 1981, Aquatic chemistry: an introduction emphasizing chemical equilibria in natural waters, Aquatic chemistry: An introduction emphasizing chemical equilibria in natural waters, p. 795-795.

Testa, B. M., 2010, RECLAIMING: ALBERTA'S OIL SANDS MINES: Earth, v. 55, p. 44-55.

Ward, B. B., 2008, Nitrification in marine systems: Nitrogen in the marine environment, v. 2, p. 199-261.

Westcott, F., 2007, Oil sands end pit lakes: a review to 2007: Prepared by Clearwater Environmental Consultants Inc. for The Cumulative Environmental Management Association-End Pit Lakes Subgroup.